การเคลือบผิวอนุภาคด้วยฟลูอิดไดซ์เบดที่เสริมด้วยไฟฟ้าสถิต

นางสาว ยุวดี พูนเพชรมงคล

PARTICLE COATING IN FLUIDIZED BED COATER ENHANCED WITH ELECTROSTATICITY

Miss Yuwadee Phoonphetmongkon

Thesis Title   PARTICLE COATING IN FLUIDIZED BED COATER
                      ENHANCED WITH ELECTROSTATICITY
By   Miss Yuwadee Phoonphetmongkon
Field of study   Chemical Engineering
Thesis Advisor   Associate Professor Tawatchai Charinpanitkul, D.Eng.
Thesis Co-advisor   Associate Professor Poj Kulvanich, Ph.D.

_____

       Accepted by the Faculty of Engineering, Chulalongkorn University in Partial Fulfillment of the Requirements for the Master 's Degree

……………………………………………….. Dean of Faculty of Engineering
       (Professor Direk Lavansiri, Ph.D.)

THESIS COMMITTEE

…………………………………………….. Chairman
       (Professor Wiwut Tanthapanichakoon, Ph.D.)

…………………………………………….……. Thesis Advisor
       (Associate Professor Tawatchai Charinpanitkul, D.Eng.)

…………………………………………….. Thesis Co-advisor
       (Associate Professor Poj Kulvanich, Ph.D.)

…………………………………………….. Member
       (Associate Professor Sirikalaya Suvachitanont, D.Eng.)

…………………………………………….. Member
       (Nattaporn Tonanon, M.Sc.)

นางสาวยุวดี พูนเพชรมงคล : การเคลือบผิวอนุภาคด้วยฟลูอิดไดซ์เบดที่เสริมด้วยไฟฟ้าสถิต (PARTICLE COATING IN FLUIDIZED BED COATER ENHANCED WITH ELECTROSTATICITY) อ. ที่ปรึกษา : รศ.ดร. ธวัชชัย ชรินพาณิชกุล, อ.ที่ปรึกษาร่วม: รศ.ดร. พจน์ กุลวานิช, 115 หน้า. ISBN 974-17-6855-9.

จากผลของการศึกษาการเคลือบผิวอนุภาคลูกแก้วด้วยสารเคลือบ Hydroxypropyl Methylcellulose (HPMC) ภายในเครื่องเคลือบผิวแบบฟลูอิดไดซ์เบดขนาด 16 ลิตร ที่เสริมด้วยการป้อนไฟฟ้าสถิตที่หัวฉีด โดยการปรับเปลี่ยนตัวแปรกระบวนการ ซึ่งได้แก่ ความเร็วอากาศที่ใช้ในการฟลูอิดไดซ์ (2.2 ถึง 4.3 ม/ว) อัตราการป้อนสารเคลือบแก่หัวฉีด (10 ถึง 20 มล./นาที) ขนาดของอนุภาคแกน (590 และ 1,033 ไมโครเมตร) และศักย์ไฟฟ้าที่ป้อนแก่หัวฉีด (0 ถึง (-4) กิโลโวลต์) พบว่าตัวแปรดังกล่าวมีผลต่อค่าประสิทธิภาพในการเคลือบผิว ความหนาของชั้นฟิล์มเคลือบที่วิเคราะห์โดยใช้โปรแกรมวิเคราะห์ภาพถ่ายจากกล้องจุลทรรศน์ และความหนาแน่นปรากฏขณะอัดที่วิเคราะห์โดยใช้เครื่องทดสอบสมบัติวัสดุผง โดยการเพิ่มค่าความเร็วอากาศที่ใช้ในการฟลูอิดไดซ์ จะทำให้ประสิทธิภาพในการเคลือบและความหนาของฟิล์มเคลือบมีค่าลดลง เนื่องจากความเร็วอากาศที่เพิ่มขึ้นจะทำให้ตัวทำละลายของสารเคลือบระเหยได้เร็วขึ้น ส่งผลให้กลายเป็นอนุภาคขนาดเล็กฟุ้งกระจายหนีไปก่อนที่จะสัมผัสกับอนุภาคแกน ในขณะที่เมื่อใช้อนุภาคแกนขนาดใหญ่ขึ้นจะทำให้ปรากฏการณ์ฟลูอิดไดเซชันเกิดได้ยากขึ้น การสัมผัสกันของหยดละอองกับอนุภาคแกนจึงเกิดได้น้อยลง ส่งผลให้ความหนาของชั้นฟิล์มเคลือบลดลง ในทางตรงกันข้าม การเพิ่มอัตราการป้อนสารเคลือบให้สูงขึ้น จะทำให้ความหนาของฟิล์มเคลือบและประสิทธิภาพในการเคลือบผิวเพิ่มขึ้น เนื่องจากขนาดของหยดสเปรย์ที่เกิดจะใหญ่ขึ้น และมีโอกาสสัมผัสกับอนุภาคแกนมากขึ้น สำหรับการเพิ่มศักย์ไฟฟ้าที่ป้อนให้กับหัวฉีดให้สูงขึ้น จะส่งผลให้เกิดแรงดึงดูดทางไฟฟ้าระหว่างหยดสเปรย์และอนุภาคแกนเพิ่มขึ้น ดังนั้นจึงทำให้ได้ประสิทธิภาพในการเคลือบผิวสูงขึ้น

ภาควิชา............วิศวกรรมเคมี..................   ลายมือชื่อนิสิต..

สาขาวิชา..........วิศวกรรมเคมี...............   ลายมือชื่ออาจารย์ที่ปรึกษา.......................................

ปีการศึกษา........2547…..   ลายมือชื่ออาจารย์ที่ปรึกษาร่วม...............................

Experimental results of coating of glass beads with aqueous solution containing HPMC as a coating liquid within a 16 liters top-spray fluidized bed enhanced by electrostaticity was significantly dependant on operating variables which were fluidizing air velocity (2.2 to 4.3 m/s), flow rate of coating agent (10 to 20 ml/min), size of core particles (590 and 1,033 μm) and electricity potential applied to a spraying nozzle (0 to (-4) kV).   Coating efficiency, coating film thickness and packed bulk of coated particles were affected by those operating variables. Increasing of fluidizing air velocity, coating efficiency and coating film thickness became hindered due to the higher evaporating rate of sprayed droplets became promoted with the increasing air velocity then they transformed to fine particulate dispersing away before coming into contact with core particles. While larger core particles led to more difficulty to be fluidized, resulting in a less contact among the core particles and sprayed droplets. On the other hand, an increase in flow rate of coating liquid could increase the coating film thickness and the coating efficiency. This could be implied that the higher the flow rate the larger the droplets sprayed out from the nozzle which increased the possibility of contact among the core particles and droplets. Meanwhile, an increase in electrical potential applied to the nozzle would lead to an increase in the attractive force among the charged droplets and the core particles therefore the coating efficiency could become more enhanced.

Department……Chemical Engineering…   Student's signature……………………....

Field of study....Chemical Engineering…   Advisor's signature……………………....

Academic year ...…2004…...   Co-advisor's signature………………...….…

ACKNOWLEDGMENTS

CONTENTS

CONTENTS (Continued)

CONTENTS (Continued)

สถาบันวิทยบริการ
จุฬาลงกรณ์มหาวิทยาลัย

LIST OF TABLES

LIST OF FIGURES

LIST OF FIGURES (Continued)

LIST OF FIGURES (Continued)

LIST OF FIGURES (Continued)

NOMENCLATURE

ρ_p	particle density (kg/m^3)
d_p	particle diameter (μm)
Q_L	coating agent flow rate (ml/min)
E	applied potential (kV)
U	fluidizing air velocity (m/s)
σ	fluid surface tension (N/m)
ρ	fluid density (kg/m^3)
μ	fluid viscosity (mPa/s)
U_{sol}	fluid volumetric flow rate (m^3/s)
U_{at}	air volumetric flow rate (m^3/s)
q	charge of particle (C)
r	distance between charge (m)
k	Coulomb constant

CHAPTER I

INTRODUCTION

1.1 Background

Coating is a process to form deposition of an ingredient on surface of another substance or objects of various sizes. Categories of coating usually depend on the applications to be used. For pharmaceutical industry, film coated on particulate material is employed to protect the active ingredients against environment hazard, light, air as well as hiding bad tastes odor or appearance. It is, therefore, well known that coating technology is widely usable for controlled release applications.

Nowadays, fluidized bed coaters are very important equipment for surface treatment of particulate material, in particular for pharmaceutical industry due to their various advantages. For instance, several operations such as particle mixing, liquid spreading and particle evaporation of solvent from the particle surface could be carried out within the same apparatus. It should be noted that top spray fluidized bed coater has another advantage of being simple to set up. However, such coater has some disadvantages that some coating agents will rapidly be vaporized or be entrained out of the vessel before coming into contact with core particles because of the countercurrent flow between coating agent droplet and core particles.

Meanwhile, electrostaticity that provides an attractive force between the different charged substances is broadly applied in many industries. For example, electrostatic spray-painting utilizes charged droplets for coating onto the surface of an object. Other industrial electrostatic applications include textile flocking, sand paper

manufacture and xerography. Use of charged spray droplets has been shown to improve the efficiency of deposition in agricultural pesticide applications.

For this reason, the objective of this study is to develop a top spray fluidized bed coater by applying different charge onto core particles and droplets of coating agent for improving coating efficiency by the attractive force of the different charges.

1.2 Objective of The Present Study

1. To develop a fluidized bed coater by applying electrostatic potential to core particles and coating droplets in order to enhance the deposition of coating agent onto the surface of the core particles.

2. To test performance of the developed fluidized bed coater under various conditions to study their effects on properties of the coated particles and the coating efficiency.

1.3 Scope of Study

1. To develop a fluidized bed coater of which coating efficiency could be enhanced by electrostaticity

2. To investigate the effects of process variables to the properties of film coated on glass beads. Aqueous Hydroxypropyl Methylcellulose (HPMC) was employed as film coating agent.

   The process variables of interest are

   2.1 Fluidized velocity: 2.9, 3.6, 4.3 m/s

   2.2 Voltage applied to the nozzle: 0, 1000 volt

   2.3 Flow rate of coating agent: 10, 15, 20 ml/min

   2.4 Average size of core particles: 590 and 1033 μm

3. The properties of coated particle investigated are

    3.1 Packed bulk density

    3.2 Film thickness

    3.3 Morphology and surface by using Scanning Electron Microscope (SEM)

1.4 Expected Benefit

1. Understand the principle of coating process using fluidized bed coater

2. Understand how the mentioned factors affect the coating process using fluidized bed coater enhanced with electrostaticity.

CHAPTER II

LITERATURE REVIEWS

A. Wolny and W. Kazmierczak [1] used a special method of electric charge measurements on single polystyrene particles in a fluidized bed. The method consisted in an analysis of the trajectory of particles ejected from the bed into a homogenous electric field by means of a local pneumatic impulse. The fluidized bed was either made of pure polystyrene particles or modified by humid air or by addition of fines (aluminium powder or sodium chloride).

Poul Betesen et al. [2] examined the differences between the efficiency of organic solvent-based membranes applied by countercurrent coating and by Wurster-based, concurrent coating were examined by coating KCl crystals with an ethylcellulose-based membrane. The dissolution from crystals coated by the concurrent process was slower than that achieved by the countercurrent process as assessed at the time for dissolution of 63.2%. The cause of this higher efficiency was examined. The coated crystals were examined by sieve analysis, by measuring the specific surface area, the film thickness, the amount of coating dry matter applied, by scanning electron microscopy of surface and cross-sections, and by determining the porosity of the membranes. It was shown that only the membrane porosity can explain the differences in coating efficiency.

A. J. Yule et al. [3] investigated a burner using electrostatic method to produce and control a fuel spray for non-burning sprays. The burner had a charge injection nozzle and liquid flow rate and charge injection rate were varied using hydrocarbon liquid of differing viscosities, surface tensions and electrical conductivities. Droplet size distributions were measured and it was shown how the dropsize, spray pattern, breakup length depend on the above variables, and in particular on the specific charge achieved in the spray. The data are valuable for validating two computer models under development. Electrostatic disruptive forces can be used to atomize oils at flow rates commensurate with practical combustion systems and that the charge injection technique is particularly suitable for highly resistive liquids.

J.Guardiola et al. [4] studied the influence of particle size, fluidization velocity, and relative humidity on the degree of electrification reached by a fluidized bed of glass beads. The static electrification of the bed was measured by means of the potential difference observed between an electric probe and the metallic distributor. The effect of relative humidity appeared to be complex and was connected with the quality of fluidization - bubbling or slugging-existing in the bed. The static electrification of the bed cannot be measured accurately when the relative humidity is lower than a critical value because the adhesion of particles to the probe led to irreproducible voltage values. Also, the degree of electrification increased with particle size and air velocity.

R.K. Johnson, R.C. Anantheswaran and S.E. Law [5] used an embedded-electrode, two-fluid, electrostatic-induction spray-charging nozzle to atomize and charge spray droplet in a pilot-scale spray-drying unit. A dielectric barrier made out of Teflon® (PTFE) was installed within the spray-dryer to impede deposition of charged droplets onto the walls of the sprays-dryer. Concentrated whole milk (500g/kg solids) was atomized with induction electrode potentials of 0, 300, 600, 750, and 900 V and atomizing pressures of 140, 280, and 410 kPa. Charging voltage had a significant effect on the solubility index. Particle size analysis and scanning electron microscopy revealed that 140 kPa was insufficient for complete atomization.

Hiroshi Yuasa, Tatsu Nakano and Yoshio Kanaya [6] studied the suppression of agglomeration in fluidized bed coating by adding NaCl. The coating was carried out with aqueous spray solution at various additional amounts of NaCl, using water-soluble hydroxypropyl cellulose (HPC) or hydroxypropylmethyl cellulose (HPMC) as membrane material, and spherical granules made of crystalline cellulose (Celphere™) as core particle. Agglomeration of particles was clearly suppressed by adding NaCl to the aqueous spray solution in both cases of HPC and HPMC. The mean particles diameter of the coated particles decreased with the increasing additional amount of NaCl in the spray solution. The NaCl concentration required to reduce the viscosity of the HPC solution became lower as temperature became higher. When the viscosity of the solution decreased, turbidity and/or precipitate were observed. These results suggested that the suppression of agglomeration was caused by the reduction in the viscosity of the spray solution through salting-out of the polymeric membrane materials.

Koen Dewettinck and Andre Huyghebaert [7] evaluated the effect of process variables on the coating efficiency of top-spray fluidized bed coating. Sodium chloride crystals were coated with protein concentrates as a model system in a laboratory top-spray fluidized bed unit. It was established that a higher coating mass of sodium caseinate was obtained at a lower average particle size and that the highest coating mass was obtained at a critical inlet air temperature of approximately 74 $^{\circ}$C. The nozzle atomization pressure was demonstrated to act as more than a droplet size influencing factor. The highest coating efficiency of sodium caseinate was achieved at a high atomization pressure, the latter having the combined effect of producing smaller droplets with a higher velocity and decreasing the bed temperature. The functional and compositional properties of protein concentrates clearly influenced the coating efficiency when these products were used as a coating material in a top-spray fluid-bed process as was observed in studies using sodium caseinate, lysozyme and blood plasma concentrate.

M.R. Jahannama, A.P. Watkins and A.J. Yule [8] investigated a two fluid, concentric, internal mixing induction-charging nozzle suitable for electrostatic crop spraying of conducting pesticides by experimental and computational analysis. Droplet size measurements for both charged and uncharged sprays with horizontal and vertical nozzle situations were carried out. The droplet size distributions of horizontal sprays showed a significant difference between the charged and uncharged cases, where there was no remarkable difference between the vertical cases. Tests were made to assess asymmetry of the horizontal sprays comparing droplet sizes across the spray. Specific charge of the spray could was measured using a Faraday cage to collect the charge spray.

K. Saleh, D. Steinmetz and M. Hemati [9] investigated the effect of particle size on coating criteria by using sand particles as the coating support and aqueous solutions containing NaCl as coating liquid. The result showed that both growth rate and efficiency increased with decreasing the particle size. The growth was mainly governed by layering for particles larger than 200 μm, whereas for finer particles it occurred by agglomeration. As the particle size became less than 90 μm, the coating operation led to uncontrolled growth and bed quenching. However, the coating of the same particles was successfully achieved by adding some coarser particles. In addition, a mathematical model based on the population balance concept, taking into account the simultaneous growth by layering and agglomeration, was established to predict the time evolution of the particle size distribution. The comparison between experimental and calculation data permitted the establishment of a law for the size dependency of the agglomeration kernel.

M. Hemati et al. [10] studied the effect of process variables such as the excess gas velocity, atomizer location, liquid flow rate and atomizing air flow rate and physicochemical properties of the solid and liquid such as viscosity of solution and initial particle mean size on the growth of solid particles in fluidized bed. The binding aqueous solution which was aqueous of polymer or inorganic salts was introduced in the bed using a pneumatic atomizer located in the top of the column. They found that the fluidizing air velocity was the most important factor affecting the growth kinetics and stability of the operation. An increases of the relative humidity depending on the liquid flow rate as well as the air flow rate, favor agglomeration mechanism especially for values greater than 0.4. An increase in the particle initial size led to an enhancement of the layering mechanism especially for value greater than 300 μm.

M. Murtomaa et al. [11] studied an inductive method for charge generation measurement by using monohydrate, microcrystalline cellulose and glass beads as materials for fluidization. The system consisted of an electrostatic ring probe, which allowed charge scanning across the miniaturized fluidized bed with glass or acrylic columns without disturbing the fluidization process. The charge coupling from the system to the probe has been modeled and the experimental data have been simulated using an advanced field solving software.
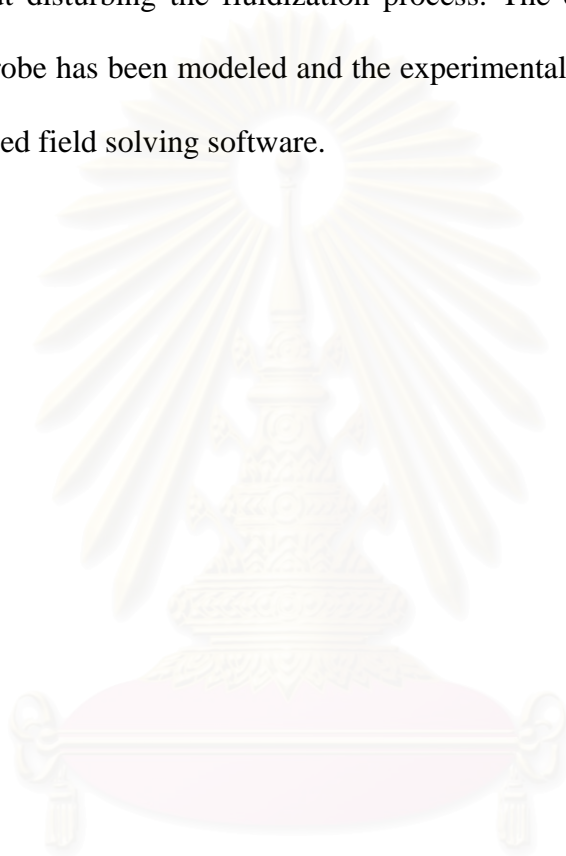
CHAPTER III

THEORY

3.1 Fluidization

Fluidization is the operation by which fine solids are transformed into a state through contact with a gad or liquid.

3.1.1 The Phenomenon of Fluidization

Pass a fluid upward through a bed of fine particles as shown in Fig. 3.1. At a low flow rate, fluid merely percolated through the void spaces between stationary particles. This is a fixed bed.
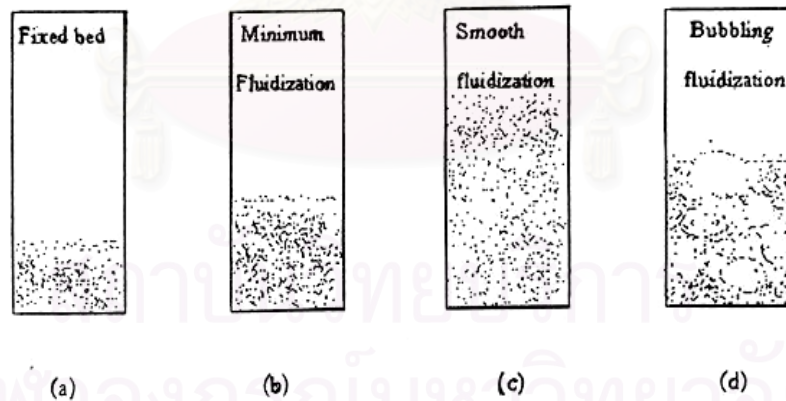
Figure 3.1 Characterization of Fluidization beds [12]

With an increase in flow rate, particles move apart and few are seen to vibrate and move about in restricted regions. This is the expanded bed.

At a still higher velocity, a point is reached when the particles are all just suspended in the upward flowing gas or liquid. At this point the fraction force between a particles and fluid counterbalances the weight of the particles, the vertical component of the compressive force between adjacent particles disappears, and the pressure drop through any section of the bed about equals the weight of fluid and particles in that section. The bed in considered to be just fluidized and is referred to as an incipiently fluidized bed or a bed at minimum fluidization.

In liquid-solid systems an increase in flow rate above minimum fluidization usually results in a smooth, progressive expansion of the bed. Gross flow instabilities are damped and remain small, and large-scale bubbling or heterogeneity is not observed under normal conditions. A bed such as this is called a particulately fluidized bed, a homogeneously fluidized bed, a smoothly fuidized bed, or simply a liquid fluidized bed.

Gas-solid systems generally behave in quite a different manner. With an increase in flow rate beyond minimum fluidization, large instabilities with bubbling and channeling of gas are observed. At higher flow rates agitation becomes more violent and movement of solids becomes more vigorous. In addition, the bed does not expand much beyond its volume at minimum fluidization. Such a bed is called an aggregative fluidized bed, a heterogeneously fluidized bed, a bubbling fluidized bed, or simply a gas fluidized bed. In a few rate cases liquid-solid systems will not fluidized smoothly and gas-solid systems will not bubble. At present such bed are only laboratory curiosities of theoretical interest.

Both gas and liquid fluidized beds are considered to be dense-phase fluidized bed as long as there is fairly clearly defined upper limit or surface to the bed. However, at a sufficiently high fluid flow rate the terminal velocity of the solid is

exceeded, the upper surface of the bed disappears, entrainment becomes appreciable, and solid are carried out of the bed with the fluid stream. In this state we have disperse-, dilute-, or lean-phase fluidized bed with pneumatic transport of solids.

Consider briefly the quality of fluidization in a bubbling bed. Although the properties of solid and fluid alone will determine whether smooth or bubbling fluidization occurs, many factors influence the rate of solid mixing, the size of bubbles, and the extent of heterogeneity in the bed. These factors include bed geometry, gas flow rate, type of gas distributor, and vessel internal such as screens, baffles, and heat exchangers.

As an example considers slugging, a phenomenon is strongly affected by the vessel geometry. Gas bubbles coalesce and grow as they rise, and in a deep enough bed they may eventually become large enough to spread across the vessel. Thereafter the portion of the bed above the bubble is pushed upward, as by a piston. Particles rain down from slug and it finally disintegrates. At about this time another slug forms and this unstable oscillatory motion is repeated. Slugging is usually undesirable since it increases the problems of entrainment and lowers the performance potential of the bed for both physical and chemical operations. Slugging is especially serious in long, narrow fluidized beds.

3.1.2 The Geldart Classification of Particles

A full classification of powder according to their behavior in fluidization is complex their behavior depends on many particle properties. Geldart and co-worker have identified two parameters to classify powder for fluidization i.e. the particle size, the particle density. This classification, for fluidization by air ambient conditions, shower Fig. 3.2
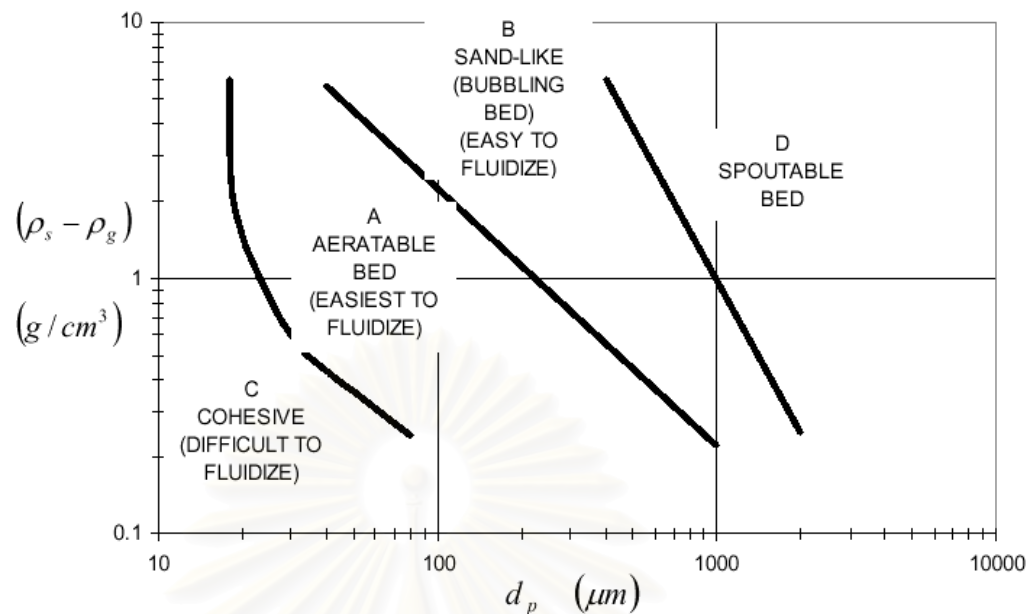
Figure 3.2 Geldart classification of fluidized beds. Particle properties are related to the type of fluidized beds [13].

Powder in group A, sometimes referred to as slightly cohesive, (typically cracking catalysts), are size range 50 to 200 microns. This particles exhibit large bed expansion after minimum fluidization and before start of bubbling; the bubble size is limited.

Powder in group B (e.g. sand, pellets and granules) bubble at the minimum fluidization velocity and the bed expansion is small.

Group C (cohesive) is size range less than 20 microns. This group is difficult to fluidize at all, they exhibit a tendency to form channeling. The denser and larger crystal are behave like group D. With group D the bed expansion is minimal, even less than for the group B. This group can form stable spouted bed if the gas is admitted only through a centrally-positioned hole. Moreover, the transition group AC, size range 20 to 50 microns, has been recognized as "semi-cohesive", between groups A and C.

The key fluidization properties of solids from the different group appear in table 3.1

Table 3.1 Summary of group properties

	A	B	D
Most obvious Characteristic	Bubble-free range of fluidization	Start bubbling at Minimum fluidization velocity	Coarse solids
Typical Pharmaceutical substrates	Microparticles	Pellets; granules; Light, small crystals	Tablets; capsules; Heavy, large crystals
1. Bed expansion	High	Moderate	Low
2. Deaeration rate	Slow, linear	Fast	Fast
3. Bubble properties	Splitting/recoalescence predominate Maximum size exists Large wake	No limit on size	No know upper Size Small wake
4. Solids mixing	High	Moderate	Low
5. Slug properties	Axisymmetric	Axisymmetric; Asymmetric	Horizontal voids, Solids slug, wall Slugs
6. Spouting	Not except in very shallow beds	Shallow beds only	Even in deep beds

3.2 Coating

3.2.1 Purpose of Coating

The first coated pharmaceutical dosage forms were medication with sugar coatings for the purpose of masking unpleasant tastes and imparting a more elegant appearance. For a long time lasting gloss was therefore the major prerequisite. Nowadays there are other important reasons for pharmaceutical particle coating:

- protection of active ingredients against light, air and moisture

- increase mechanical stability during manufacture, packing and shipment

- protection the active ingredients against the influence of digestive fluids

- ensuring their controlled release

- avoidance of side effect

- increasing drug safety by better identification

3.2.2 Type of Coating

Coating materials usually consist of a mixture of a mixture of substances. The matrix formers are responsible for the stability of the coating structure, and they also determine the coating process. Depending on the type of matrix former or binder used, three coating categories can be distinguished.

1.Coating with sucrose and other sugar: It permits application of copious amount of mass to the core and is widely used in the manufacture of pharmaceuticals and confectionery. Coating pans are the preferred type of equipment, belt coaters being the exception.

2.<u>Hot melts</u>: It also a considerable amount of mass while cooling is required for solidification of the coating on the core. They are mainly use for confectionery. The most important raw materials are fats, mostly cocoa fat and the sugar/alcohol mixture xylitol/sorbitol. Process is conducted in pan or on belts.

3.<u>Film coating</u>: They require less material, forming thin membranes that largely follow the contours of the substrate, e.g. score and engravings. The film formers affect the partly pH-dependent solubility and selective permeability of coatings. Coating pans and fluidized bed equipment are generally used for processing.

Film and sugar coatings differ substantially in thickness and therefore also in the necessary mass of coating material (table 3.2)

Table 3.2 Comparison between film and sugar coating

	Sugar-coated tablets	Film-coated tablets
Coating thickness (μm)	0.2-0.5	0.05-0.03
Film former (mg/cm^3)		0.5-3
mg mass/cm^2	30-100	1-12

3.2.3 Fundamental of Film Coating

Among these three coating methods, film coating has gained wider attention especially for application of controlled released. Uniformity of distribution of the film and evaporative efficiency to inhibit core penetration by solvents or water are common to the three types of fluidized bed processing: top-spray, bottom-spray, and tangential-spray. However, each of the techniques has limitations, are they are by no mean equivalent.

Application of a film to a solid is indeed vary complex. A layer of coating does not occur during a single pass through the coating zone, but relies on many passes to produce complete coverage of surface. Droplet formation, contact, spreading, coalescence, and evaporation, as illustrated in figure 3.3, are occurring almost simultaneously during the process.

The nozzles typical used in fluidized bed coating process are binary type nozzles: liquid is supplied at a low pressure and is sheared into droplet by air. Droplet size and distribution are more controlled with the type of nozzle than with a hydraulic nozzle, especially at low liquid flow rate. However, the air used for atomization also contributes to evaporation of the coating solvent. This evaporation results in increasing the droplet's viscosity, and it may inhibit spreading and coalescence upon contact with the core material. Another factor affecting droplet viscosity is the distance that the droplets travel through the primary evaporation media (the fluidization air) before impinging the core. This problem becomes more stress with the use of organic solvents which evaporate much more quickly than water. Films whose viscosity is very sensitive to change in solids concentration also give rise to such problem. In all three fluidized bed processes, the nozzle is positioned to minimize droplet travel distance.
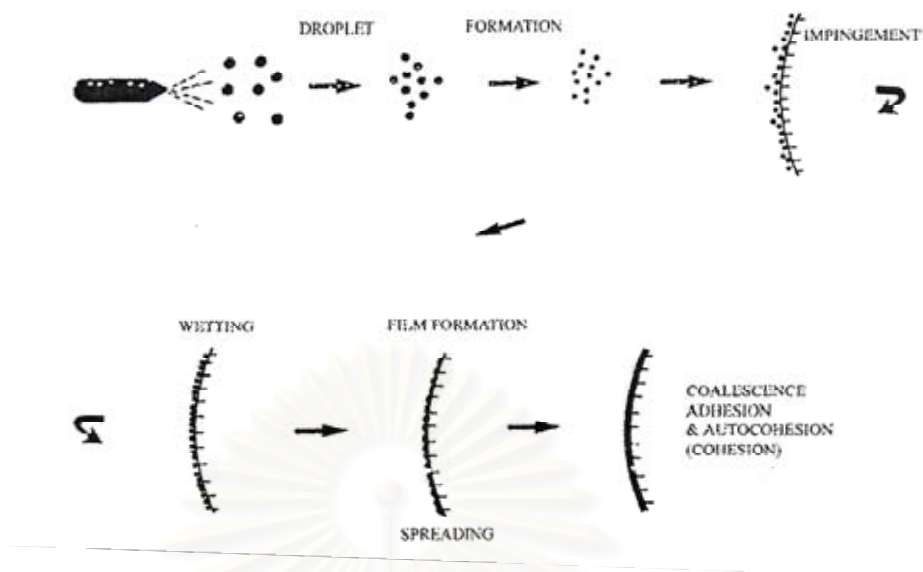
Figure 3.3 Schematic of the film coating process [14].

3.2.4 Process Variables

The rate of evaporation of the coating application media can significantly affect film formation in both aqueous and organic solvent systems. Fluidization air volumetric flow rate, temperature, and humidity are the three factors, which have strong influence on efficiency of coating process.

For organic solvent, low fluidization air temperature may be chosen to accommodate the solvent's low heat of evaporation. The danger in allowing absolute humidity to vary is that enthalpy, which determines evaporation rate, increases at a given dry bulb temperature as the absolute humidity increases. Additionally, if absolute humidity is high, evaporation cooling by the solvent in the coating zone may locally depress the air temperature below the dew point, causing condensation of water onto the substrate surface, as the film forming. If the film is incompatible with water, the coating would not perform as desired.

Consistency in absolute humidity is recommended, but removal of all moisture is not required. In fact, in many organic solvents coating processes, a quantity of moisture in the process air is usually helpful in dispelling static electricity, which develops after surface of the particles is completely covered.

Coating uniformity is a result of the rapid cycling of particles or the number of times the particles are exposed to the spray. The rate which the coating is applied (on a solid basis) is dependent on the solution concentration and the spray rate. However, the droplet size and spreading characteristics will affected by the increased viscosity.

Spray rate is dependent on three factors: (1) capacity of air for the solvent being used; (2) the tackiness of the coating being applied; (3) the speed with which the particles travel through the coating zone. The rate-limiting factor is generally the tackiness of the coating solution as it changes from a liquid to a solid. In the fluidized bed process, coating is applied to paticles suspended in the air stream. However, particle-machine and particle-particle collisions do occur and have strong effect on the coating efficiency.

3.2.5 Factors Affecting The Quality of Film Coating

Film coating is a process in which the results obtained are attributable to the complex interaction of numerous factors. In order to better understand those factors that influences the quality of the finish product, it is necessary to examine the factors that have an effect on the coating phenomena. These factors are interaction between the core material (substrate) and the applied coating, the drying process and the uniformity of distribution of substrate in the equipment during coating process. Some

of these important factors are spray equipment, solid content of coating liquid and fluidizing air velocity etc.

3.2.6 Ingredients Used in Film Coating

In general, film coating formulations consist of an extensive list of ingredients, including film formers, plasticizers, colorants, surfactants, flavors, grossing agents and solvents. Nowadays, typical formulation contains polymer, plasticizers, colorant and solvent.

Film coatings consist mainly of polymer, which are applied to the core in the form of solutions or dispersion in which other excipients are dissolved or suspended. After drying the solvents or dispersing agents, the polymer and other excipients remain on the core as a coherent, uniform film.

Pharmaceutical film coating formulations consist of organic solutions and aqueous dispersions. Film coating which use organic solvents produces good results but has a limitation due to its serious drawbacks such as associated flammability, toxicity, and environmental pollution hazard. However, this technique is still widely used and probably always has application where specialized polymers are used for coating.

1.Polymer

A polymer is a large molecule built up by the repeat of small, simple chemical units. The repeat unit of the polymer is usually equivalent to the monomer, or stating material from which the polymer is formed. In the majority of film coating formulations, the polymer is the major ingredient. Consequently, this material has the greatest impact on the final properties of the coating.

Polymers have various chemical types and grades. When selecting a polymer for film coating, it is thus necessary to define this material in term of chemical structure, molecular weight, and molecular distribution because molecular weight characteristics of the polymer have a significant effect on coating properties. Nowadays, there are numerous commercially synthetic polymers, which have found wide range of usage in pharmaceutical formations.

For aqueous-based coating systems, the polymers can be divided into essentially two classes: aqueous-soluble polymers and water-insoluble or pH-dependent soluble polymers.

The most commonly used aqueous-soluble polymers consist primarily of:

1.1 Acrylate copolymers: Eudragit E® (catonic copolymer based on dimethylamioethyl methacrylate and other neural methacrylate)

1.2 Cellulosic polymers: Carboxymethylcellulose sodium, Hydroxypropyl-cellulose, Hydroxypropyl methylcellulose, Methylcellulose, Methyl hydroxcellulose, Polyethylene glycols, Povidone

On the other hand, Enteric coatings constitute the major portion of the water-insoluble or pH-dependent polymers. These polymers can be solubilized by adjusting the pH of the coating solution, or they can be formulated to be suspended in the aqueous media and applied as insoluble polymer particles. The water-insoluble polymers are used when an enteric coating or a special controlled-release delivery system is desired. Some of most common insoluble polymer candidates are: Methacrylic acid copolymer, Eudragit L and S®, Cellulose acetate phthalate, Hydroxypropyl methylcellulose phthalate, Polyvinyl acetate phthalate, Etylcellulose.

Among these coating polymers, HPMC is one of the most widely employed coating materials and it is of interest in this work. Therefore information of HPMC will shortly introduced as follows,

Hydroxypropyl methylcellulose (HPMC)

PhEur: Methylhydroxypropylcellulosm

USPNF: Hydroxypropyl methylcellulose, Pharmacoat®, Methocel®

Type of HPMC for film coating: It is available in several grades, which vary in viscosity and extend of substitution. HPMC defined in the USP XXII specifies the substation type by appending a four digits number to the nonproperprietary name. The first two digits refer to the approximate percentage content of the methoxy group (OCH_3). The second two digits refer to the approximate percentage content of the hydroxypropoxy group ($OCH_2CHOHCH_3$). The substation affects the solubility-temperature relationship.

The majority of HPMC used in pharmaceutical products is primarily used as a tablet binder, in film coating and as an extended release tablet matrix. Concentrations of between 2-5% w/w may be used as a blinder in either wet or dry granulation processes. HPMC 2910 of lowlabeled viscosity (3-15 mPa.s) is commonly used film coating.

Structure formula

R=-H$_2$-CH$_2$-CH$_2$CH(OH)CH
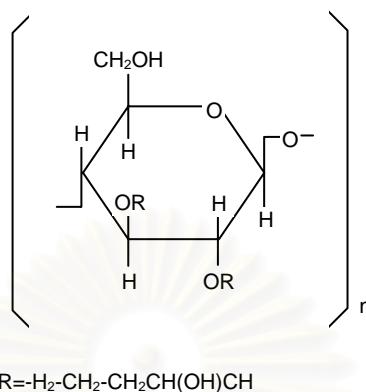
Figure 3.4 Hydroxypropyl methylcellulose [15].

Properties of HPMC: HPMC is and odorless and tasteless, white or creamy-white colorless fibrous or granular powder.

Ash: 1.5-3.0 % depending upon the grade.

Melting point: 190-200 $^{\circ}$C

Moisture content: depending upon the initial moisture content and the temperature and relative humidity of the surrounding air.

Solubility: soluble in cold water, forming a viscous colloidal solution; practically insoluble in chroloform, ethanol (95%) and ether, but soluble in mixtures of ethanol and dichloromethane, and mixtures of methanol and dichloromethane.

Specific gravity: 1.26

2. Plasticizers

Plasticizers are usually high-boiling liquids – sometimes also polymeric substances – of low molecular weight that should disperse as homogeneously as possible in the film former to be modified. By interacting with the film-forming

polymer, they alter certain physical and mechanical properties by enhancing the mobility of the polymer chains. Plasticizers are added for reason of processing technique and to achieve specific properties in use, e.g. to reduce the brittleness of film former, to increase their flexibility, facilitate their distribution on the substrate and to improve film formation.

Plasticizers act by penetrating between the chains of the film-forming polymer, thereby reducing the interaction among the polymer chains in the film. The plasticizer molecule increases the flexibility of the polymer chains in the film. The glass temperature of the system decreases as a result of the increased segmental mobility, and the film becomes plastic in the temperature range for processing or use.

Plasticizers for pharmaceutical purpose must be

- colorless   - water-resistant

- odorless   - chemically resistant

- non-volatile   - non-migrating in film

- thermally stable   - physiological harmless

The effectiveness of plasticizers in the coating formulation depends on further factors, however, e.g. other excipients, solvent systems, application method etc.

In this work, PEG used as plasticizer in the coating formulation so physical properties of PEG is described below.

Polyethylene Glycol (PEG)

PhEur: Macrogolum 1000

USPNF: Polyethylene glycol

Formula: $HOCH_2(CH_2OCH_2)_mCH_2OH$

Where m represents the average number of oxyethylene groups.

Properties of PEG6000: PEG is available in the form of lumps, flakes or powders. PEG used as gloss enhancers, glidants and lubricants, plasticizers type 6000 also as a coating substance. PEG is soluble in water, hot alcohols and chlorinated hydrocarbons.

Molecular weight: 6000

Melting point: 55-63 $^{\circ}$C

Density: 1.12 g/cm^3

Solubility in water at 25 $^{\circ}$C: 1,900 mg/ml

3.Opaquants and Colorants

The colorant can be either solubilized in the solvent system of suspended as insoluble particles. Colorants are included in many film coating formulations to improve the appearance and visual identification of the coated product.

The most brilliant colorant are provided by certified Food, Drug and Cosmetic (FD&C) or Drug and Cosmetics (D&C) dyes and lakes. Lakes are prepared from dyed precipitating the colorant with alumina or talc carriers. Lakes are water-insoluble and provide the most reproducible tablet colors.

Sunset Yellow. It is generally used as coloring agent for foods and drugs.

Formula: $C_{16}H_{10}N_2Na_2O_7S_2$

Structure:
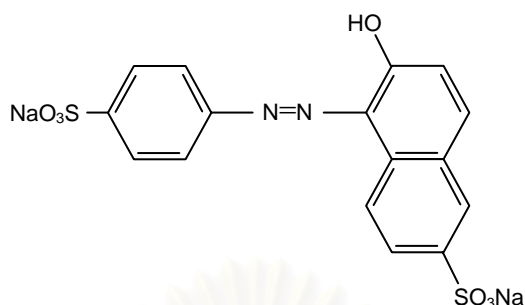
Figure 3.5 Sunset Yellow [15].

Molecular weight: 452.4

Appearance: reddish yellow powder. Aqueous solutions are bright orange colored.

Solubility in water at 25 ^{o}C: 70 g/l, slightly soluble in ethanol, in soluble in vegetable oil.

Absorption maximum: 482 nm

Incompatibilities: poorly compatible with citric acid, saccharose solutions and saturated sodium bicarbonate solutions incompatible with ascorbic acid, gelatin and glucose.

3.2.7 Fluidization in The Coating Process

1. Top Spray Coating

The most significant characteristic of the top spray method is that the nozzle sprays countercurrently or down, into the fluidizing particles. The fluidization pattern is random and unrestricted. As a result, controlling the distance the droplets travel before contacting the substance is impossible.

The top spray coating system is the complicated of the three machines. It has the largest batch capacity, and downtime between batches can be only minutes. Its biggest disadvantage is that its applications are somewhat limited.
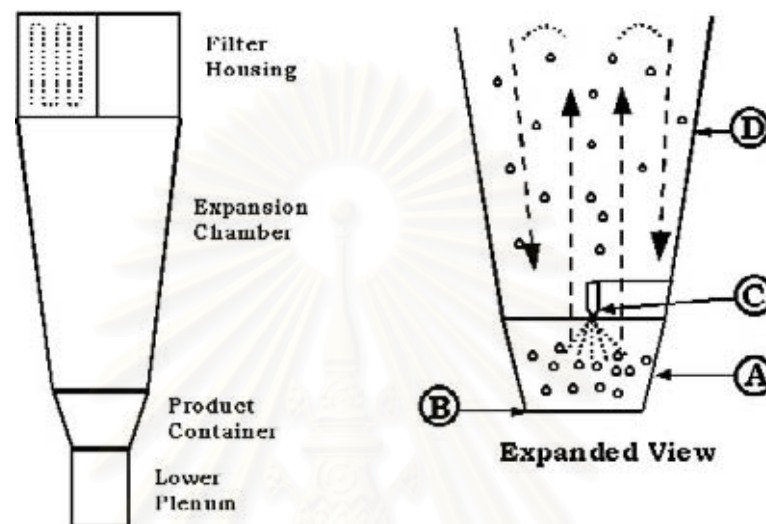
Figure 3.6 Top spray coater: (a) product container; (b) air distribution plate

(c) spray nozzle; (d) expansion chamber [16].

2. Wurster Bottom Spray Coating

This type is affected by the air distribution plate configuration and the partition height. The air distribution plate at the base of the coating chamber is divided into two sections. The open area of the plate, which is under the partition, is typically nearly fully open, allowing a high air volume and velocity to accelerate the substrate vertically past a spray nozzle that is mounted in the center of the orifice plate. On the other hand, the closed section is necessary for supporting the particle bed.

A second key process variable in Wurster processing is the height that the partition sits above the orifice plate. In general, the smaller the particles, the smaller the gap must be. This gap controls the rate of the substrate flow into the spray zone.
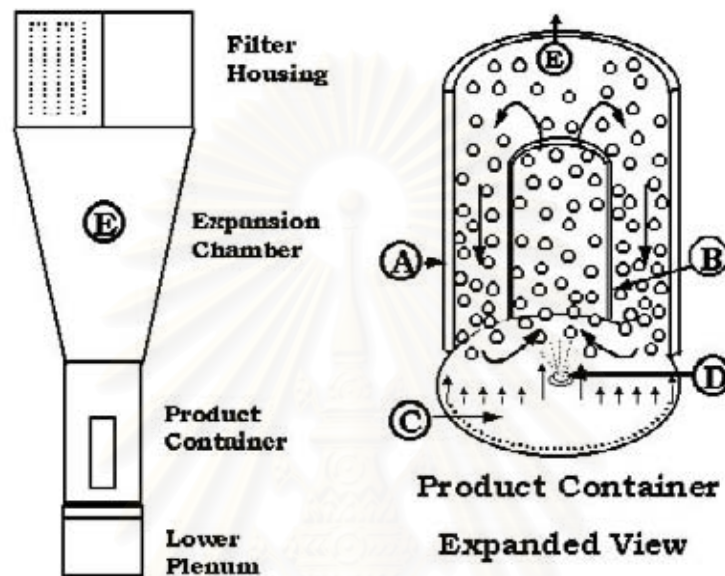
Figure 3.7 Wurster bottom spray coater: (a) coating chamber; (b) partition;

(c) air distribution plate; (d) spray nozzle; (e) expansion chamber [16].

The Wurster system has the widest application range of both water and organic solvents. The primary disadvantages of this system are that it is somewhat complicated, it is the tallest of the three types of fluidized bed machines, and the nozzles are inaccessible during the processing.

3. Tangential Spray Coating

The rotary or tangential spray system, also an immersed-nozzle, concurrent-spray technique, appears to offer film characteristics similar to the Wurster system. This system can be used with both water and organic solvents. The significance in this

equipment is that the substrate is placed into the product container and put into motion

by rotor disc, which is adjust by spinning at high speed to impart significant energy

into the bed. The disc, which is typically smooth, may be configured with a variety of

surfaces from grooves to a multi-pyramid type of the waffle plate. The gap at its

perimeter is set small to allow a high velocity but low of air. Inlet air temperature is

maintained at or near ambient.
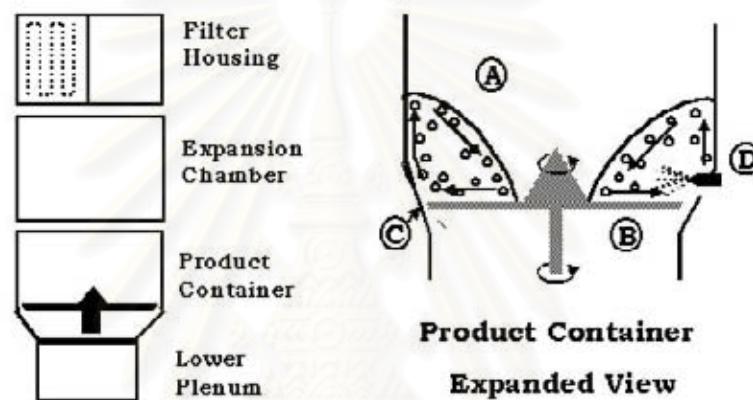
Figure 3.8 Tangential spray coater: (a) produce chamber; (b) variable speed disc

(c) disc gap or slit; (d) spray nozzle [16].

The process variables unique to the rotor system primarily involve disc slit

width, disc configuration, and rotation speed. The volume of the fluidization air is

controlled independently by adjust the slit width.

Different from the Wurster system, the rotary tangential spraying system has a

relatively wide application range, is the shortest machine in height of the three, and

allows nozzle access during processing. It has capability to produce high dose pellets

and apply coating for all types of release. Its primary disadvantage is that it exerts the

greatest mechanical stress of the three methods and, thus, is discouraged for use with friable substrates.

3.2.8 Problems in Film Coatings

Various problems occur during the coating process can be attributed to an improper coating formulation or processing condition. Some of problems are discus below.

1. Defective coatings

Defective coatings are caused by poor quality of the cores and/or inadequate formations, application or lack of process control.

2. Cracks in the film along edges

They are caused by too much internal stress, owing to differences in the thermal expansion of film and core. Cracks may also be result of swelling of the core during the coating operation.

3. Chipping

If the film does not adhere properly to the substrate surface, or its solid content too high, or it is too brittle foe want of plasticizer, this may lead to chipping. The problem can only be eliminated by total revision and optimization of the formulation for core and/or coating.

4. Blistering

If drying of spraying is performed at high speed, solvent may be retained in the film, which evaporates on post-drying and may then form blisters in the film. Normally this problem can be solved by lowering the air inlet temperature and

reducing the spray rate. Moreover, blister may also form between film and core if the adhesion of the film is inadequate.

5. Bridging

This is the phenomenon where the film fails to follow the contours of the core particles over break lines of engravings and settle in these without adherence of substrate.

6. Picking

If the film surface contains substances that are not molecularly dispersed and start to melt at the core bed temperature of the film-coating process (e.g. stearic acid, PEG) these substance may interfere with the film-forming polymer and produce holes in the film surface. This can be prevented either by replacing these substances or by lowering the core bed temperature.

Hole and defects in the film may be also be caused by too rapid spraying at too low a temperature. As a result, tablets stick together and tear off fragments of each other's film coating during drying.

7. Embedded particles

Particles broken off from the cores are embedded in the film during spraying. This may happen if the cores lack mechanical stability.

8. Dull surfaces

This happens most frequently if the droplets start to dry before reaching the cores. In this case they are too viscous to form a smooth film.

Improvement can be achieved by lowering the inlet air temperature and reducing the atomizing air quantity or pressure. Other remedial measures are additions of the substances that enhance film formation e.g. plasticizer or extra solvents.

9. Roughness

Roughness within the film is caused spray droplet. It may also be the result of porous cores, a very high concentration or relative molar mass of the film-forming pigments too large in number of size and excessive film thickness.

10. Orange Peel effect

The caused are too rapid drying or spraying, film layers that are too thick, or insufficient droplet coalescence. Orange peel may also form when small droplet dry before reaching the substrate surface or before they are able to coalesce.

Orange peel can be avoided by adjusting the spray rate and inlet temperature.

11. Twinning

The cores stick permanently together. Possible reasons are excessive spraying, a very tablet shape or very high bands.

3.3 Electrostatics

Electrostatics is that class of phenomena which is recognized by the presence of electrical charges, either stationary or moving, and the interaction of these charges, this interaction being solely by reason of the charges themselves and their position and not by reason of their motion.

3.3.1 Electrons, Protons, Neutrons, and Ions

Even at the risk of appearing too elementary, the fundamental particles of matter should be discussed. For these purposes these can be considered to be electrons, protons, and neutrons. There are others such as positrons, mesons, neutrinos, and perhaps even quarks; however, they appear and are important in fields such as high-

energy physics and nuclear physics but not in this study of electrostatics. The electron is in many processes the only important particles because it is small and relatively loosely tied to atom and molecules. It has a mass m_e of 9.1 x 10^{-31} kg and an electric charges q_e of -1.6 x 10^{-19} C. For our purposes, the electron is considered to be the smallest fundamental particle and the only one that has a negative charge.

The proton is another of the basic particles of which materials are composed. It has a positive charge q_p of 1.6 x 10^{-19} C and mass M_p of 1.7 x 10^{-27} kg. The nuclei of all atoms are made up of protons, and hydrogen, the least complex atom, is made up of a proton and an electron. Thus, the hydrogen atom is electrically neutral and has mass about the same as that of proton (since the electron mass is only 1/1837 that of the proton). A convenient source of protons is a stream of hydrogen atoms from which the electrons have been removed. These particles are also called hydrogen ions. Neutrons are the third fundamental particle. The neutron can be considered to be identical to the proton except that is electrically neutral. It has the same mass as the proton. A proton and a neutron combined form the nucleus of deuterium or heavy hydrogen, an important material in many nuclear reactors. A deuterium atom has one electron as does hydrogen.

A molecule is an electrically neutral combination of two or more atoms where the interatomic forces are strong. For example, a hydrogen molecule H_2 is made up of two atoms of hydrogen; a water molecule H_2O is two atoms of hydrogen and one of oxygen. If from any single molecule or atom, a positive ion is produced when remove one or more electrons. If extra electrons are added, a negative ion is produced. It should be noted that for many materials it is easier to produce negative ions and for others positive ions are more readily produced. Many other substances form positive or negative ions with about equal ease.

The term ion is come through its usage in electrochemistry, where it denotes the carriers of electrical current (moving charge particles) in conductive solutions. Here we make a distinction between ions and large charged particles-raindrops, for example. An ion is defined to be charged particle, either positive or negative, of atomic or molecular size. The ions may exist either in a liquid or in a gas and occasionally in a solid.

### 3.3.2 Interaction between Charges; Coulomb's Law

If a glass or ebonite rod is charged by rubbing, some of that charge may be transferred to another object, such as a light pith ball, by physical contact. By this procedure, one can, in a series of simple experiments diagrammed in figure 3.9, demonstrate that:

1. Like charge repel each other.

2. Unlike charge attract each other.

From these experiments two basic facts emerge. First, the electrostatic interaction-at-a-distance encountered so fat, the gravitational interaction; the latter is always attractive, the former may be attractive or repulsive. It is this sign reversal that hides the second important distinction; the electrostatic interaction is enormous compared to the gravitational. This tremendous difference can be appreciated from the following consideration. If two 1-kg spheres of aluminum are separated by 1 m, and if one electron from every billionth atom is transferred from one sphere to the other, leaving one negatively charged and the other positively charged, the force of attraction between the sphere will be more than 100,000 N, or more than ten thousand times the weight of each sphere. We are generally unaware of the great strength of

electrostatic forces because objects we encounter are nearly electrically neutral. They may contain a huge number of charges, but half of them will be positive, the other half negative and of equal magnitude, producing no net charge. Some small charge imbalance can be achieved and maintained. If the imbalance becomes too large, the object will discharge spontaneously, often with a great display of sparks.
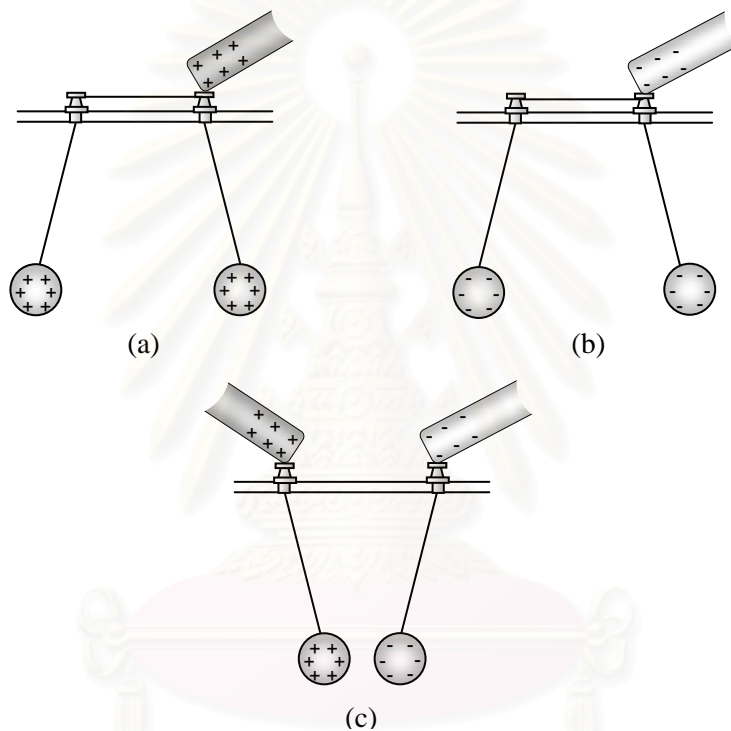
Figure 3.9 Two pith balls that have painted with aluminum paint are suspended by a metallic supports bar.

(a) and (b) Like charge

(c) Unlike charge

To probe electrostatic forces and deduce quantitative relationships, one needs a device for measuring charge. One of the earliest such instruments is the gold-leaf electroscope, shown in figure 3.10. It consists of a hollow cylinder in which a thin

gold leaf is attached at its upper end to a vertical metal rod. The rod is set in an insulating sleeve and passes out through the top of the chamber; the sides of the chamber are made of glass to permit viewing the disposition of the gold foil.

If, for example, a negative charge is deposited on the small brass sphere atop the metal rod, the many million excess electrons do not remain fixed there. They are able to move about within and on the surface of the metal, and since they repel each other, they will redistribute themselves so as keep out of each other's way as much as possible. Thus, some of that negative charge will appear on the gold leaf and metal rod; and since like charge repel, the flexible gold foil will diverge from the rod, the angle between them depending on the amount of charge deposited on the electroscope.
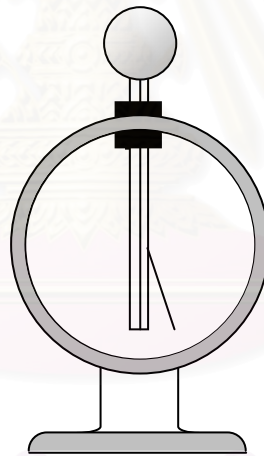
Figure 3.10 The gold leaf electroscope.

Although such instrument do not measure charge accurately, and have been replaced by more precise electronic meters, they are still used in lecture demonstrations.

The mathematical relation that governs the interaction between like and unlike charge was enunciated by Charles Coulomb in 1785. Coulomb measured the strength

of the forces as functions of the distance between the charges and their magnitudes, using a sensitive torsion balance of the sort employed by Cavendish. Coulomb concluded that the magnitude of the force between two charges in air is proportional to the product of the two charges, q_1 and q_2, and inversely proportional to the square of the distance between them. That is,

$$F = k \frac{q_1 q_2}{r^2} \tag{3.1}$$

where k is a constant. The direction of the force on the charges is along the line joining them. It is to be understood that a positive force in equation 3.1 implies repulsion, a negative, attraction. Since force is a vector quantity, the adjectives *positive* and *negative* are meaningless in any other context.

3.3.3 The Electric Field

The electric field $\mathbf{E_r}$, at the point identified by the position vector $\mathbf{r}$, is the force that a unit positive charge would experience if located at that point and if its placement did not alter the distribution of any charges in space.

In other words, E_r can be redefined as the electrostatic force per unit charge:

$$\mathbf{E_r} = \frac{\mathbf{F_{qr}}}{q} \tag{3.2}$$

where $\mathbf{F_{qr}}$ is the force that acts on a small charge q when placed at the point $\mathbf{r}$. Conversely, once $\mathbf{E}$ is know, the force acting on a charge q is given by

$$\boldsymbol{F}_q = q\boldsymbol{E} \tag{3.3}$$

If the force on a positive charge q is $\mathbf{F}$, the force acting on a negative charge of equal magnitude at the same point will be $-\mathbf{F}$. The usefulness of the field concept is

precisely that **E** fully characterizes the force on any charge throughout the region in which the field is known

3.3.4 Electric Field Lines

A very useful concept for visual representation of an electric field configuration is that of *electric field lines,* or lines of force. A precise graphic representation of an electric field requires drawing a vector of proper length and direction at every point of space, and such a map would be messy, to say the least. For example, the field map in two dimensions, of the field due to a single positive point charge would look somewhat like figure 3.11. A much simpler visualization is afforded by drawing a group of lines that obey the following conditions:

1. The lines are directed, pointing away from positive and toward negative charges, so that at any point, the tangent to a line is along the direction of the electric field at that point.

2. The number of lines that are drawn emerging from or terminating on a charge is proportional to the magnitude of the charge.

In drawing the field pattern, a few elementary rules are helpful.

1. Every field line must originate at a positive charge ad terminate on a negative charge.

A corollary of the above is the requirement that in a charge-free region the field lines must be continuous.

2. In the immediate vicinity of a point charge, the field lines are radially directed.

3. Field lines do not intersect in a charge-free region.

The last of these rules reflects the fact that the electric field vector is unique at every point in space. If two field lines did intersect, this would mean that at the point of intersection there are two equally valid directions (and possibly magnitudes) of the **E** vector and, therefore, of the net force acting on a small test charge.

(a)   (b)
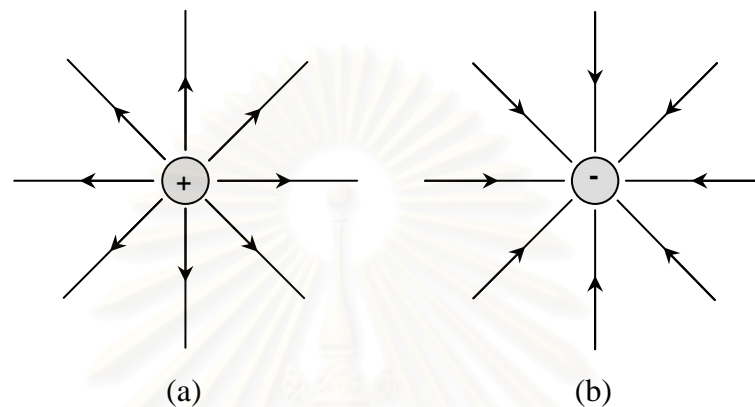
Figure 3.11 Electric field lines.

3.3.5 Principles of Charging Particles

In the following section, different electrostatic charging mechanism will be discussed.

Corona charging

The charging of particles by ions from a corona discharge was investigate in the 19th century and led to the development of the electrostatic precipitator. During corona discharge mono-polar ions migrate rapidly outwards from a source, such as the region around a sharp point, due to the Coulombic force of the intense electric field. Any particles moving through such an ion-rich region perturb the local field, effectively intensifying the field at the particles surface, in proportion to the permittivity of the particle. Ions are directed by this intensified field to the particle surface and thus charge it. Random ionic motion may be ignored under many field-

charging conditions. Field charging is considerably more efficient than charging by ion diffusion alone.

Triboelectric charging

When two dissimilar particles rub against each other, there is a transfer of electrons (charges) from the surface of one particle to the other until the potentials of the metals are aligned. This results in one of the particles being positively charged and the other being negatively charged.

Many researchers working in the field of triboelectricity have set up a "triboelectric series" similar to the "electrochemical potential series" for the metals. There is some agreement on the locations of some materials, but most of the series are very dissimilar, eve when the same materials are used. The data on individual materials used are apparently not reproducible. This is undoubtedly owing to the complexity of the surfaces of the materials themselves and also to the treatment of the surfaces in the many processes necessary for manufacture and handling. A typical triboelectric series, presented in table 3.3, serves only as an example.

Table 3.3 Atypical triboelectric series

Rabbit's fur	Cotton
Lucite	Wood
Bakelite	Amber
Cellulose acetatate	Resins
Glass	Metals
Quartz	Polystryrene
Mica	Polyethylene
Wool	Teflon
Cat's fur	Cellulose nitrate
Silk	

It is certain that this series order will only be reproducible in rare instance. Conditions such as cleanliness and humidity affect the series drastically. The materials at the top of the list are positive with respect to those lower in the list.

<u>Induction Charging</u>

Charge can be conducted to ground or from ground onto a conductor. Consider, for instance, the situation shown in the sequence of figure 3.12 (a), (b), and (c). When the positively charged glass rod is brought close to the metal sphere, which has been connected to ground by a conducting wire, negative charge electrons, are attracted toward the positively charged glass and flow from ground to the surface of the sphere. If connect the wire from the sphere without moving the less rod, whatever charge has been drawn to the sphere from ground is trapped and will remain on the sphere even after the glass rod has been withdrawn.

This method of charging a conducting object is called charging by induction. The charge is induced on the conductor by the proximity of another charged object, not transferred to it directly as in charging by conduction by conduction. Note that when a conductor is charged by induction, its charge is of a sign opposite to that on the charging object. Note also the convenience of charging by induction; the charging objected of its charge, and the process can be repeated innumerable times without the need of renewed electrification by friction, that is, rubbing with silk cloth.
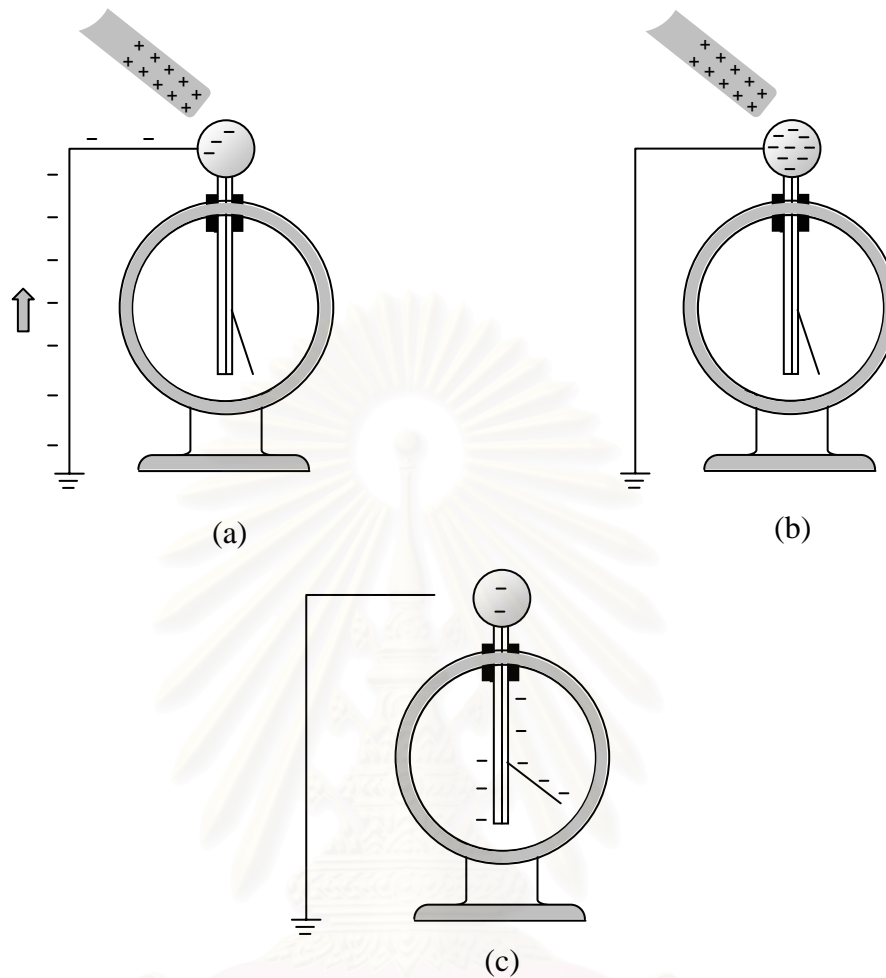
Figure 3.12 Charging by induction.

(a) The electroscope is connected to ground. As the glass rod is brought near the metal sphere, negative charges are attracted to the sphere from the ground.

(b) The ground connection is removed while the glass rod is kept in position.

(c) If the glass rod is then withdrawn, the negative charge on the electroscope, which redistributes itself over this region, causes a deflection of the gold leaf, showing that there is a net charge on the instrument.

CHAPTER 4

EXPERIMENTAL PROCEDURE

4.1 Materials

1. Core particles   - Glass beads (average size 590 and 1,033 µm)

2. Film former   - Metochel E5 (hydroxypropyl methylcellulose, HPMC)

3. Plasticizer   - Polyethylene glycol 6000

4. Colorant   - Yellow sunset lake

5. Solvent   - Distilled water

6. Others   - Grease

                     - Glass slide

4.2 Equipments

The experiment setup used in this work is shown in Figure 4.1. At the upper section of the fluidized bed coater which is made of acrylic (Ekasilp Bangkok Co., Ltd.), equipped with bag filter (made from polyester 25 µm, Golden Fitech Cooperation Co., Ltd.) to prevent entrainment of particles, whose sizes are very fine. The fluidizing air was drawn from the blower (model DBR-010-1A, Paisan Machinery) and heated by heated coil (model PMB075U240 and PMB150U240, Utility Electric Co., Ltd.) which is located at the bottom of air distributor. The thermocouple (model JB-10 type CA (k), Sang Chai Meter Co., Ltd.) and the temperature controller (model Digicon type DD-6, Sang Chai Meter Co., Ltd.) are used to control the fluidizing air temperature in the range studied.
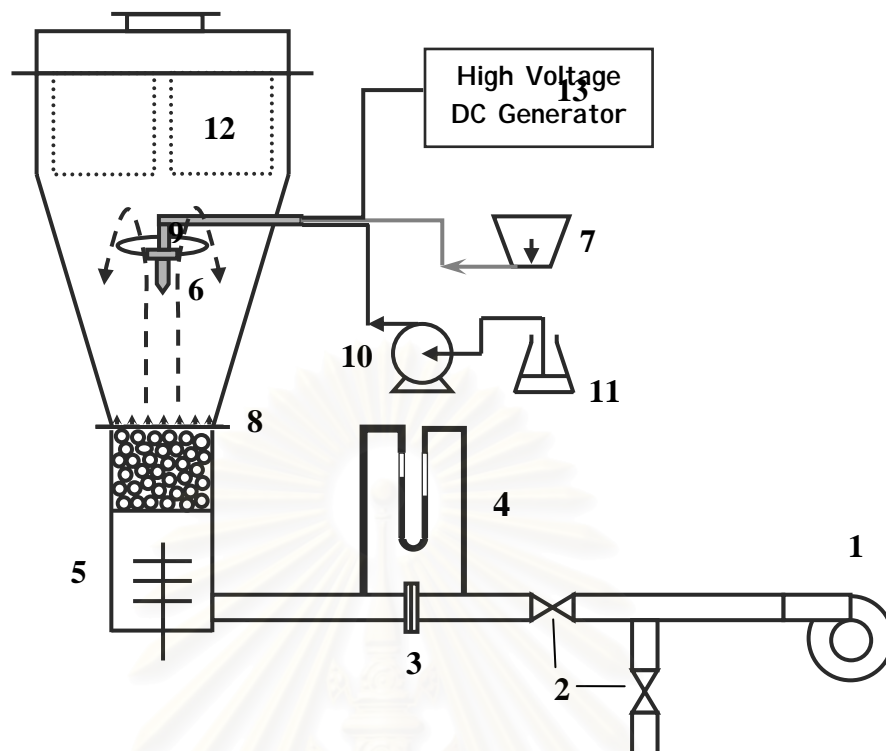
Figure 4.1 Schematic diagram of the fluidizing bed coater develop in this work

1) Blower 2) Ball Valve 3) Orifice plate 4) Manometer 5) Heater 6) Nozzle

7) Air compressor 8) Distributor 9) Fluidized bed Chamber 10) Peristaltic pump

11) Coating solution 12) Bag filter 13) High Voltage DC Generator

Nozzle

The nozzle used in this work is binary nozzle made from stainless steel (model Wide-Angle round spray, Pawin Engineering Co., Ltd.), body type 1/8J equips with fluid cab No. 40100 and air cap No. 120. The nozzle is held up by PVC tube to fit the nozzle at the center of the column. The spray is directed downwards from the nozzle to the core particles. Atomizing air is supplied to the nozzle by air compressor (model SVP-202, Swan Pneumatic Corporation Ltd.,)

High voltage DC generator

The high voltage DC generator circuit, figure 4.2, used in this work is simply set up. Alternating electric current is passed through variac (model TBS-10M, Yokoyama Electric Works, Co., Ltd.) which used to control the input electrical potential. The controlled electric current is increased to high potential by neon transformer (model 909, Scharoensap Electric Co., Ltd.) after leaving the variac. High voltage diodes (model X100FF5, Voltage Multiplier Inc.) which connected to bridge pattern are used to convert alternating current to direct current.
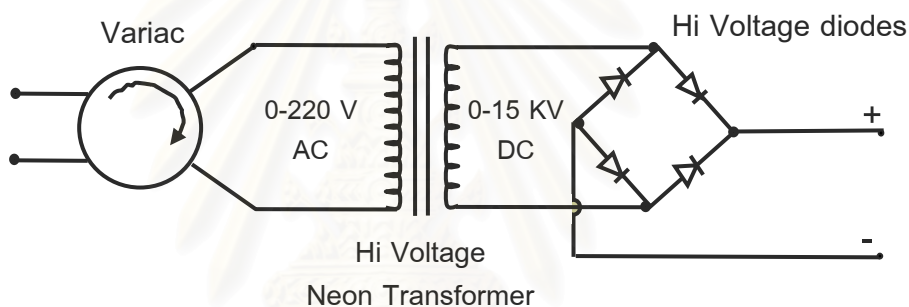
Figure 4.2 Schematic diagram of high voltage DC generator circuit

Hot Plate & Magnetic Stirrer

The hot plate & magnetic stirrer (model Fish Erband, Fisher Scientific, USA.) is used to prepare coating solution and to stir continuous the solution while feeding solution to the nozzle.

Peristaltic Pump

The peristaltic pump (model 7554-95, Cole-Parmer Instrument Co., Ltd.), figure 4.3 is used to feed coating solution to the nozzle combined with a MasterFlex L/S drive to control constant flow rate. The high performance precision tubing, series

number 6429 model L/S 15, is selected to transport solution. Additionally, interrupter timer (model H3CR, Omron Corporation, Japan) is used to control pulse spraying.

Figure 4.3 Peristaltic pump

4.3 Experimental Conditions

This work study affect of process variables e.g. fluidizing air velocity, coating solution flow rate, core particle size and applied potentials to physical properties of coated particle such as film thickness, packed bulk density, coating efficiency and surface morphology by using other equipment.

Fluidizing Air Velocity

The range of fluidizing air velocity was selected from trial and error by selected in the range that core particles can be fluidized. However, in order to prevent the particles strike the bag filter on the top of column, the fluidizing air velocity was not more than. Thus, the range of fluidizing air velocity in this study was 2.2, 2.9, 3.6 and 4.3 m/s respectively.

Flow Rate of Coating Agent

Minimum flow rate of coating agent adjusted by the peristaltic pump in this work is 10 ml/min. If the flow rate of coating agent is too much, the core particle will agglomerate to large particle and cannot fluidize. In order to prevent the agglomeration, the range of coating agent flow rate in this study was 10, 15 and 20 ml/min

Core Particle Size

For purpose of comparison with the average size of glass beads that used as core particles in this study, the difference sizes of glass beads are 590 and 1033 µm.

Applied Electrical Potential

The voltage applied to the nozzle were -1 and -4 kV due to the high voltage diodes which used to bridge connection in the circuit cannot apply the potential higher than -5 kV. Moreover, electrostatic coating in various industry applied voltage at least -3 kV to charge the droplet so the highest voltage applied to the nozzle in this work was -4 kV.

The other conditions in this work were fixed:

- film coating is hydroxpropyl methylcellulose

- concentration of film coating is 5 % w/v

- solvent is distilled water amount 150 ml

- duration to spray coating agent is on 7 s. and off 20 s.

- drying time in fluidized bed after the coating process about 10 minutes

- height of spray nozzle from air distributor is 20 cm.

4.4 Experimental procedure

4.4.1 Preparation of Coating Solution

The composition of coating solution is present in table 4.1

Table 4.1 Composition of coating solution

Ingredients	%w/v
Polymer (Methocel E5, hydroxypropyl methylcellulose, HPMC)	5
Plasticizer (polyethylene glycol 6000)	1.6
Lake (yellow sunset lake)	0.6
Distilled water	92.8

- Dissolve plasticizer and lake in distilled water (about half of total amount coating solution, 75 millimeters)

- The solution was heated to 60 ^{o}C and stirred until the solution is homogeneously.

- Added the polymer into the solution.

- The solution should be moderate agitation during mix the solution and heated the solution to 70 ^{o}C.

- When HPMC dissolve ready, cold distilled water is added to produce the required volume.

- A clear solution is obtained after cooling within a day on standing room temperature.
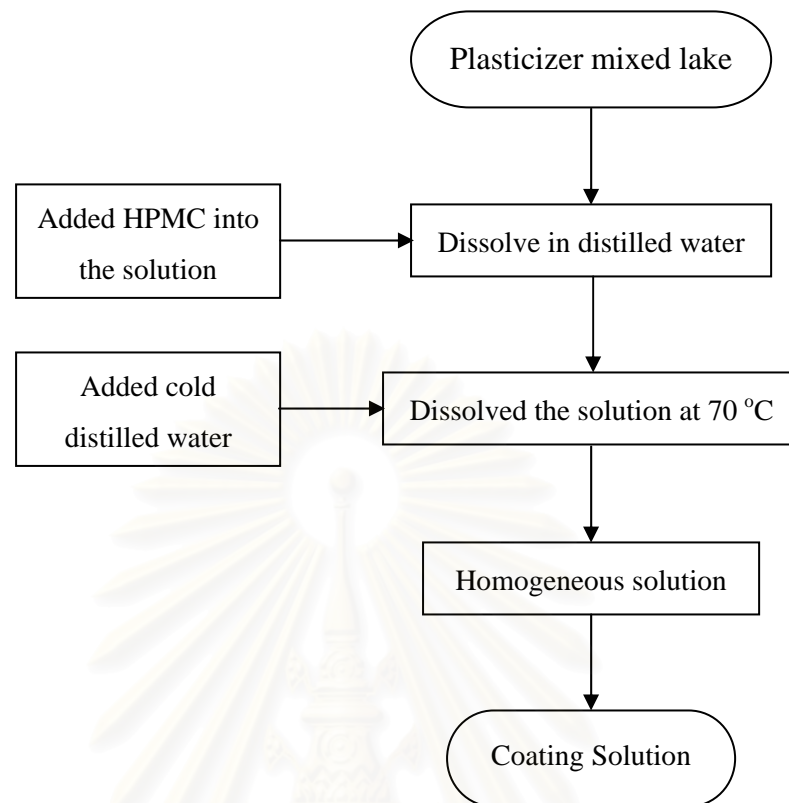
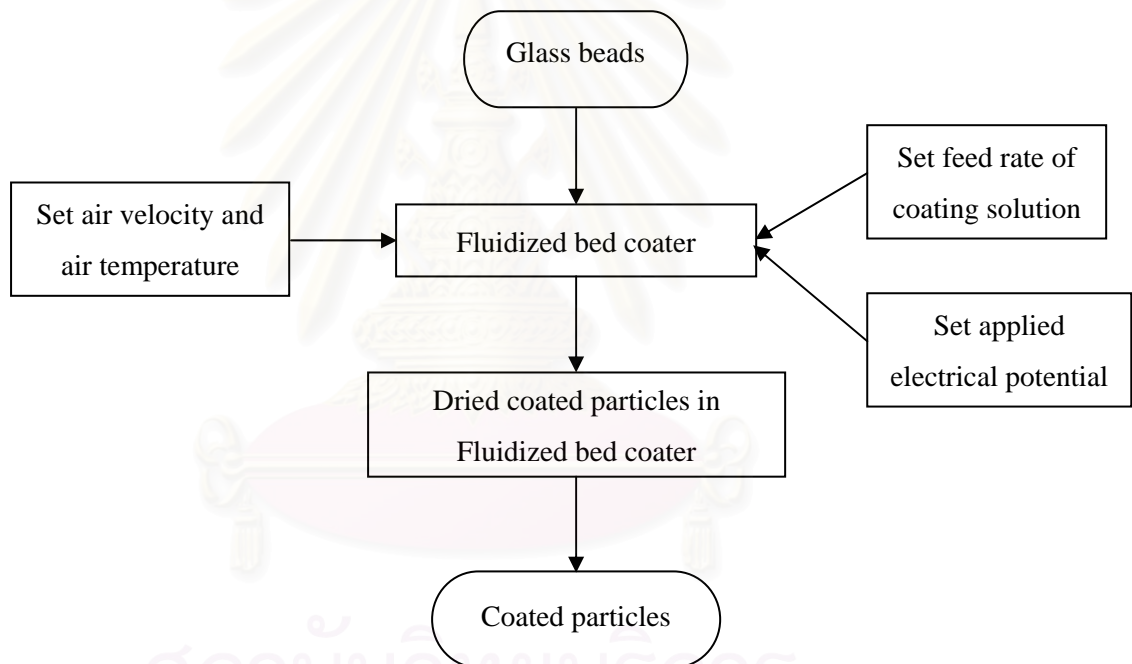**Figure 4.4 Flowchart of preparation of coating solution**

4.4.2 Preparation of Coated Particles.

- Glass beads 180 grams were transferred into the fluidized bed coater.

- Turned on the switch of air blower and controlled constant fluidizing air velocity at set point.

- Turned on the switch of temperature controller and set fluidizing air temperature at 70 °C.

- Turned on the peristaltic pump and set feed rate of the coating solution to the nozzle.

- Turned on the air compressor and opened pressure valve at 2 bar.

- When the air temperature and velocity moved to set point set the interrupter timer that is sprayed coating solution for on 7 seconds and stopped 20 seconds. The coating solution was fed until all of coating solution is used up.

- After the coating process, the coated particles were dried in coater chamber at the same temperature and air flow about 10 minutes.

Remark During the coating operation, the coating solution was stirred continuously to prevent sedimentation of the insoluble particles.

Figure 4.5 Flowchart of preparation of coated particles

4.4.3 Characterization of Coated Particles

After the coating experiments, the coated particles were screened using two sieve screens with different in aperture sizes, e.g. 600 and 1,180 μm, on a vibration shaker (Ratch, Type Vibro, West-Germany) to remove portion of the coated particles

that formed agglomerates. The coated particles were then placed in a hot-air oven (model UM400, Memmert, Germany) over a night to reduce the moisture content in the product. The coated particles were characterized for the following properties: the percentage of coating efficiency, the coating film thickness, the percentage of growth rate, the packed bulk density and the surface morphology.

Coating Efficiency

To determine the coating efficiency of the developing process, the weights of coated particles (after the coating experiment) and uncoated particles (before the coating experiment) were determined using 4-digits analytical balance. The coating efficiency is then calculated by using the following formula:

Coating efficiency

$$= \frac{\text{weight of coated particles} - \text{weight of uncoated particles}}{\text{total weight of coating material input (water-free)}} \times 100$$

Film Thickness

To measure the film thickness of coated particles, the SLR camera (Panasonic,WV-CP240/G) equipped with an optical microscope (model CX31, Olympus) was used to capture images of coated particles which were preliminary washed in boiling water. The average diameter of coated particles, about 30 particles, was determined in triplicate and the results averaged by the picture analysis method, using a picture analyzing package (Image Pro V. 3.0). The film thickness of coated particles can be calculated by using the following equation:

Film thickness

$$= \frac{\text{averaged diameter of coated particle} - \text{averaged diameter of uncoated particle}}{2}$$

Growth Ratio

The growth ratio of coated particles is given by the following equation

$$= \frac{\text{average diameter of coated particle} - \text{average diameter of uncoated particle}}{\text{average diameter of uncoated particle}} \times 100$$

Packed Bulk Density

The packed bulk density of coated particles was measured by using the Powder Characteristic Tester (model PT-N, Hosokava Micron). Each sample was determined in triplicate and the results averaged.

Morphology

The shape and the surface characteristics of the coated particles were observed using scanning electron microscope (SEM, model JSM-S400 JEOL). Before the SEM observation, the particle samples were coated with gold using an ion sputter coater under vacuum conditions.

CHAPTER V

RESULTS AND DISCUSSION

Operating variables which exhibit effects on the properties of coated particles are summarized in table 5.1. Two glass beads of which average sizes are 590 and 1,033 μm are used as core particles in the experiments. The coating agent is a mixture of Polyethylene glycol and Methocel E5 Hydroxypropyl methycellulose (HPMC) with distilled water (conc. was fixed 5%). After coating, the coated particles are characterized to get information of evaluating film thickness, packed bulk density, coating efficiency and morphology. These effects will be reported and discussed later by using the experimental data obtained in this work.

Table 5.1 Operating conditions

Parameter	U (m/s)	Q_L (ml/min)	E (kV)	d_{P0} (μm)
Fluidizing air velocity	2.2 2.9 3.6 4.3	20	0	590 1,033
Coating agent flow rate	2.9	10 15 20	0	590 1,033
Electrostaticity	2.2 4.3	10 20	0 -1 -4	590 1,033

where   U   =   Fluidizing air velocity (m/s)

             Q_L =   Coating agent flow rate (ml/min)

             E   =   Applied electrical potential (kV)

             d_{po} =   Core particle size (μm)

5.1 Influence of Fluidizing Air Velocity

To study the influence of fluidizing air velocity on the coating efficiency, the fluidizing air velocity was varied between 2.2 and 4.3 m/s while the coating agent flow rate was kept constant at 20 ml/min. The efficiency of glass bead core particles with nominal size of 590 and 1,033 µm are illustrated in figure 5.1. The efficiency dropped from 73 to 55% and 65 to 55%, for the core particles of 590 and 1,033 µm respectively when the fluidizing air velocity was increase from 2.2 to 4.3 m/s. It is also observed that in the vessel wall and filter bag there was depositing of small particles of coating agent which is solodified by evaporating of its solvent. It is reasonable to consider that the evaporation rate of the solvent in the coating agent was increased due to the increase in the fluidizing air velocity. The coating agent droplets turned to solid particles and were entrained away from the coating zone to filter bags by the fluidizing air before contacting and spreading on the surface of core particles. Moreover, higher fluidizing air velocity is the cause of film attrition. Therefore the coating efficiency was hindered. Such result could also be confirmed by data of film thickness and growth ratio of coating film as shown in figure 5.2 and 5.3, respectively.

Comparison between 590 and 1,033 µm core beads could result in an understanding that smaller particles could be coated with higher coating efficiency. This could be explained by the fact that smaller particles capture more binder than larger particles because of their greater specific area and higher possibility of contact with droplets in atomizing zone. This is in and agreement with the result of K. Saleh et al. [9] who proposed a following the linear correlation to reveal the coating efficiency with particle specific area.

$$\eta = 0.00080 a_p + 53 \qquad (60,000 > a_p > 9,000 \text{ m}^2/\text{m}^3) \qquad (5.1)$$

where

$$a_p = \frac{6}{d_p} \qquad (5.2)$$

when η :   coating efficiency (%)

     a_p :   specific surface area (m^2/m^3)

     d_p :   particle diameter (m)

Based on the above mentioned equations, while a higher coating efficiency would be aspected but due to their greater specific area, the thinner coating film would oppositely be expected when smaller core particles were employed. Therefore, as a consequence, under the same condition, the growth ratio of the coating film of smaller core particles would be lower than that of larger particles.

On the contrary, figure 5.4 presented the effect of fluidizing air velocity on the packed bulk density of coated particles. The packed bulk density of coated particles was increased by increasing fluidizing air velocity. It is known that the density of HPMC which is employed as the coating agent (1.037 g/cm^3) is lower than that of glass beads (2.562 g/cm^3). Hence, a decrease in the coating film thickness due to the increasing air velocity would lead to the lower bulk density of the coated particles.

The morphology of the oroginal glass beads and the coated one was qualitatively examined by using a scanning electron microscope at different magnifications as illustrated in figure 5.5, 5.6 and 5.7. The uncoated particles exhibit smooth surface and spherical shape. The SEM micrographs of coated particles after coating by varying fluidizing air velocity exhibit remarkably rough surface. In order

to evaluate the surface roughness of the coated particles, the fractal geometry obtained by analysis microscopic images using image processing software is taken into account. Also visual observation of the surface of the coated particles reveals that the surfaces of the coated particles are more irregular. With the fractal analysis it is found that before coating the fractal dimension of glass bead perimeter is 0.947 but after coating the fractal dimension of the coated particle perimeter is increased to 1.01.
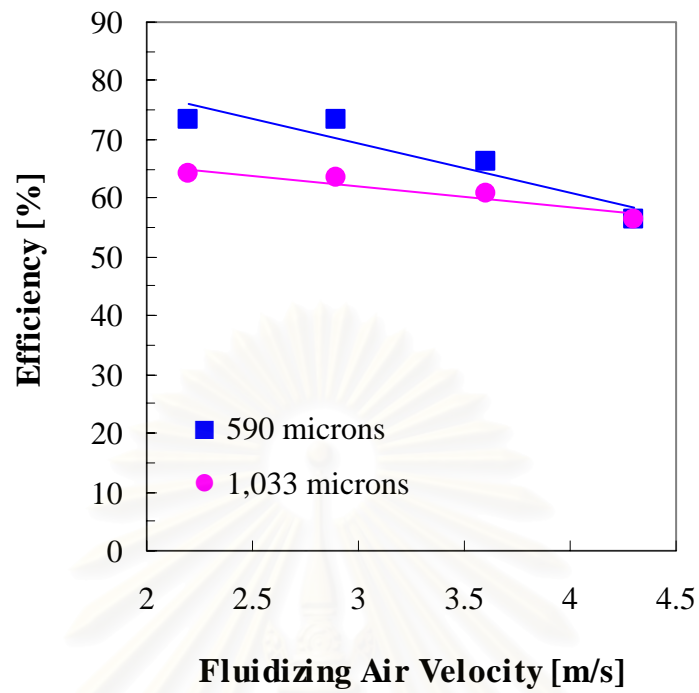
Figure 5.1 Effect of fluidizing air velocity on the coating efficiency
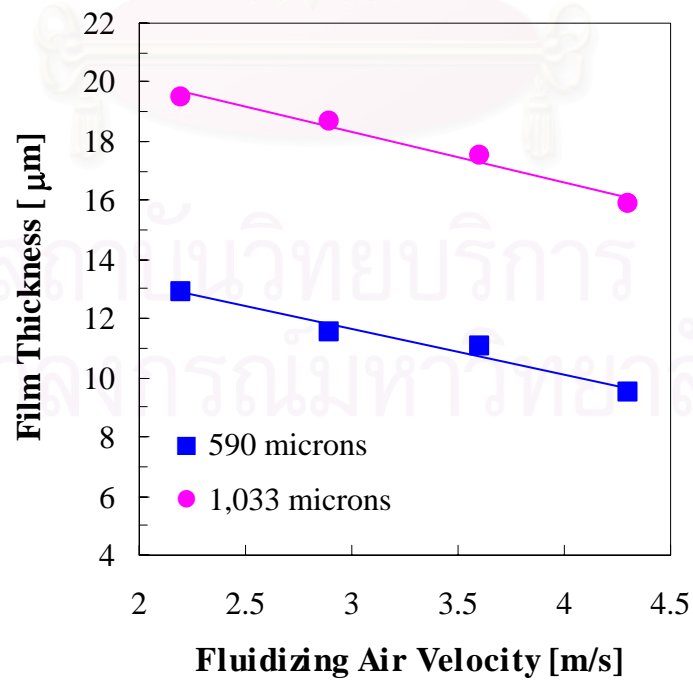
Figure 5.2 Effect of fluidizing air velocity on the film coated thickness
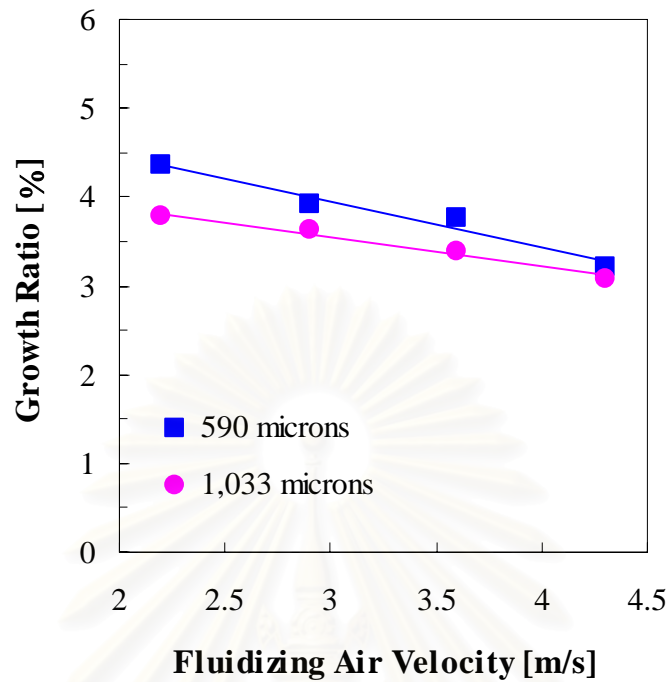
Figure 5.3 Effect of fluidizing air velocity on the growth ratio of coating film
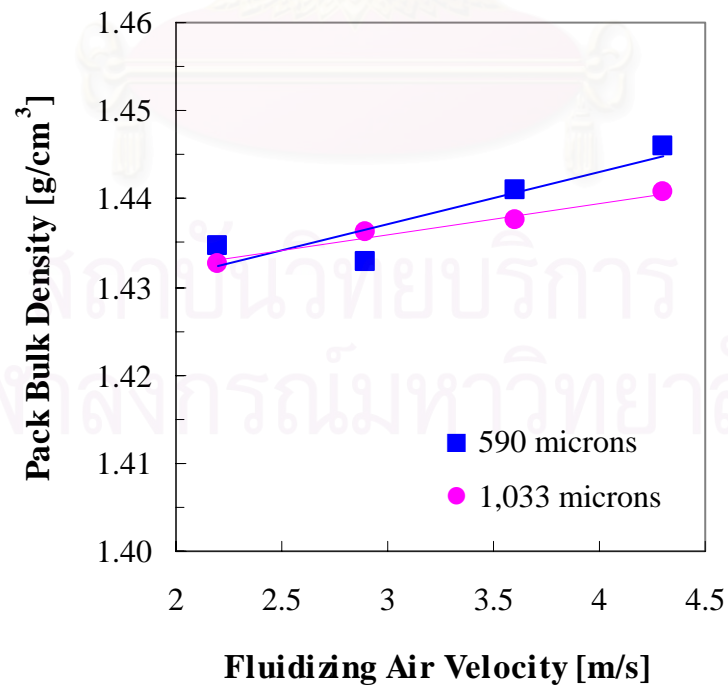
Figure 5.4 Effect of fluidizing air velocity on the packed bulk density
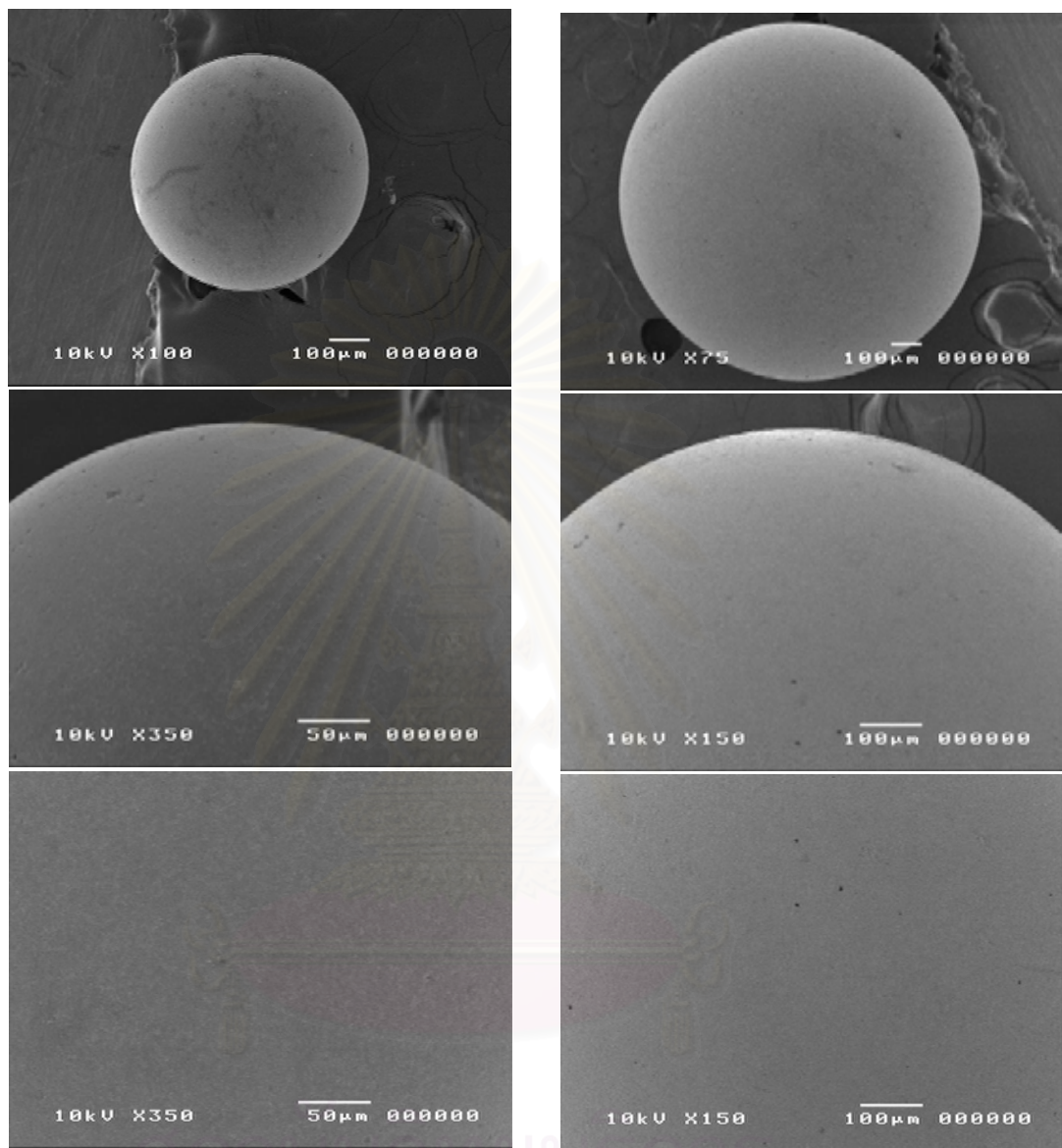
Figure 5.5 SEM micrographs of initial glass beads. (a), smaller size (590 μm) at

the magnification of 100 and 350. (b), larger size (1,033 μm) at the magnification
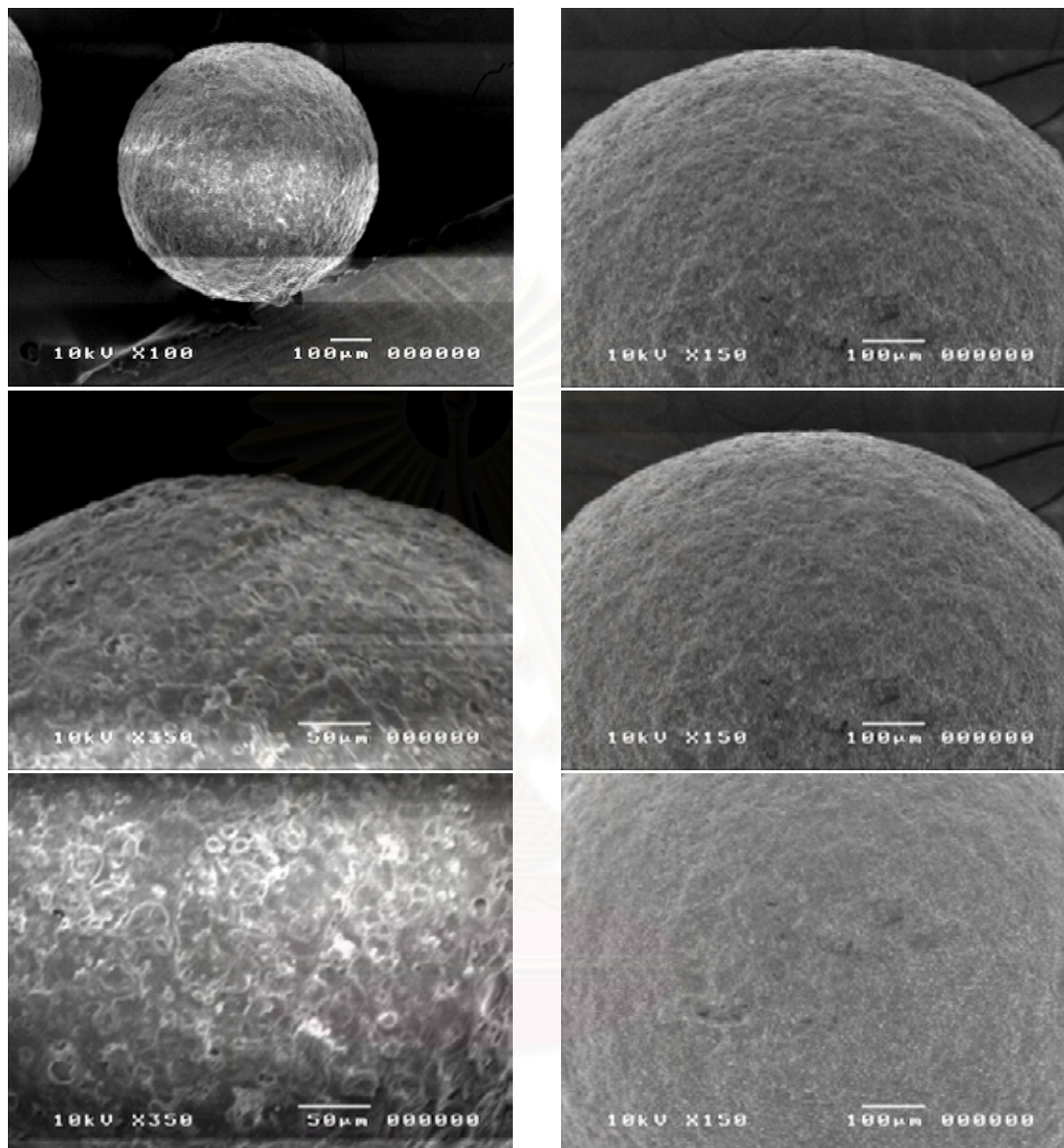
of 75 and 150

(a)   (b)

Figure 5.6 SEM micrographs of particle coated at liquid flow rate of 20 ml/min

and 2.2 m/s fluidizing air velocity. (a), smaller size of 590 μm at magnification of

100 and 350. (b), larger size of 1,033 μm at magnification of 75 and 150.
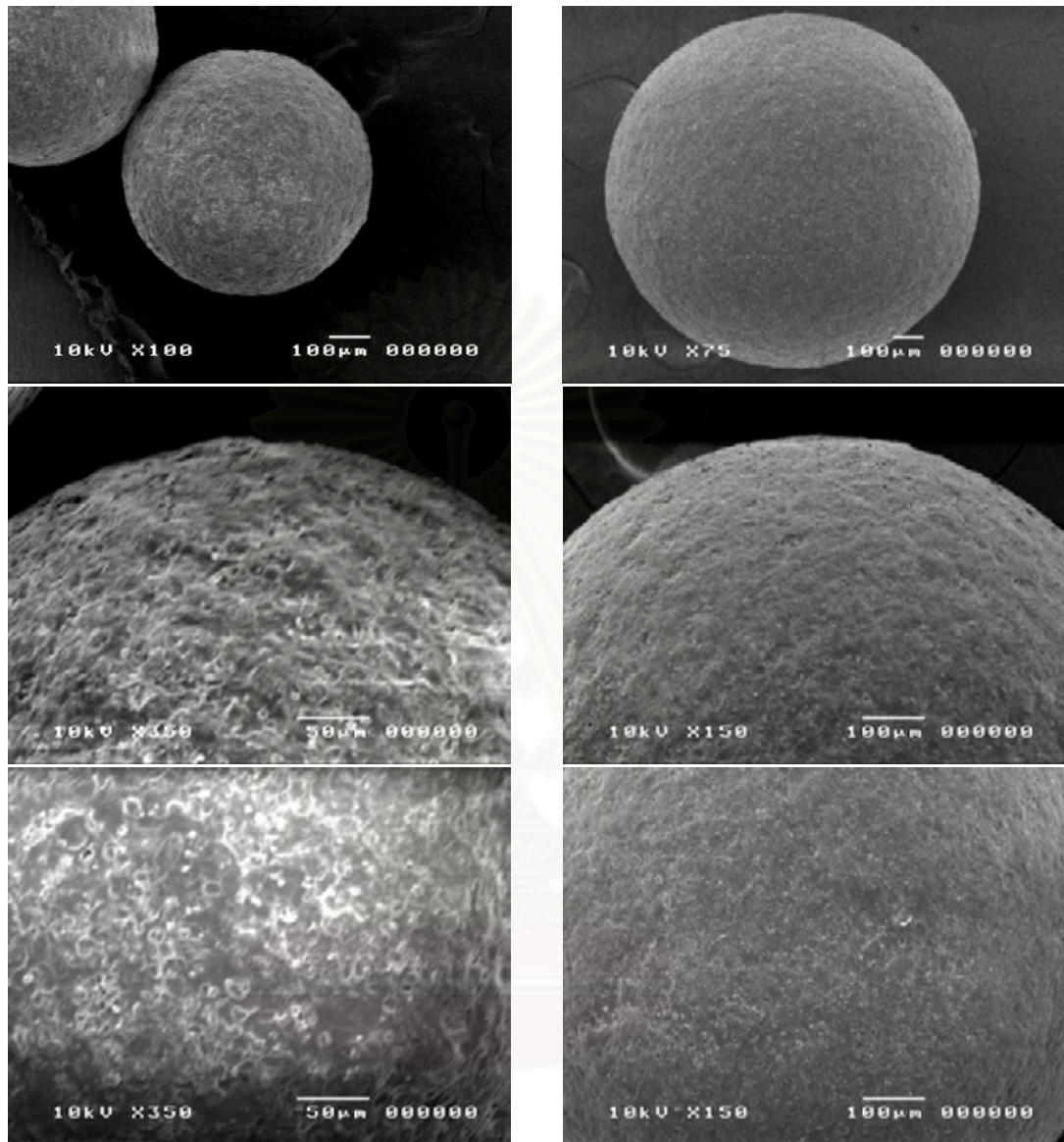
(a)   (b)

Figure 5.7 SEM micrographs of particle coated at liquid flow rate of 20 ml/min

and 4.3 m/s fluidizing air velocity. (a), smaller size of 590 μm at magnification of

100 and 350. (b), larger size of 1,033 μm at magnification of 75 and 150.

5.2 Influence of Coating Agent Flow Rate

The coating agent flow rate was varied between 10 and 20 ml/min at a constant atomizing air pressure and a fluidizing air velocity of 2 bar and 2.9 m/s, respectively. The effects of the liquid flow rate on the coating efficiency are shown in figure 5.8. For core particles of either 590 or 1,033 μm the coating efficiency becomes higher when liquid flow rate is increased. Maximum coating efficiency of about 73 and 63 % for the core particles of 590 and 1,033 μm, respectively, can be obtained at the liquid flow rate of 20 ml/min. Meanwhile effects of the liquid flow rate on the film thickness and growth ratio of the coating film are illustrated in figure 5.9 and 5.10, respectively.

Regarding to K. Dewettinck et al. [7], it could be implied that an increase in the liquid flow rate at constant atomized air pressure could result in larger droplet. K. Dewettinck et al. has purposed an equation which explains the droplet size dependence on the flow rate (equation 5.3)

$$D_d = \frac{585 \times 10^3 \sqrt[3]{\sigma}}{v_{REL}\sqrt{\rho}} + 597\left(\frac{\mu}{\sqrt{\sigma\rho}}\right)^{0.45}\left(\frac{1,000 U_{sol}}{U_{at}}\right)^{1.5} \tag{5.3}$$

when: σ = fluid surface tension (N/m)

ρ = fluid density (kg/m^3)

μ = fluid viscosity (mPa/s)

U_{sol} = fluid volumetric flow rate (m^3/s)

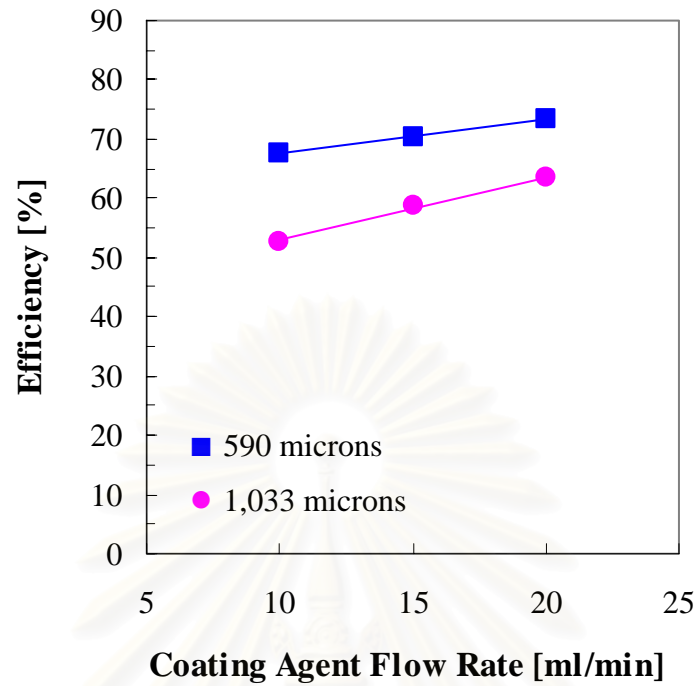U_{at} = air volumetric flow rate (m^3/s)

Figure 5.8 Effect of coating agent flow rate on the coating efficiency
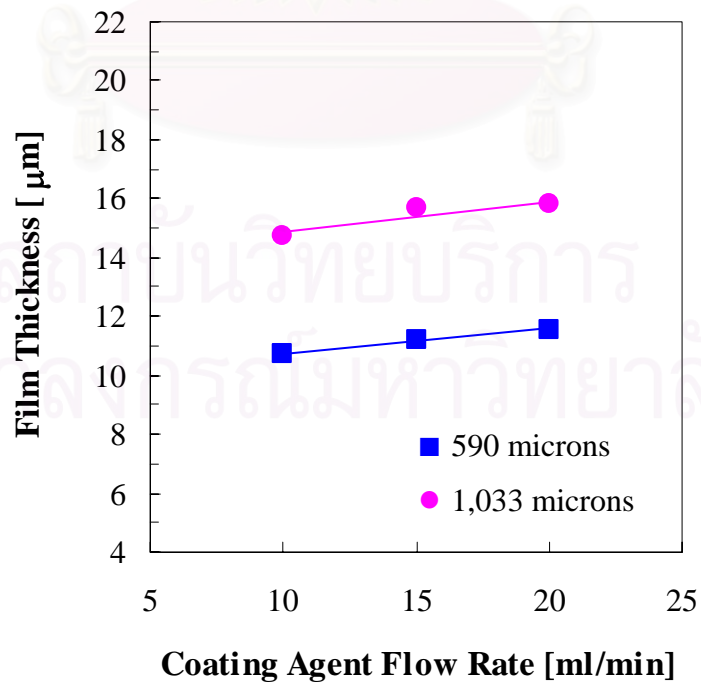

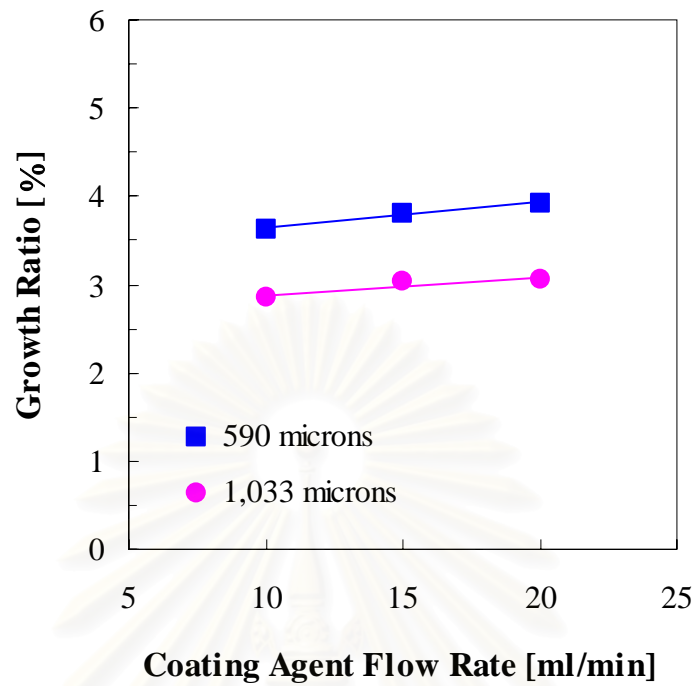**Figure 5.9 Effect of coating agent flow rate on the film thickness**

Figure 5.10 Effect of coating agent flow rate on the growth ratio of coating film
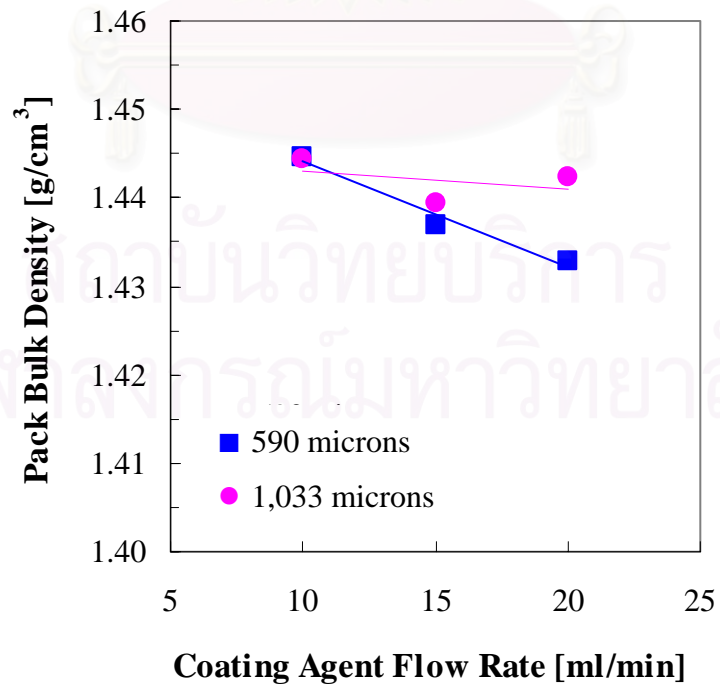

Figure 5.11 Effect of coating agent flow rate on the packed bulk density

Meanwhile larger droplet size resulting in less premature droplet evaporation before particle-droplet contact due to its smaller specific surface area leading to higher coating efficiency. It is known that higher spraying rate could result in the formation of larger droplets and a lower fluid-bed temperature. Therefore it is reasonable that the increased flow rate of coating agent could give rise to a higher deposition coating mass. Consequently, thicker coating film could also be obtained with the increased rate of spreading. It should be further noted that at constant flow rate of coating agent with larger core particles, thicker coating film is obtained as shown in figure 5.9 due to their lower specific surface area. This result is consistent with the previous reported result shown in figure 5.2. Effect of coating agent flow rate on the growth ratio of coating film is in good agreement with the previously described results as shown in figure 5.10.

Figure 5.11 also illustrates the effect of coating agent flow rate on the packed bulk density of the coated particles. It is found that the increased coating agent flow rate could result in the reducing packed bulk density due to higher mass fraction of coating film on the coated particles. From experiment, it could be observed that weight of particles after coating process increases with declining rate when the coating agent flow rate is increased.

Micrographs of coated particles obtained under conditions of various liquid flow rates are introduced in figure 5.12-5.13. It is found that after coating the surface of coated particles were rougher than glass beads but it morphology is still sphere.

(a)   (b)
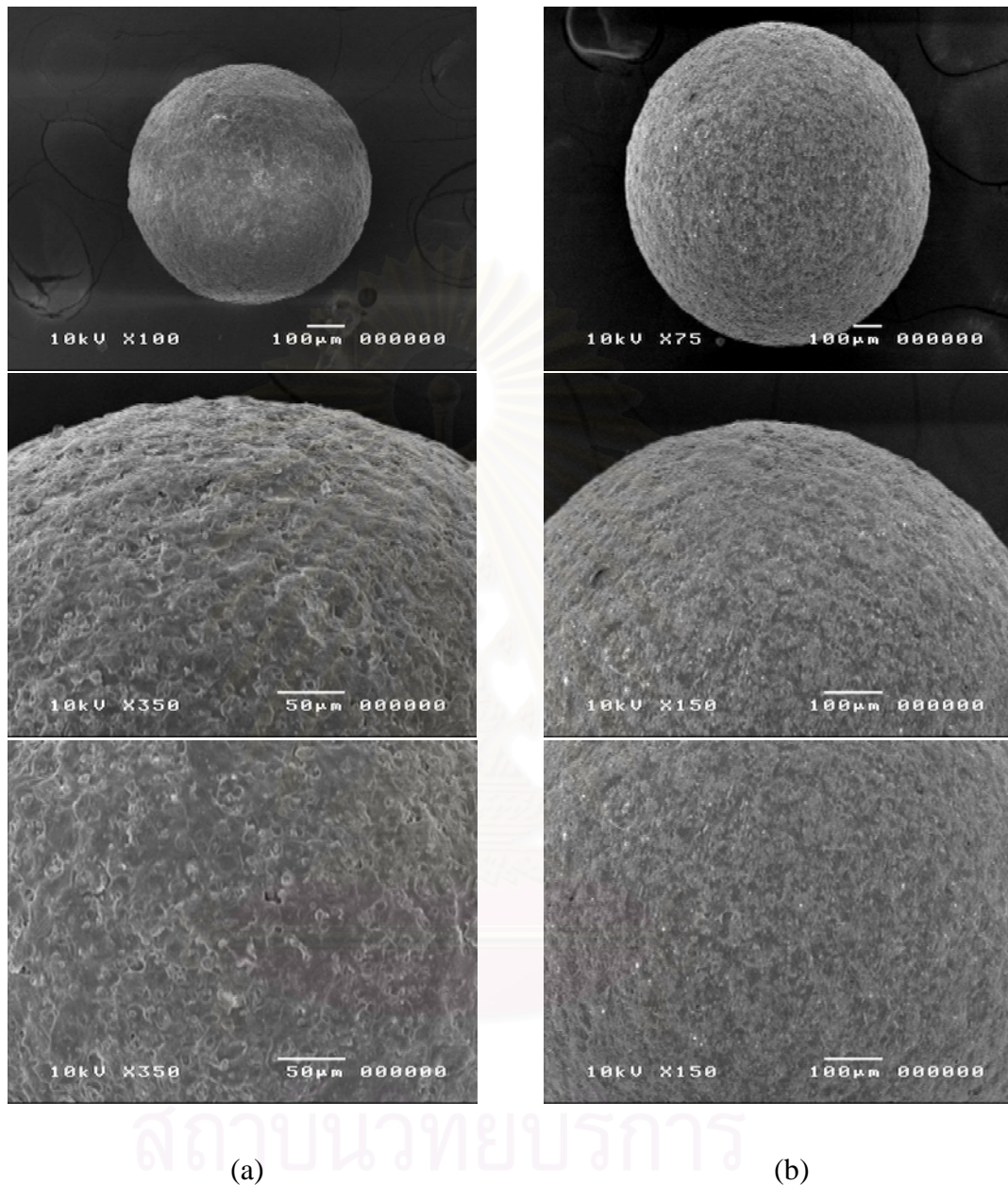
Figure 5.12 SEM micrographs of particle coated at fluidizing air velocity of 2.9 m/s and liquid flow rate 10 ml/min. (a), smaller size of 590 μm at magnification of 100 and 350. (b), larger size of 1,033 μm at magnification of 75 and 150.
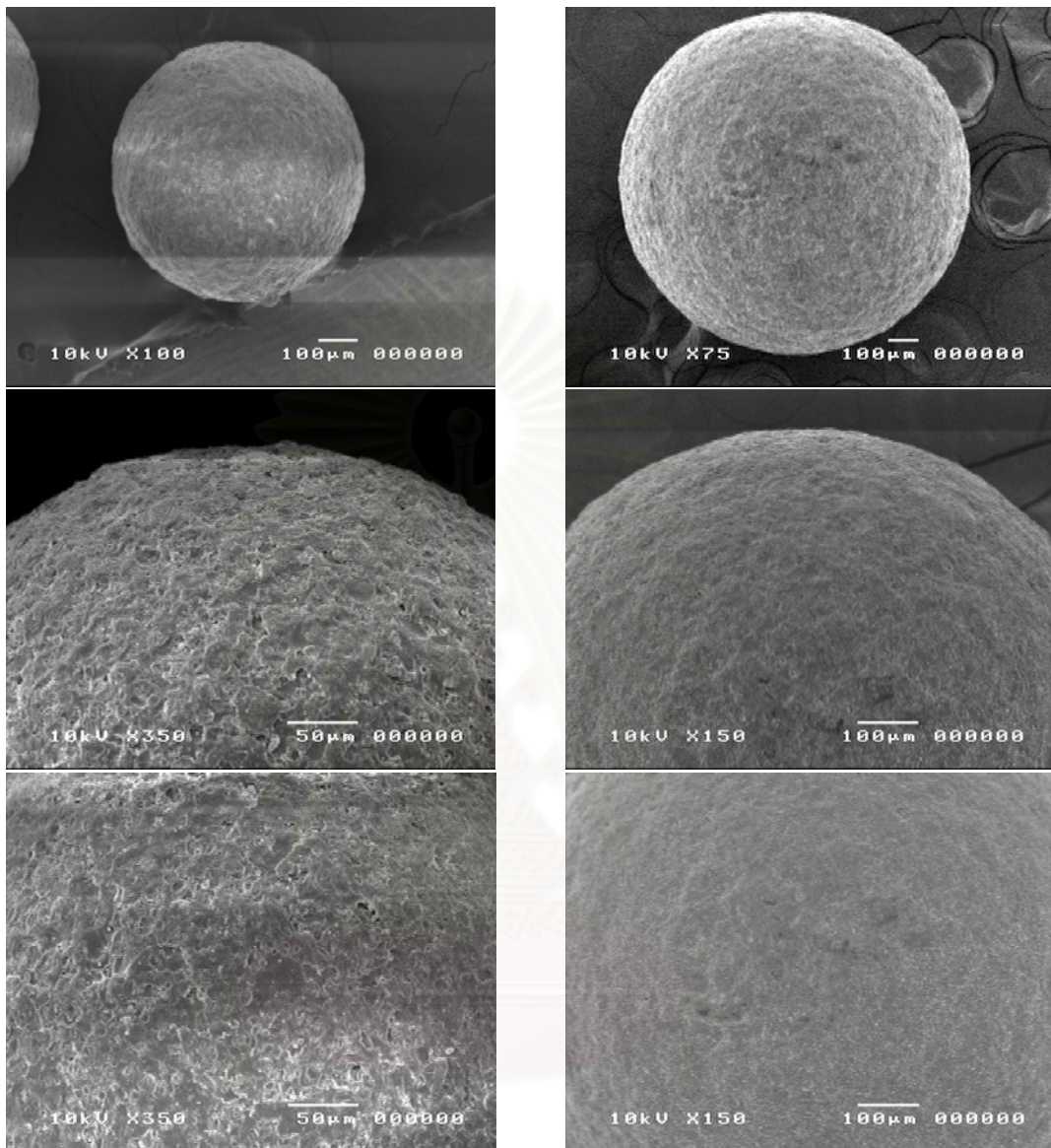
(a)   (b)

Figure 5.13 SEM micrographs of particle coated at fluidizing air velocity of 2.9

m/s and liquid flow rate 20 ml/min. (a), smaller size of 590 μm at magnification

of 100 and 350. (b), larger size of 1,033 μm at magnification of 75 and 150.

5.3 Influence of Electrostaticity

The influence of electrostaticity on the coting efficienty, film thickness, growth ratio and morphology of coated particles is investigated by varying the electrical potential applied to the nozzle between 0 to -4 kV. Similarly, effects of fluidizing air velocity, coating agent flow rate and core particle size on these coating characteristics are also discussed here.

5.3.1 Influence of Applied Electrical Potential

The effect of applied electrical potential on the coating efficiency is examined by varying the electrical potential applied to the nozzle between 0 to -4 kV under condition of constant coating agent flow rate and fluidizing air velocity of 20 m/min and 4.3 m/s, respectively. The results are shown in figure 5.14. Higher applied potential could lead to the increasing percentage of the coating efficiency. The coating efficiency increases from 60 to 75 % and 57 to 67 % for the case of 590 and 1,033μm, respectively when the applied potential is increased from 0 to -4 kV. This might be attributed to an increase in the specific charge on atomizing droplets of coating agent. According to A. J. Yule et al. [3], an increase in the applied electrical potential could lead to higher specific charge of atomized droplets. The average specific charge is the charge per unit volume could be calculated from the following equation 5.4

$$\rho_s = \frac{I_S}{Q_L} \qquad\qquad 5.4$$

where ρ_s = Specific charge density (C/m^3)

I_s = Spray current (A)

$$Q_L \quad = \quad \text{Volume flow rate (m}^3\text{/s)}$$

From the above equation, the specific charge density could be calculated when the applied electrical potential is varied and then after the charge per droplet was calculate too, the result were shown in table 5.2.

Table 5.2 Effect of applied potential at a coating agent flow rate of 20 ml/min on the spray current, specific charge and charge of single droplet

Applied Potential (kV)	I_s (A)	ρ_s (C/m^3)	q_d (C)
0	0	0	0
-1	4.0×10^{-8}	0.12	2.91×10^{-16}
-4	2.4×10^{-7}	0.72	1.56×10^{-15}

An increase in charge of single droplet leads to stronger attractive force estimated approximately by equation 5.5. Because such attractive force is interaction between charged droplets and core particles which are induced by attrition due to fluidizing air, it could lead to higher coating efficiency. Figure 5.14 indicated that an increase in electrical potential could result in an increase in coating efficiency. The increase in coating efficiency might be attributed to higher adherence probability because of higher potential difference between coating agent droplet and core particles.

$$F = k \frac{q_1 q_2}{r^2} \tag{5.5}$$

where q_1, q_2 = Charge of particle (C)

$$r \quad = \quad \text{Distance between charge (m)}$$

$$k \quad = \quad \text{Constant}$$

Effect of electrical potential on the coating efficiency is consistent with that on the film thickness and growth ratio of coated particles as shown in figure 5.15 – 5.16. The film thickness and growth ratio of coated particles become increased when higher electrical potential is applied. It should be noted that film thickness of smaller core particles is thinner than larger ones. This could be implied that these smaller core particles have higher specific surface area which could be available for wetting process, similar to previous results.

Figure 5.17 illustrates effect of packed bulk density of coated particles. It could be clearly observed that the packed bulk density of coated particles become lower with the increasing potential applied to the nozzle. This could be concluded that the increasing potential could help increase the deposition of coating film of which density is lower than that of core particles. Therefore, the thicker coated particles should exhibit density lower than the thinner ones.

Micrographs of the coated particles obtained from the experiment are shown in figure 5.18 and 5.19. They reveal that surface of the coated particles are rougher after coating. There is no significant difference between the coating layers on either small or larger particles. Moreover, morphology of the coated particles is still spherical. Comparison of the coated particles obtained from experimental either with or without application of electrical potential also revealed that the coating layer exhibits the similar roughness. These show that the equipment developed in this work could provide consistent coating layer on the core particles.
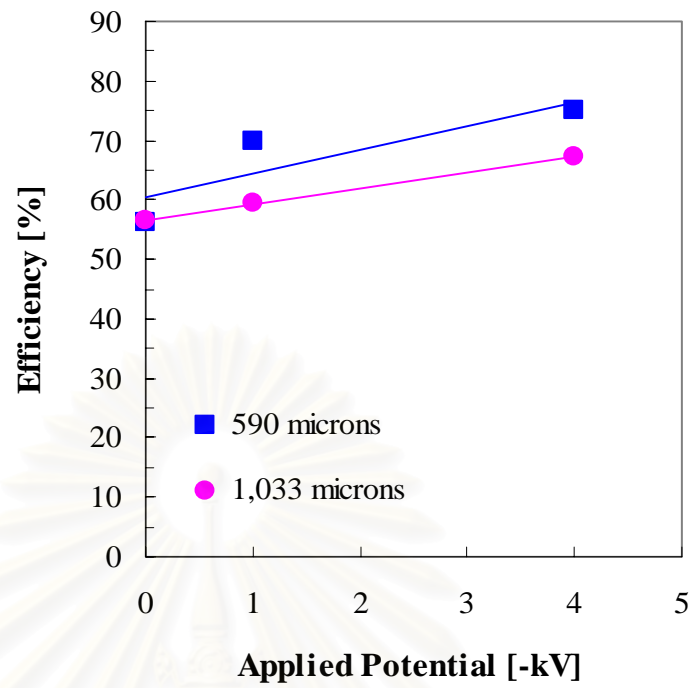
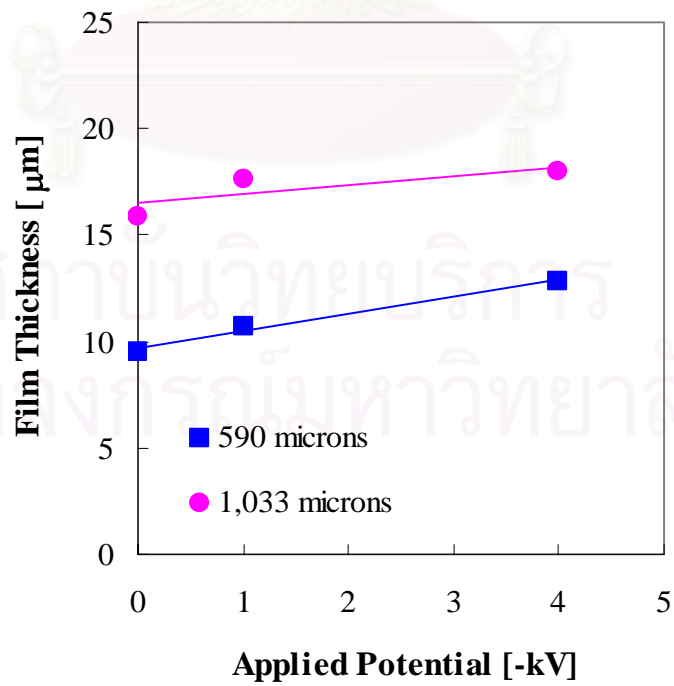**Figure 5.14 Effect of applied potential on the coating efficiency**

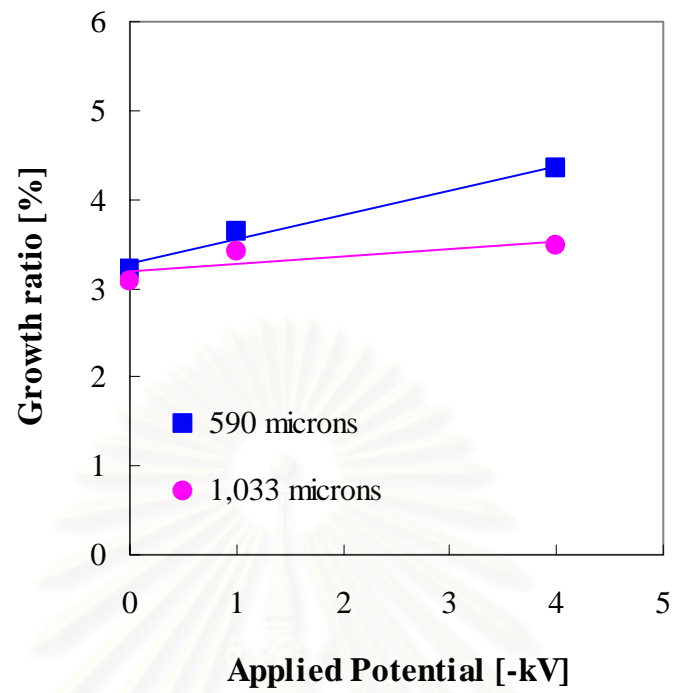**Figure 5.15 Effect of applied potential on the film thickness**

Figure 5.16 Effect of applied potential on the growth ratio of coating film
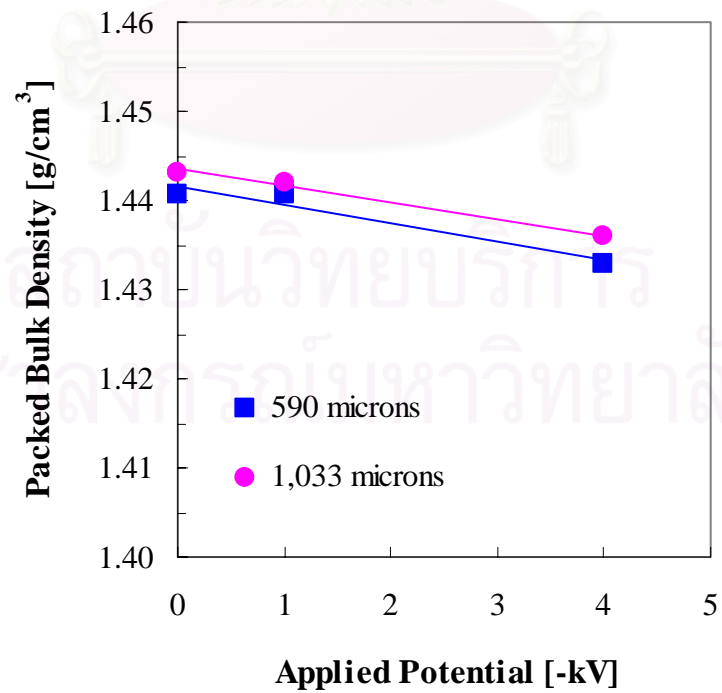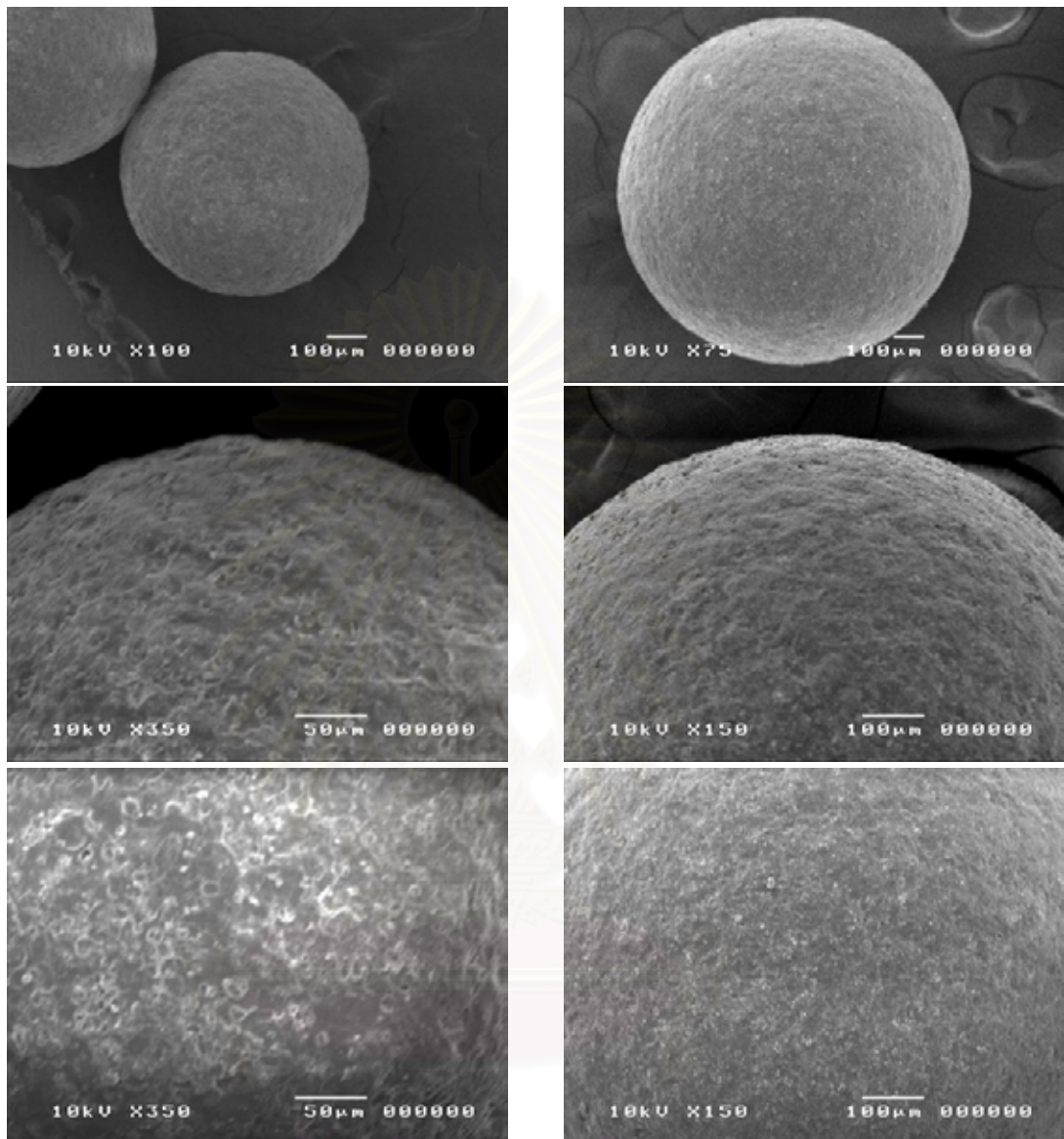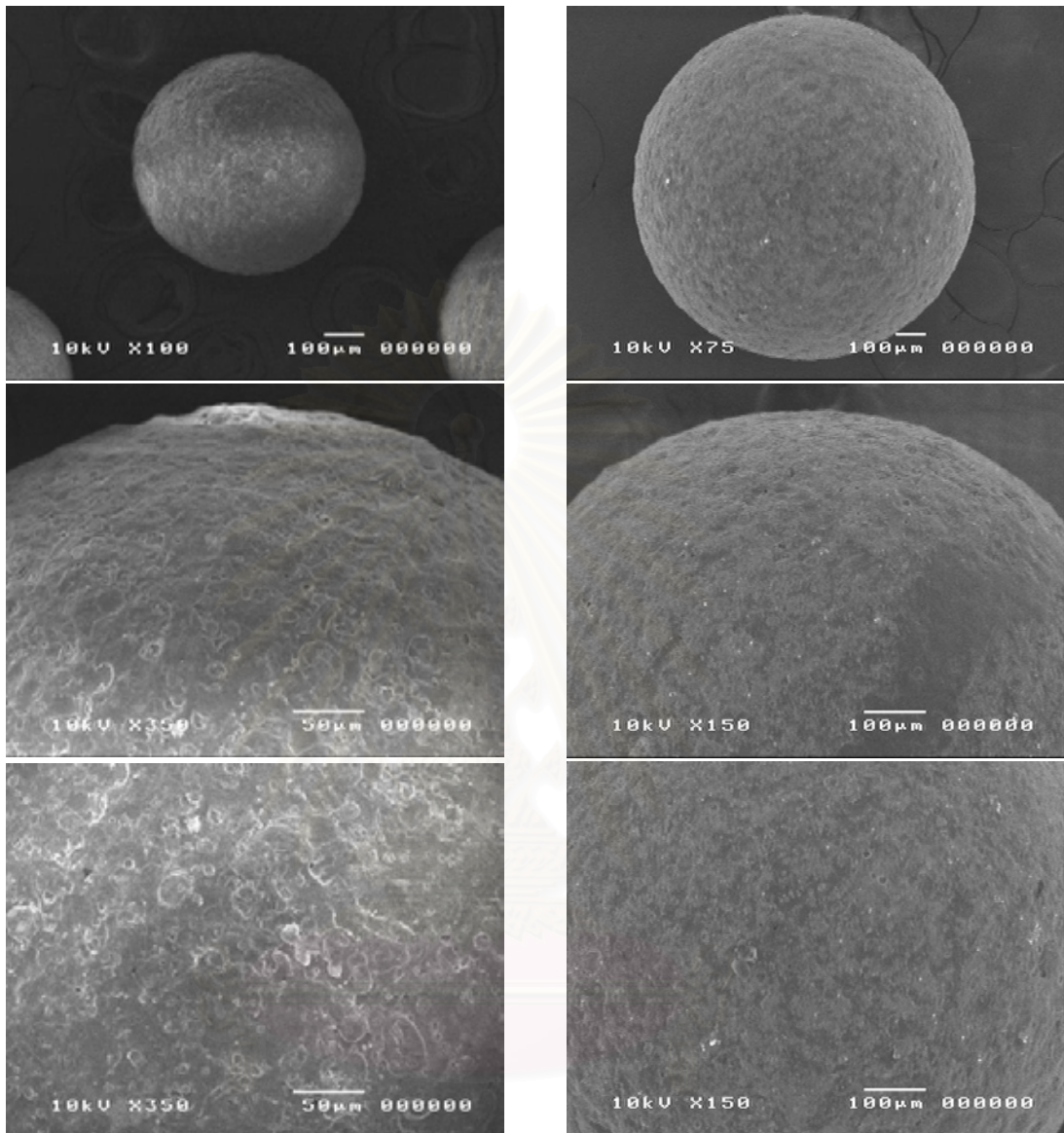

Figure 5.17 Effect of applied potential on the packed bulk density

(a)   (b)

Figure 5.18 SEM micrographs of particle coated at 0 kV of potential applied to the nozzle, 4.3 m/s of fluidizing air velocity and 20 ml/min of liquid flow rate. (a), smaller size of 590 μm at magnification of 100 and 350. (b), larger size of 1,033 μm at magnification of 75 and 150.

(a)   (b)

Figure 5.19 SEM micrographs of particle coated at -4 kV of potential applied

to the nozzle, 4.3 m/s of fluidizing air velocity and 20 ml/min of liquid flow rate.

(a), smaller size of 590 μm at magnification of 100 and 350. (b), larger size of

1,033 μm at magnification of 75 and 150.

5.3.2 Influence of Fluidizing Air Velocity

The influence of fluidizing air velocity on the coated particles characteristics is investigated by varying the air velocity between 2.2 and 4.3 m/s, electrical potential applied to the nozzle is also varied between 0 to -4 kV. Glass bead with nominal size of 590 and 1,033 μm are used as core particle in this study while the coating agent flow rate is kept constant at 20 ml/min. Figure 5.20 illustrates the coating efficiency as a function of the fluidizing air velocity and the electrical potential. The coating efficiency is increased when the fluidizing air velocity is increased. It should be noted that at the fluidizing air velocity of 4.3 m/s, the increasing electrical potential could enhance the coating efficiency. However, such enhancing effect of the electrical potential at the fluidizing air velocity of 2.2 m/s is comparative low. The coating efficiency was slightly increased form 73 to 75% and 64 to 69% for the 590 and 1,033 μm core particles, respectively, at fluidizing air velocity of 2.2 m/s. This could be explained that higher air velocity could provide the formation of bigger bubbles which could induce more rigorous motion of the core particles and resulting in augmenting static charge on the core particles [4]. Meanwhile, it should be noted that the increasing air velocity could also lead to higher entrainment of coating agent droplet. Therefore, with higher air velocity, the increasing electrostatic potential on the core particles would be prominent, leading to stronger dependence of the coating efficiency on the increasing electrical potential. On the other hand, with higher air velocity, the entrainment of the coating droplets would be more enhanced, resulting in the lower dependence of the coating efficiency on the increasing potential.

Considering the effect of core particle size from figure 5.21, it could be observed that the coating layer thickness on the smaller core particles is thinner than

that of the bigger core particles. This could be again explained by the higher specific surface area of the smaller which could provide higher probability of contacting between the atomized droplets and the core particles. The consistent results in dependence of the film thickness, the growth ratio and the packed bulk density of the coated particles on the fluidizing air velocity are also shown in figure 5.22 and 5.23.

SEM images of the surface of the coated core particles at two difference of fluidizing air velocity are shown in figures 5.24 and 5.25. Similar to previous results, no significant difference among the surface roughness of the coating layer on either big or small core particles. It should also be noted that the coating layer exhibits the very porous characteristics. This should be implied for the slow released of the coated particles if it is applied with core particles containing drug [17].
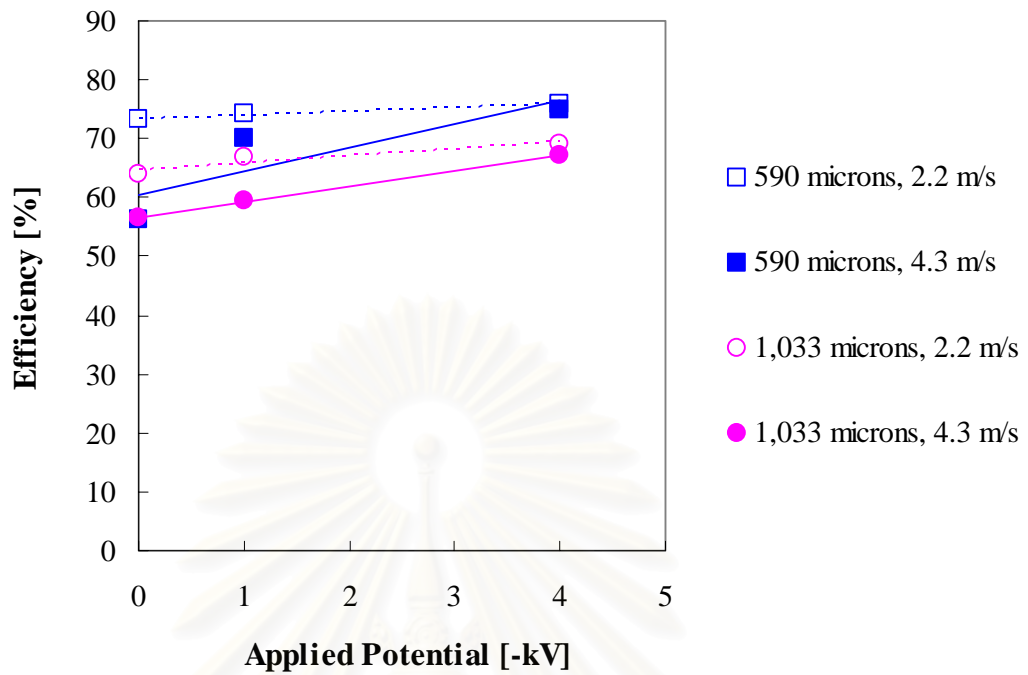
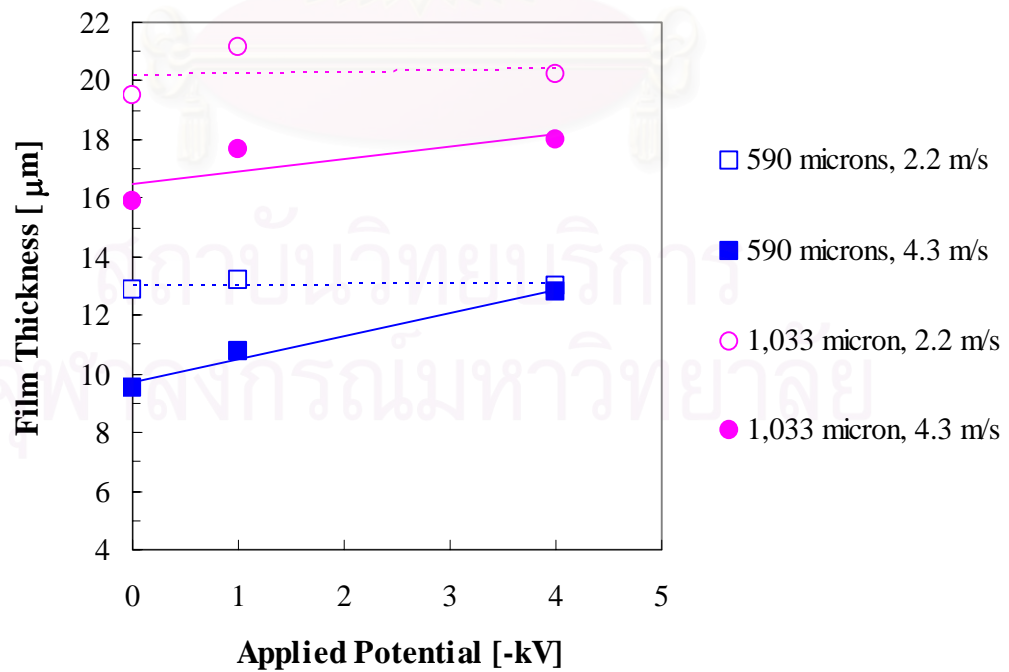**Figure 5.20 Effect of applied potential on the coating efficiency**

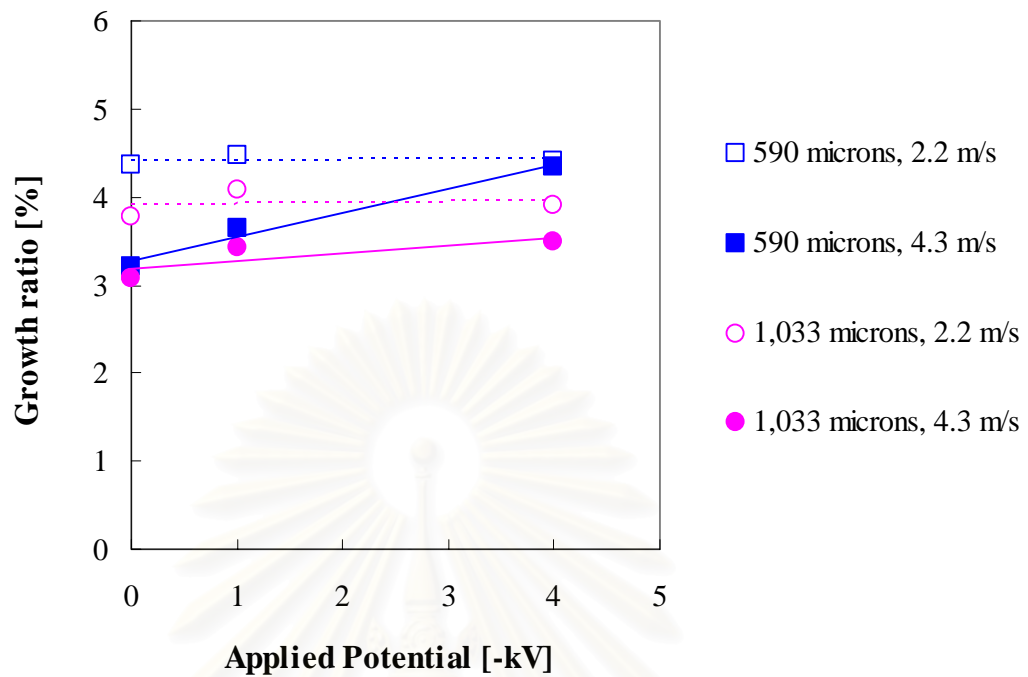**Figure 5.21 Effect of applied potential on the film thickness**

Figure 5.22 Effect of applied potential on the growth ratio of coating film
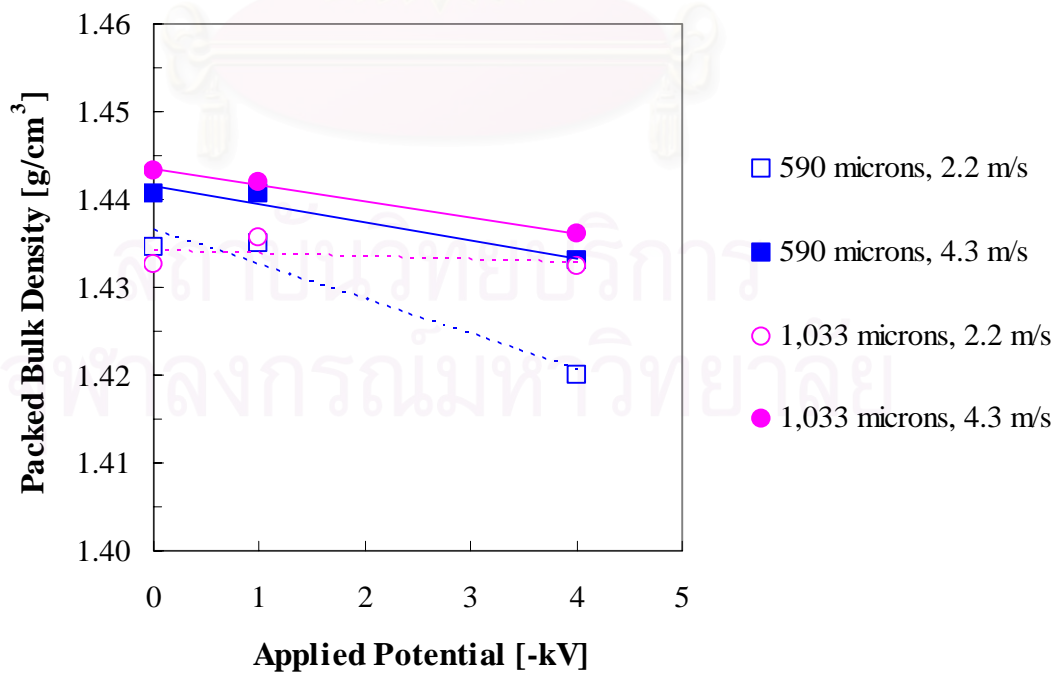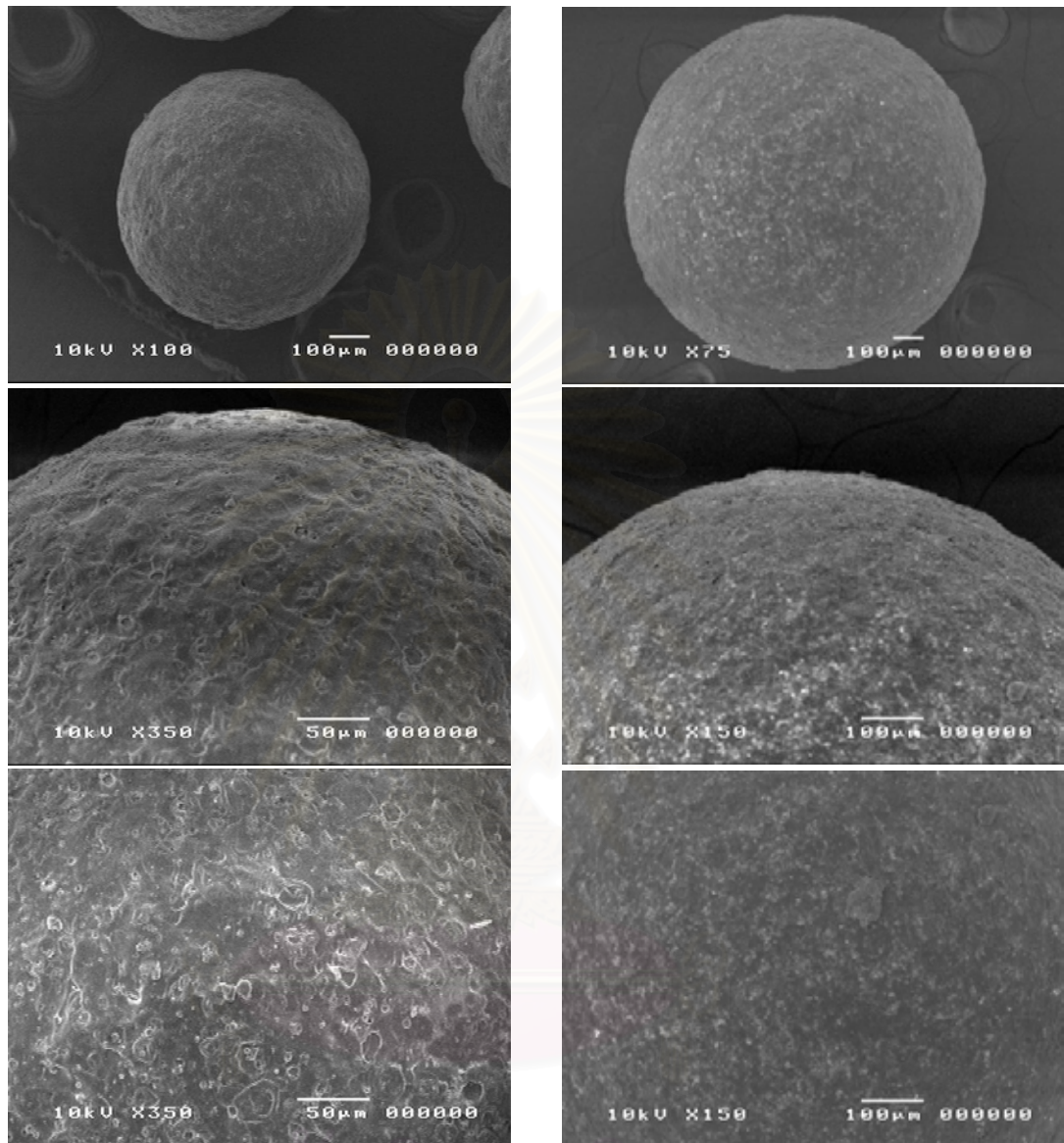

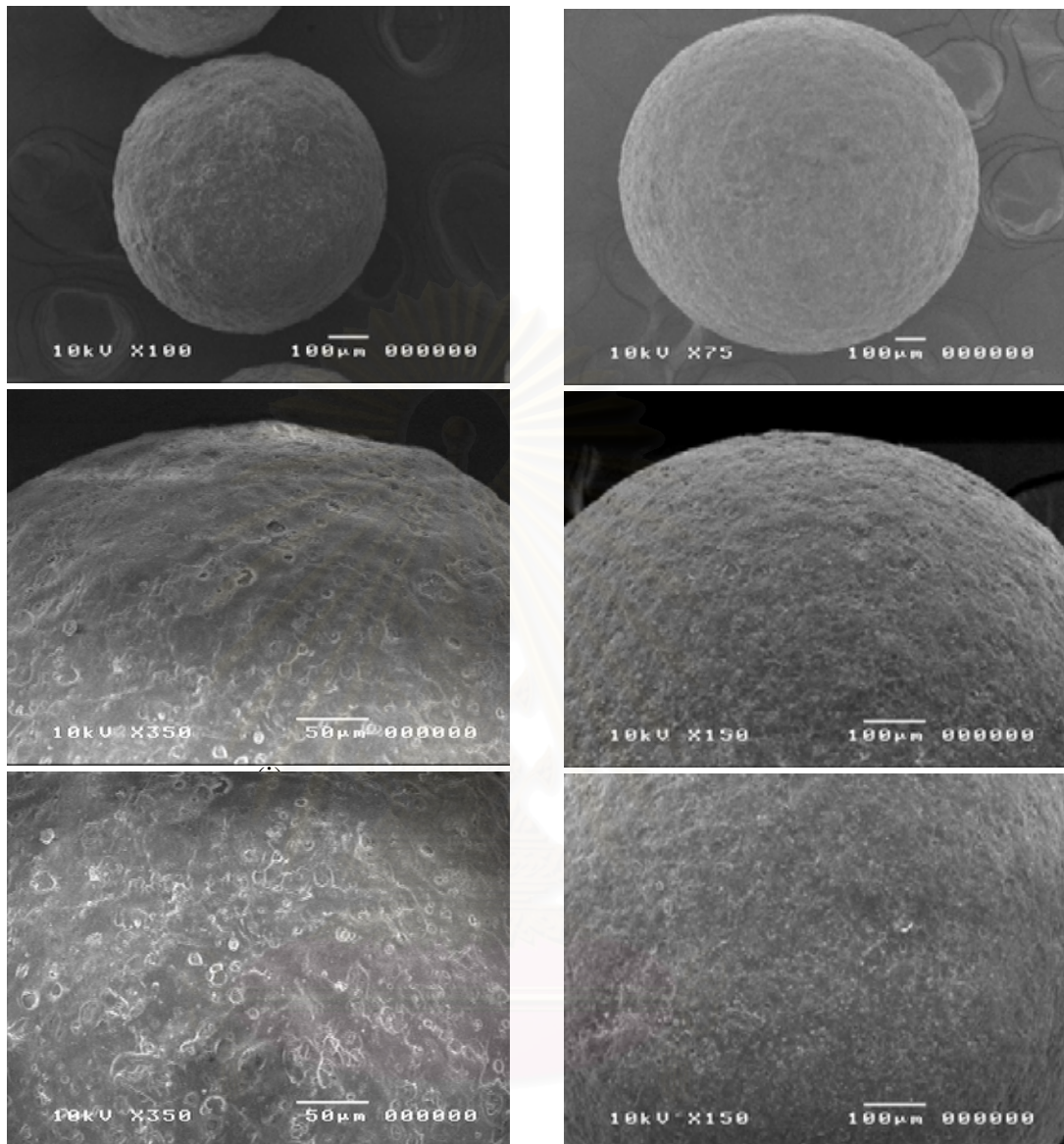**Figure 5.23 Effect of applied potential on the packed bulk density**

(a)   (b)

Figure 5.24 SEM micrographs of particle coated at 2.2 m/s of fluidizing air

velocity, -4 kV of potential applied to the nozzle and 20 ml/min of liquid flow rate.

(a), smaller size of 590 μm at magnification of 100 and 350. (b), larger size of

1,033 μm at magnification of 75 and 150.

Figure 5.25 SEM micrographs of particle coated at 4.3 m/s of fluidizing air

velocity,-4 kV of potential applied to the nozzle and 20 ml/min of liquid flow rate.

(a), smaller size of 590 μm at magnification of 100 and 350. (b), larger size of

1,033 μm at magnification of 75 and 150.

5.3.3 Influence of Coating Agent Flow Rate

Under the higher fluidizing air velocity which provides lower coating efficiency, effect of the flow rate of the coating agent on all coating characteristics of interest is summarized in theses subchapter.

Figure 5.26 -5.28 showed that at air velocity of 4.3 m/s, the effect of liquid flow rate on the coating efficiency, film thickness and growth ratio become more enhanced as the liquid flow rate is increased. It should be noted that with higher flow rate of the coating agent the duration of the operation could be shorten. Meanwhile the packed bulk density of the coated particles become slightly decreased with the increasing flow rate of the coating agent as shown in figure 5.29. This could be explained that lose of the coating agent become lower when the flow rate of the coating agent is increased because larger atomizing droplet could be obtained.

However, referring to equation 5.4, it is found that the specific charge of the atomized droplets would be reduced for the higher liquid flow rate therefore the lower coating efficiency would be expected. With this reason, higher coating efficiency could be obtained at the higher flow rate of the coating agent which gives rise to larger droplets even though there was less specific charge on the surface of the droplets. This electrostatic force could be increased the probability of among the core particles and the atomized droplets. As mention previously, these effects of the atomized droplet size, the fluidized air velocity and the electrical potential on the coating characteristic should be integrated. Because of these effects the amount of the coating layer could be rapidly increased when higher electrical potential is employed and higher the liquid flow rate is supplied.

Figure 5.30-5.31 represented the SEM micrographs of the coated particle affected by the change of the liquid flow rate when the applied potential is kept

constant at -4 kV. It is found that the coated particle surface is rougher than that of the uncoated particle. Figure 5.31(a), illustrates the orange-peel like surface observed at the magnification of 350. It could be noted that the orange-peel like surface is one defection of the coated particles inevitably obtained when using HPMC polymer [6].

At the magnification of 1500, the ring or donut-like shapes at the surface of coated particles could be investigated as shown in figure 5.32. This appearance indicates that solute precipitation occur already inside the droplets during droplets flight. It could be explained that the solvent evaporation of atomized droplets, which are moving relative to the ambient, is faster on the leading surface of the droplet. Therefore, the solute concentration at the front surface of the droplet is higher and crust formation starts at the front side when the surface concentration exceeds the equilibrium saturation. Subsequently, the crust grows at the front of the droplet without any precipitation at the backside of the droplet due to the evaporation rate is much smaller at this location. The crust grows further and a cup-shaped particle is created with a certain wall thickness depending on the total amount of solute and the drying conditions. A schematic representation of the formation of these ring - and doughnut-like shapes is depicted in figure 5.34 [10]. Moreover, some doughnut shapes may be produced due to impinging and spreading of droplets with rippling of droplet edge on the surface of core particles.
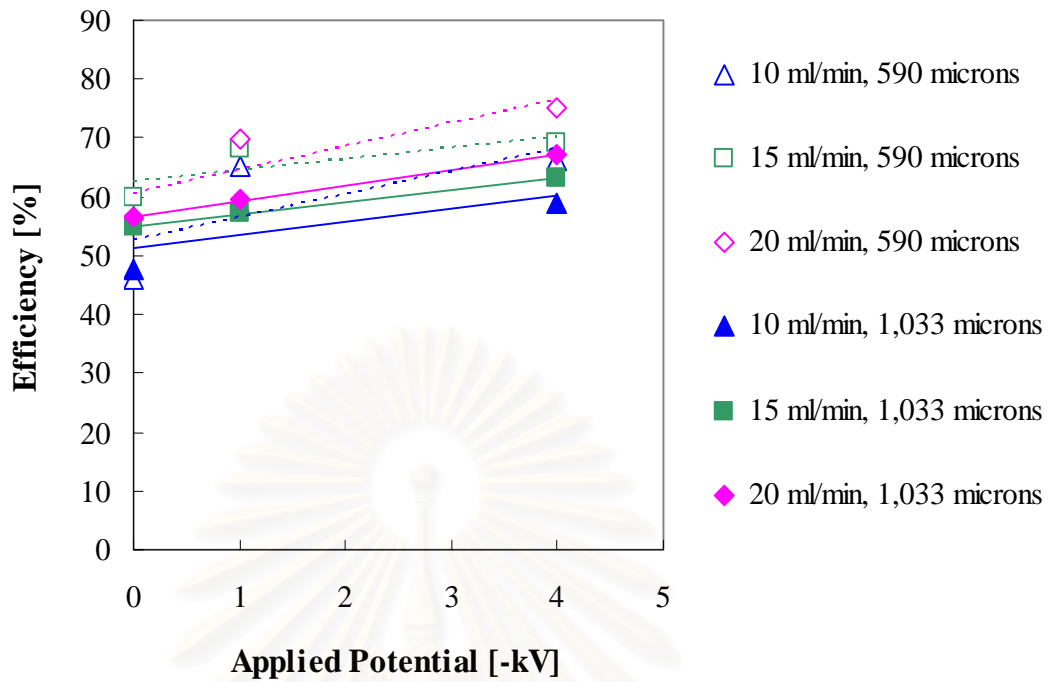
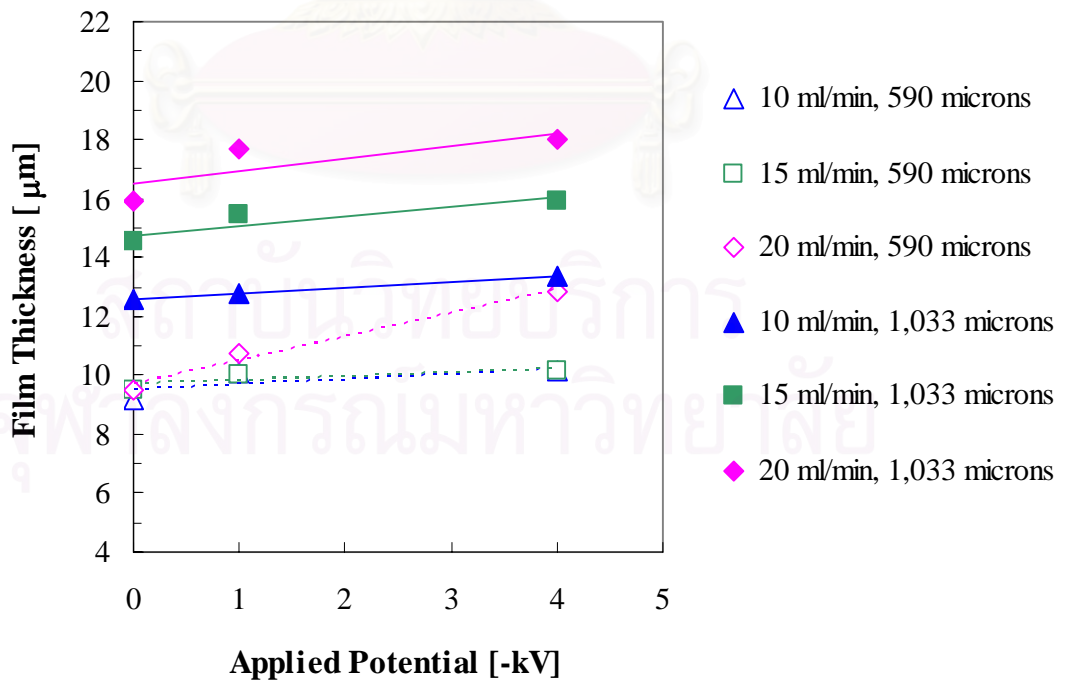**Figure 5.26 Effect of liquid flow rate on the coating efficiency**

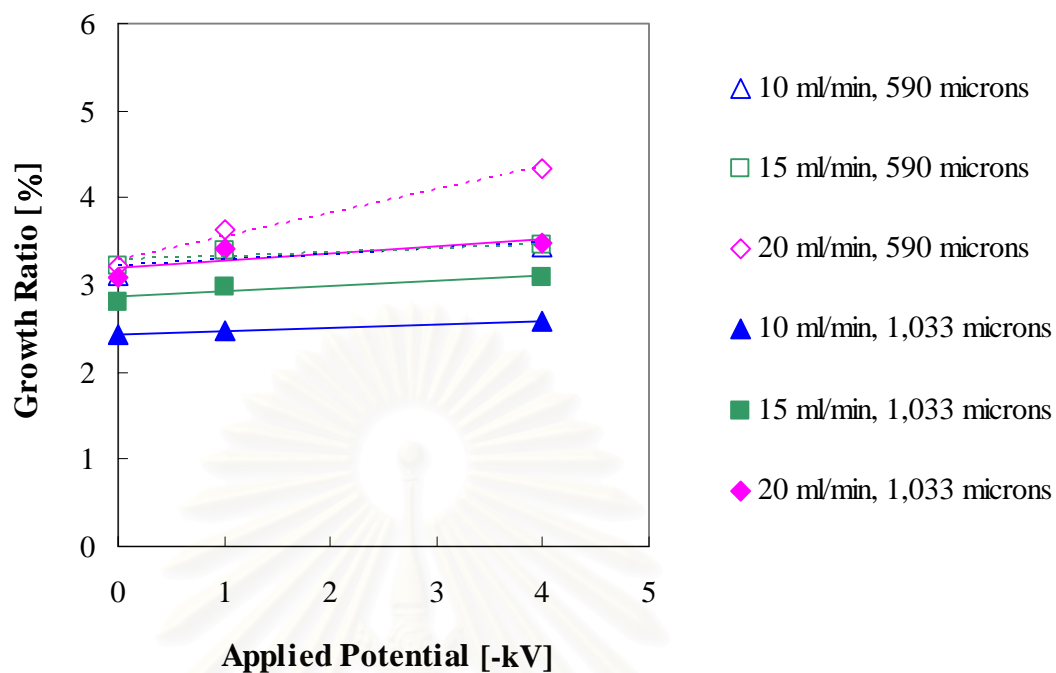**Figure 5.27 Effect of liquid flow rate on the film thickness**

Figure 5.28 Effect of liquid flow rate on the growth ratio
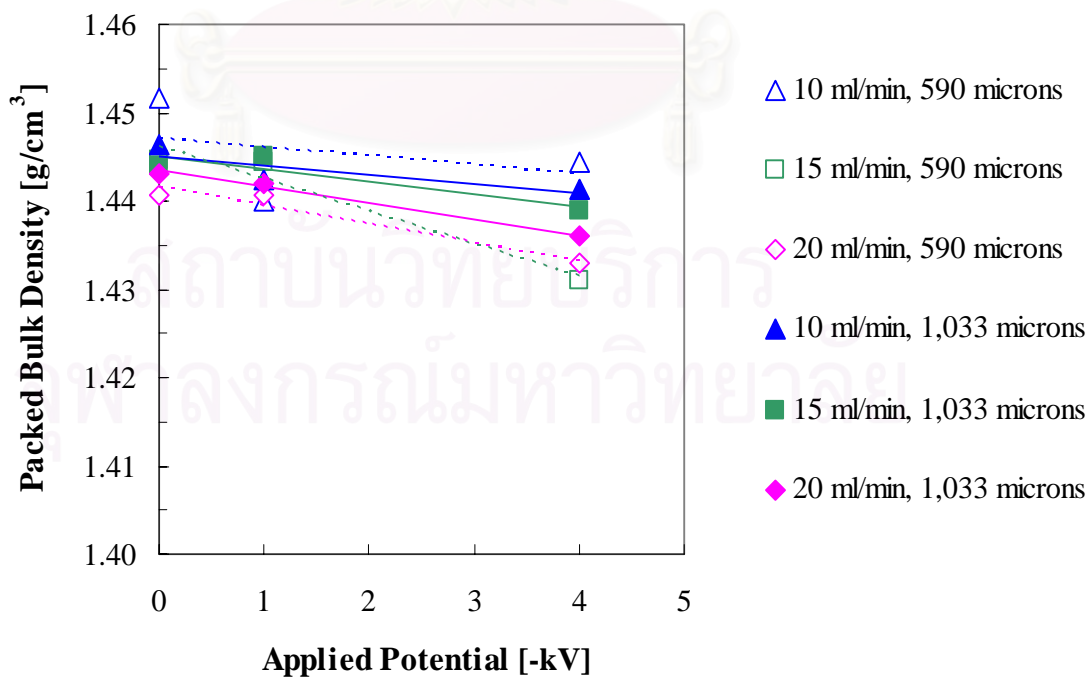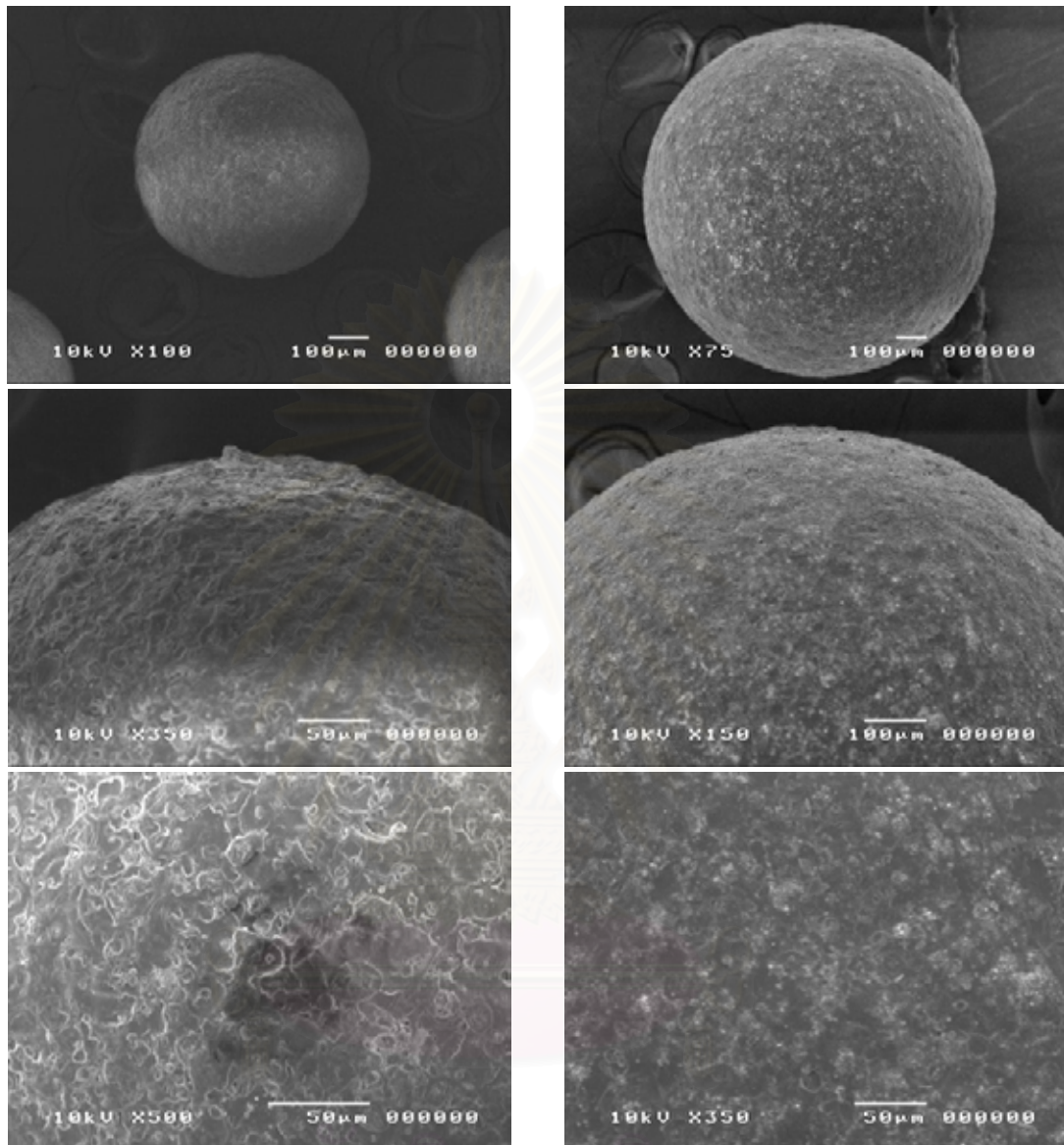

Figure 5.29 Effect of liquid flow rate on the packed bulk density
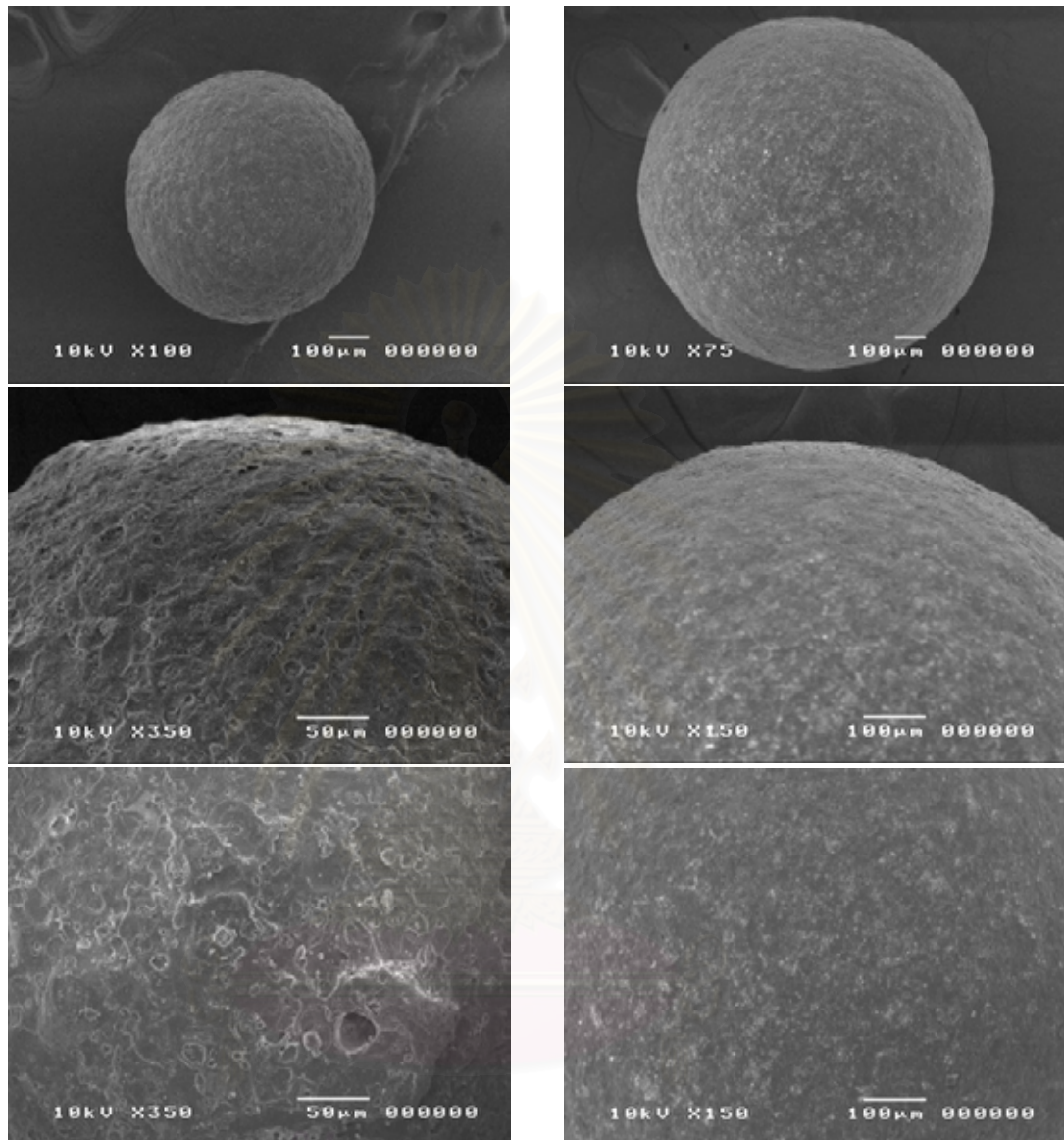
(a)   (b)

Figure 5.30 SEM micrographs of particle coated at 4.3 m/s of fluidizing air

velocity,-4 kV of potential applied to the nozzle and 10 ml/min of liquid flow rate.

(a), smaller size of 590 μm at magnification of 100 and 350. (b), larger size of

1,033 μm at magnification of 75 and 150.

(a)   (b)
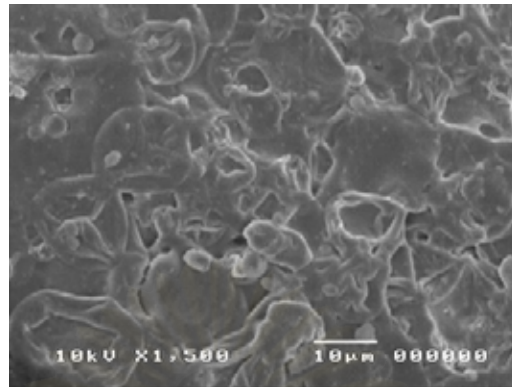
Figure 5.31 SEM micrographs of particle coated at 4.3 m/s of fluidizing air

velocity,-4 kV of potential applied to the nozzle and 20 ml/min of liquid flow rate.

(a), smaller size of 590 μm at magnification of 100 and 350. (b), larger size of

1,033 μm at magnification of 75 and 150.

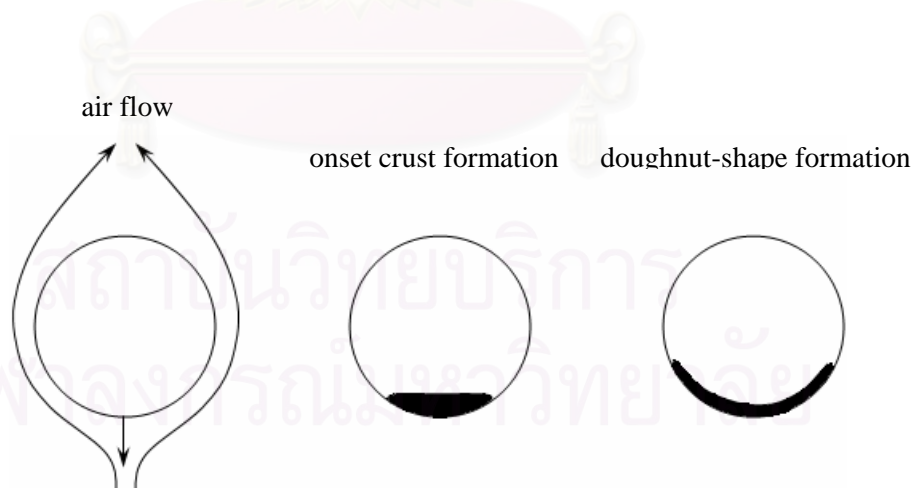**Figure 5.32 SEM micrographs of particle coated at 4.3 m/s of fluidizing air velocity,-4 kV of potential applied to the nozzle and 10 ml/min of liquid flow rate of 590 μm core particle size at the magnification of 1500.**

air flow

onset crust formation   doughnut-shape formation

Figure 5.33 Development of doughnut shape by means of solute precipitation inside spray droplets

CHAPTER VI

CONCLUSION AND FUTURE WORKS

6.1 Conclusion

The effects of major operating variables, i.e. fluidizing air velocity (2.2 to 4.3 m/s), coating agent flow rate (10 to 20 ml/min) and applied potential (0 to (-4) kV), on the characteristics of the coated particles, including the coating film thickness, the percentage of coating efficiency, the percentage of growth rate, the packed bulk density and the surface morphology, were investigated. From the experimental results, it could be concluded as follows,

1. The solvent evaporation rate that could be modulated by adjusting the fluidizing air velocity and the flow rate of coating agent was the major factor that effected losing of coating agent.

2. The coating efficiency was enhanced when smaller core particles were employed in the coating process due to higher specific area of the smaller core particle.

3. Losing of coating agent could be reduced by increasing the electrical potential applied to the nozzle due to the enhanced deposition of coating agent droplets on the surface of core particles promoted by the attractive force between the electrical charges on the droplet and core particle surfaces.

4. The production of finer liquid droplets could be obtained from the nozzle assisted with electrical potential due to less coalescence of the charged droplets.

6.2 Future Works

1. The humidity of the fluidizing air before entering the coater chamber should be kept constant to investigate the effect of the humidity on the moisture content in the coated particles.

2. The developing process should be studied for its applicability for coating drugs of different models.

3. An investigation of the effect of an increase in electrical potential that applied to the nozzle on the coating efficiency should be carried out.

4. Use different techniques to generate electrical charges on the surface of core particles, e.g. corona discharge technique, to obtain a better control of electrical charge concentration on the surface of core particles.

REFERENCES

[1]   A. Wolny, and W. Kazmierczak. Triboelectrification in fluidized bed of polystyrene. Chemical Engineering Science 44 (1989): 2607-2610.

[2]   P. Bertelsen, F. N. Christensen, P. Holm, and K. Jorgensen. Comparison of organic solvent-based ethylcellulose coatings on KCl crystals applied by top and bottom spraying in fluidized-bed equipment. International Journal of Pharmaceutics 111 (1994): 117-125.

[3]   A. J. Yule, J. S. Shrimpton, A. P. Watkins, W. Balanchandran, and D. Hu. Electrostatically atomized hydrocarbon sprays. Fuel 74 (1995): 1094-1103.

[4]   J. Guardiola, V. Rojo, and G. Ramos. Influence of particle size, fluidizion velocity and relative humidity on fluidized bed electrostatics. Journal of Electrostatics 34 (1996): 1-20.

[5]   R.K. Johnson, R.C. Anantheswaran and S.E. Law. Electrostatic-enhanced atomization for spray drying of milk. Lebensmittel Wissenschaft und Technologie-Food Science and Technology 29 (1996): 71-81.

[6]   H. Yuasa, T. Nakano, and Y. Kanaya. Suppression of agglomeration in fluidized bed coating I. Suppression of agglomeration by adding NaCl. International Journal of Pharmaceutics 158 (1997): 195-201.

[7]   K. Dewettinck, and A. Huyghebaert. Top-spray fluidized bed coating: effect of process variables on coating efficiency. Lebensmittel Wissenschaft und Technologie-Food Science and Technology 31 (1998): 568-575.

[8]   M. R. Jahannama, A. P. Watkins, and A. J. Yule. Examination of electrostatically charged sprays for agricultural spraying applications. Proc. ILASS-Europe 52 (1999): 252-260.

[9]   K. Saleh, D. Steinmetz, and M. Hemati. Experimental study and modeling of fluidized bed coating and agglomeration. Powder Technology 130 (2003):116-123.

[10]   M. Hemati, R. Cherif, K. Saleh, and V. Pont. Fluidized bed coating and granulation: influence of process-related variables and physicochemical properties on the growth kinetics. Powder Technology 130 (2003): 18-34.

[11]   M. Murtomaa, et al. Electrostatic measurements on a miniaturized fluidized bed. Journal of electrostatics 57 (2003): 91-106.

[12]   Kunii, D., Levenspiel, O. Fluidization engineering. USA: Wiley and Sons, 1969.

[13]   D. Geldart. Types of gas fluidization. Powder Technology 7(1973): 285-292.

[14]   H. A. Liberman, L. Lachman, and J. B. Schwartz. Pharmaceutical dosage forms:Tablet. vol 3., 2nd ed. New York: Marcel Dekker, 1990.

[15]   A Wade, , Weller, P.J. Handbook of pharmaceutical excipients. 2nd ed. London: The pharmaceutical press, 1994.

[16]   James W. McGinity. Drugs and the pharmaceutical sciences: aqueous polymeric coatings for pharmaceutical dosage forms. vol.79, 2nd ed. New York: Marcel Dekker, 1997.

[17] Bauer, K.H., Lehmann, K., Osterward, H.P., Rothang, G. <u>Coated pharmaceutical dosage forms</u> Florida: CRC Press, 1998.

APPENDICES

APPENDIX A

Calibration Curve

The fluidizing air velocity versus height of water difference in difference orifice diameter is presented in table A.1 and A.2 respectively. The calibration curve obtained by pressure drop between orifice that shown in height of water difference in manometer are depicted in figure 1, 2 and 3, respectively.

Table A.1 Height of water difference in orifice diameter 20 mm.

Height of water difference in manometer (cm)	Fluidizing air velocity (m/s)					
	No.1	No.2	No.3	No.4	No.5	Average
3	0.5	0.4	0.4	0.5	0.4	0.4
6	0.9	0.9	0.9	0.9	1.1	0.9
7.5	1.1	1.1	1.0	1.1	1.2	1.1
13	1.5	1.5	1.5	1.5	1.5	1.5
15	1.7	1.7	1.7	1.7	1.7	1.7
18	2.1	2.1	2.1	2.1	2.1	2.1
22	2.4	2.4	2.4	2.4	2.5	2.4

Fluidizing air velocity is measured at room temperature ($\approx 30\,^0C$)

Table A.2 Height of water difference in orifice diameter 27 mm.

Height of water difference in manometer (cm)	Fluidizing air velocity (m/s)					
	No.1	No.2	No.3	No.4	No.5	Average
2	2.1	2.1	2.0	2.1	2.1	2.1
3	2.4	2.5	2.5	2.5	2.5	2.5
5	3.2	3.3	3.2	3.2	3.2	3.2
8	4.3	4.3	4.3	4.3	4.3	4.3
12	5.0	5.1	5.0	5.0	5.0	5.0
14	5.2	5.3	5.2	5.2	5.2	5.2
15	5.4	5.4	5.3	5.3	5.4	5.4

Fluidizing air velocity is measured at room temperature ($\approx 30\,^{0}C$)
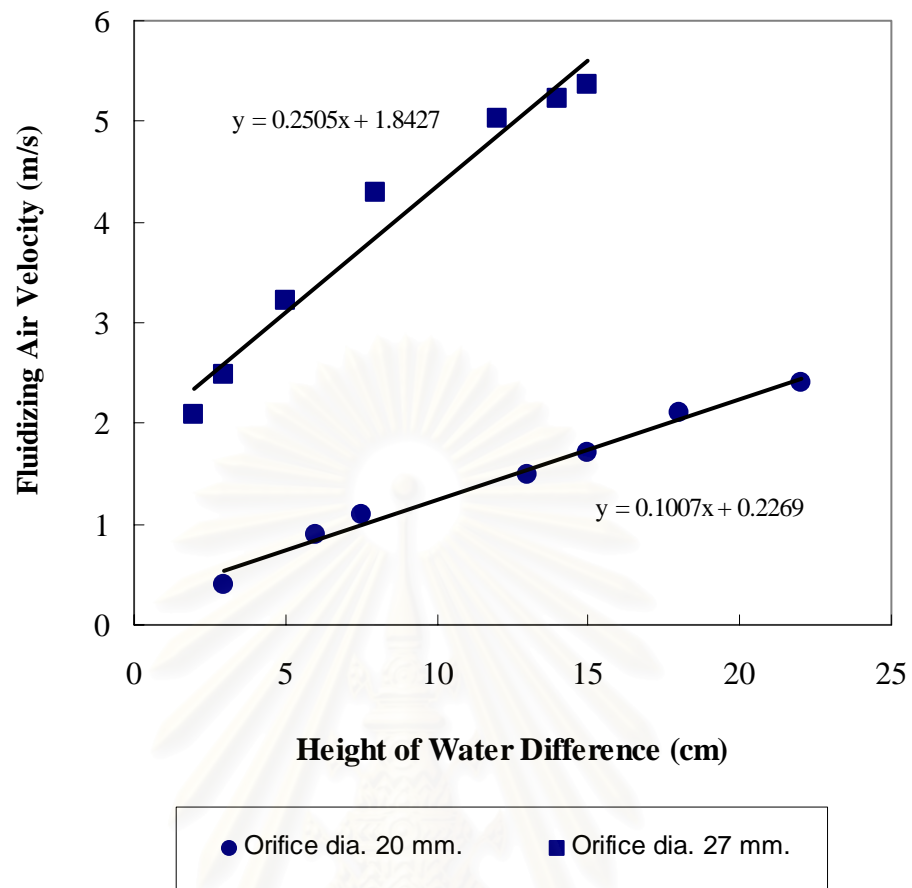
Figure A.1 Calibration curve of orifice diameter 20 and 27 millimeters

APPENDIX B

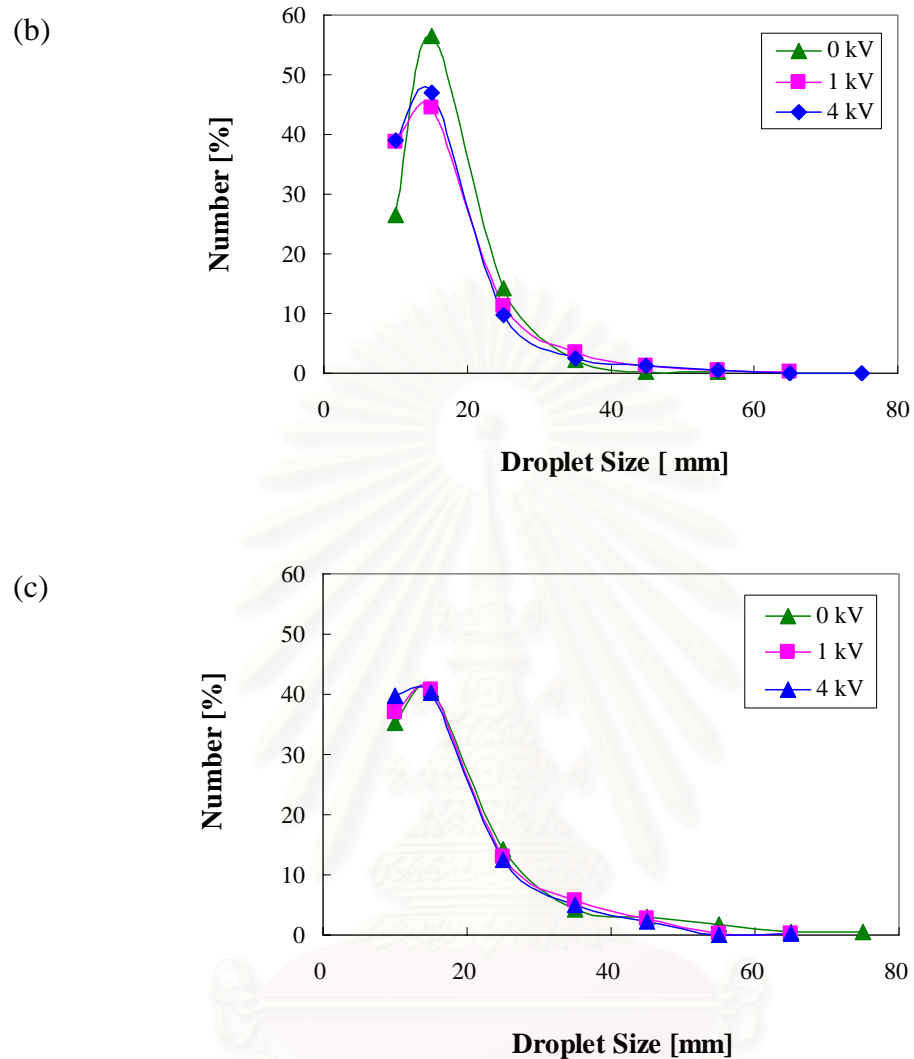**Averaged Droplet size and droplet size distribution**

Feed Rate (ml/min)	Applied Potential (kV)	Average Droplet Size (μm)
10	0	15.48
15	0	15.73
20	0	17.60
10	1	15.40
15	1	15.61
20	1	16.67
10	4	15.15
15	4	15.19
20	4	16.05

(a)
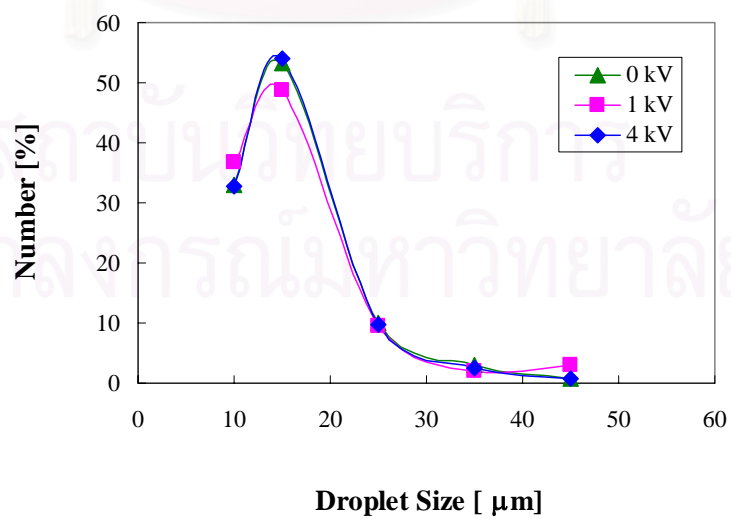
Droplet Size [μm]

Figure B. Droplet size distributions at different flow rate and applied potentials.

Flow rate: (a) 10 ml/min, (b) 15 ml/min (c) 20 ml/min.

APPENDIX C

Table C.1 Experimental result of 590 μm glass beads coating in the fluidized bed

coater

Process variable ($U/Q_L/E$)	Total weight of coated particles	Coating efficiency [%]	Pack bulk density [g/cc]	Film thickness [μm]	Growth ratio [%]
2.2/10/0	187.36	68.15	1.443	11.85	4.02
2.9/10/0	187.32	67.75	1.445	10.70	3.63
3.6/10/0	186.56	60.60	1.444	9.28	3.15
4.3/10/0	184.97	46.05	1.452	9.15	3.10
2.2/15/0	187.68	71.07	1.436	12.21	4.14
2.9/15/0	187.61	70.44	1.437	11.22	3.80
3.6/15/0	187.33	67.72	1.440	10.46	3.55
4.3/15/0	186.47	59.86	1.445	9.50	3.22
2.2/20/0	187.91	73.24	1.435	12.90	4.37
2.9/20/0	187.92	73.23	1.433	11.57	3.92
3.6/20/0	187.16	66.19	1.436	11.10	3.76
4.3/20/0	186.09	56.32	1.441	9.49	3.22
2.2/10/-1	187.73	71.56	1.436	12.49	4.23
2.9/10/-1	187.48	69.07	1.439	12.09	4.10
3.6/10/-1	187.49	69.29	1.439	10.45	3.54
4.3/10/-1	187.05	65.25	1.440	10.11	3.43
2.2/15/-1	187.94	73.54	1.432	12.58	4.26
2.9/15/-1	187.83	72.44	1.434	11.93	4.04
3.6/15/-1	187.57	70.09	1.437	9.99	3.38
4.3/15/-1	187.35	68.04	1.444	10.02	3.40
2.2/20/-1	188.01	74.11	1.435	13.21	4.48
2.9/20/-1	187.99	73.92	1.435	11.88	4.03
3.6/20/-1	187.64	70.71	1.440	11.80	4.00
4.3/20/-1	187.56	69.94	1.441	10.74	3.64
2.2/10/-4	187.55	69.80	1.437	12.52	4.24
4.3/10/-4	186.82	66.02	1.445	10.13	3.43
2.2/15/-4	187.95	73.49	1.435	12.44	4.22
4.3/15/-4	187.50	69.27	1.431	10.18	3.45
2.2/20/-4	187.95	75.94	1.420	13.01	4.41
4.3/20/-4	188.30	75.00	1.433	12.81	4.34

Table C.2 Experimental result of 1,033 μm glass beads coating in the fluidized bed coater

Process variable (U/Q_L/E)	Total weight of coated particles	Coating efficiency [%]	Pack bulk density [g/cc]	Film thickness [μm]	Growth ratio [%]
2.2/10/0	185.89	54.48	1.443	15.01	2.91
2.9/10/0	185.68	52.56	1.444	14.75	2.86
3.6/10/0	185.83	53.95	1.442	14.32	2.77
4.3/10/0	185.15	47.63	1.446	12.55	2.43
2.2/15/0	186.78	62.56	1.436	16.31	3.16
2.9/15/0	186.38	58.85	1.439	15.65	3.03
3.6/15/0	186.18	57.27	1.440	15.35	2.97
4.3/15/0	185.92	54.80	1.444	14.51	2.81
2.2/20/0	186.92	64.11	1.433	19.50	3.78
2.9/20/0	186.85	63.35	1.436	18.70	3.62
3.6/20/0	186.57	60.85	1.438	17.50	3.39
4.3/20/0	186.10	56.43	1.443	15.90	3.08
2.2/10/-1	186.42	59.37	1.441	16.26	3.15
2.9/10/-1	186.31	58.44	1.442	15.79	3.06
3.6/10/-1	185.30	49.08	1.447	13.28	2.57
4.3/10/-1	185.30	49.08	1.448	12.75	2.47
2.2/15/-1	186.82	63.17	1.442	18.42	3.57
2.9/15/-1	186.01	55.57	1.444	15.88	3.07
3.6/15/-1	185.66	52.37	1.448	14.17	2.74
4.3/15/-1	186.18	57.17	1.445	15.42	2.99
2.2/20/-1	187.21	66.79	1.436	21.12	4.09
2.9/20/-1	186.67	61.78	1.441	19.73	3.82
3.6/20/-1	186.48	60.01	1.436	19.11	3.70
4.3/20/-1	186.43	59.53	1.442	18.06	3.50
2.2/10/-4	186.44	59.59	1.442	17.66	3.42
4.3/10/-4	186.49	60.11	1.440	16.99	3.29
2.2/15/-4	186.36	58.87	1.441	13.33	2.58
4.3/15/-4	187.01	64.92	1.438	18.13	3.51
2.2/20/-4	186.82	63.10	1.439	15.93	3.08
4.3/20/-4	187.48	69.21	1.432	20.21	3.91

where   U   =   fluidizing air velocity (m/s)

      Q_L =   coating agent flow rate (ml/min)

      E   =   applied electrical potential (kV)

APPENDIX D

Image Processing Procedure (Image-Pro Plus 3.0)

Calibration Program

- Start up program by clicking at icon of **Image-Pro Plus 3.0**. (See Figure D.1)

- Open a file of calibration scale image. (See figure D.2)

- Click at "Measure" on the menu bar and click at "Calibration", then select "Spatial" Command. (See figure D.3)

- Click at "New" command and set a new name of this scale at name label and change measurement unit to microns. (See figure D.4)

- Click back to the picture and then zoom picture at the position of scale. After clicking at the image of calibration scale, a white line will appear. Then using mouse to click at the edges of the line to move it overlay on the line of reference scale image. If the scale was completely equal to the reference, then define the value in "Scaling" window as 1 and then click OK. The program will be automatic save this scale. (See figure D.5)
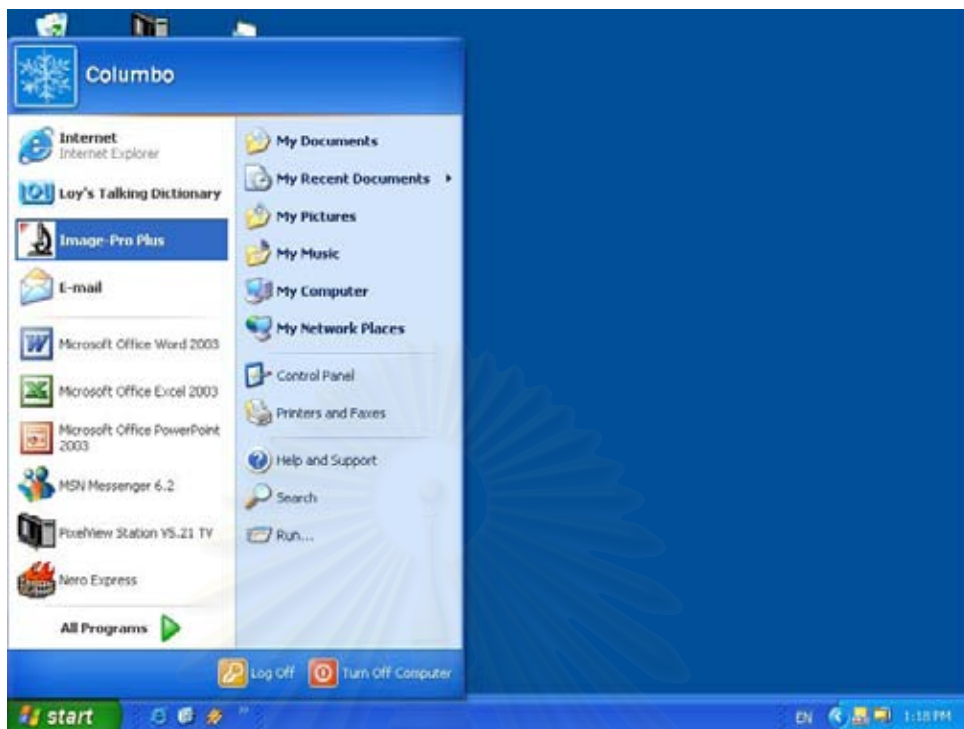
Figure D.1 Calibration procedure
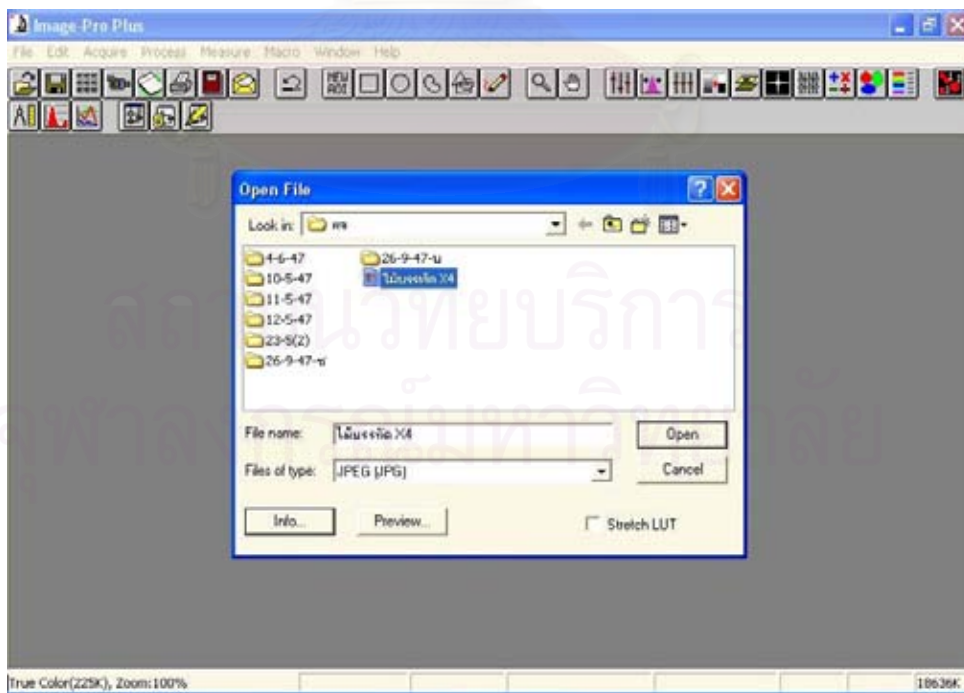
Figure D.2 Calibration procedure
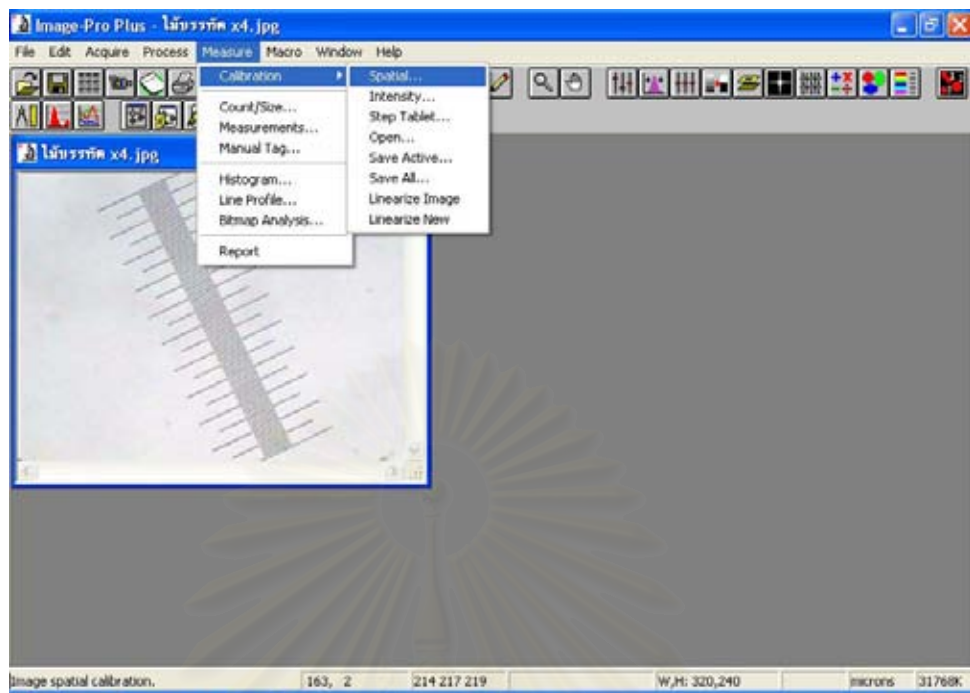
Figure D.3 Calibration procedure
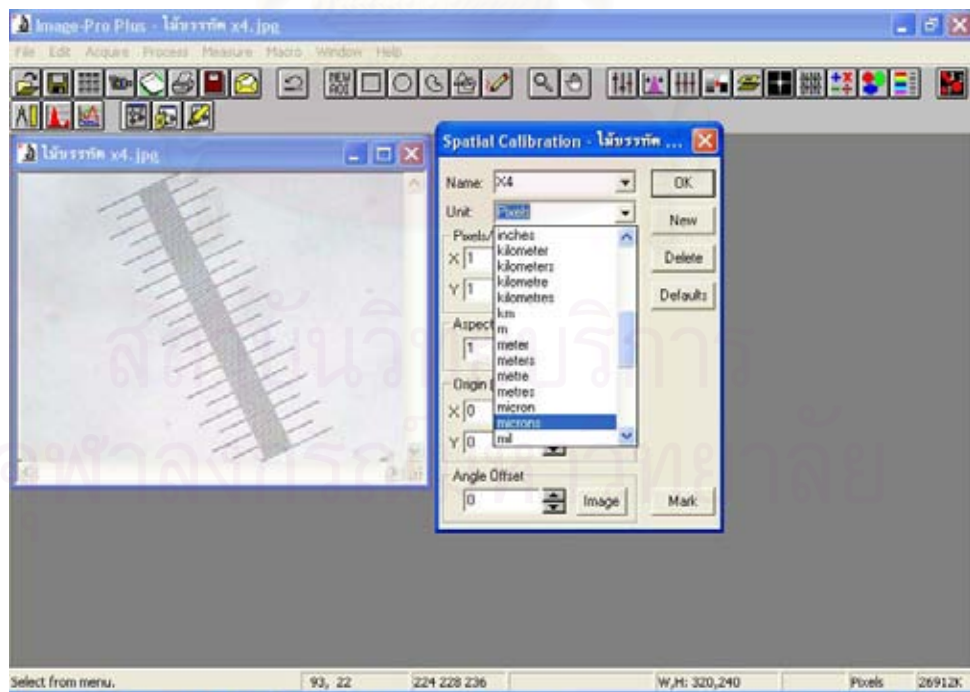
Figure D.4 Calibration procedure

Figure D.5 Calibration procedure

Particle diameter measurement

- Open the particle image file. (See figure D.6)

- Click at "Edit" command on the menu bar and choose at "Convert to"

command then choose "Gray Scale" command for converting the image into Black

and White format. (See figure D.7)

- Click at the binarized image, "Threshold" window will be shown. One has to

adjust the value of threshold for eliminating the noise present in the images. Adjusting

can be done by clicking mouse at the adjusting arrow and sliding it to right or left

until the image can be seen clearly. (See figure D.8)

- Click at Measure command in the menu of "Count/Size" to choose "Select

Measurement" command. Then select measurement type which was "Diameter (ave)"

by sliding vertical scroll bar at the left of measurement window. Diameter (ave) command will appear at the right hand side of Filter ranges. (See figure D.9)

- Click at ""Diameter (ave)"" in "Filter ranges" textbox and change the lower and upper limit size of the selected object by filling the appropriate value into at start and end box, respectively. After click "OK" button, "Count/Size Option" window was disappears. (See figure D.10)

- After clicking at "Options" command in "Count/Size" window, select type of outline style which should be "Filled", label style as "Object" and label color s "Yellow" and then click at "Fill Holes" checkbox. Then click OK. (See figure D.11)

- After clicking at "Count" command, the program will start and mapping the object (particle) whose size was in the range determine. (Figure D.12)

- Measurement data can be observed for confirmation by select "View" command in "Count/Size" windows. After choosing "Select Measurement" command, another window of "Measurement Data" will be shown. One can sort the object's size from minimum to maximum by selecting "Sort up" ratio button. (See figure D.13)

- Procedure of transferring the data can be done b clicking at "File" on menu bar of the measurement data window, then click at "DDE to Excel". The data will be automatically transferred to the Excel. (See figure D.14 and D.15)
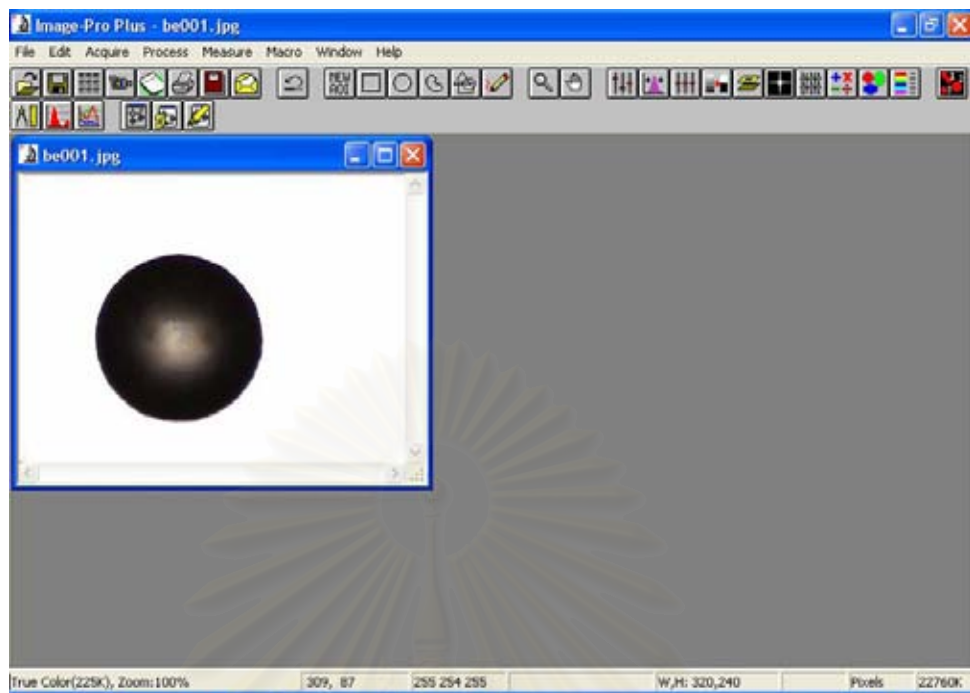
Figure D.6 Particle diameter measurement
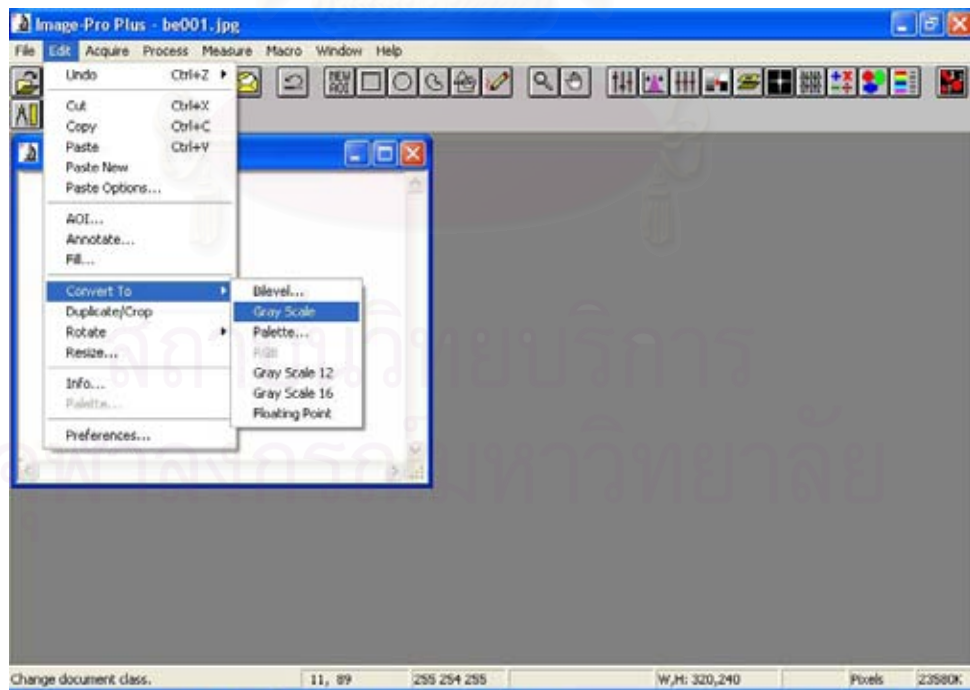
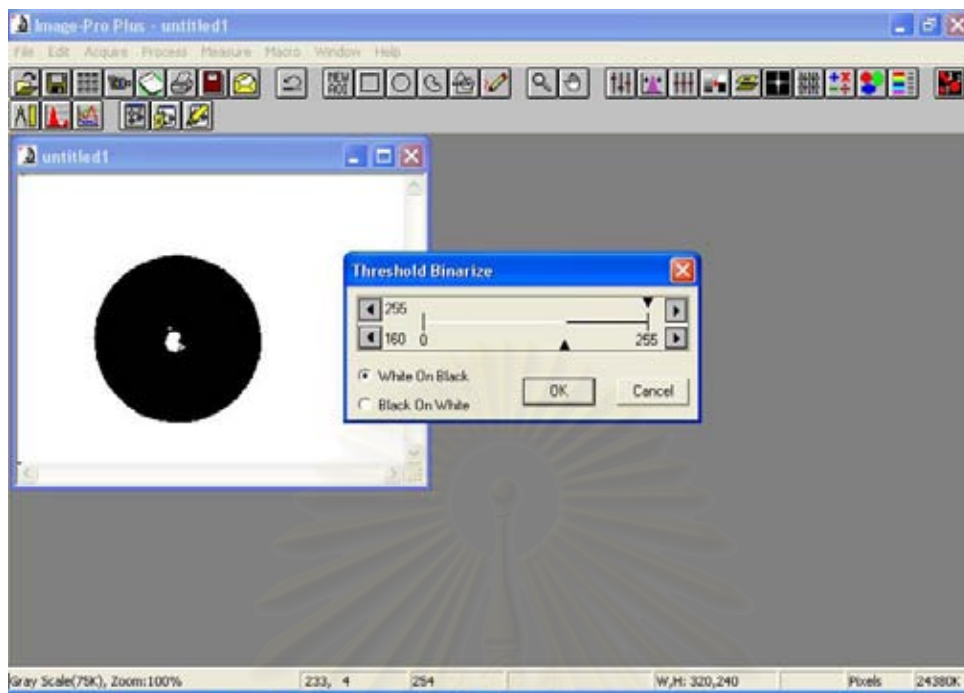**Figure D.7 Particle diameter measurement**
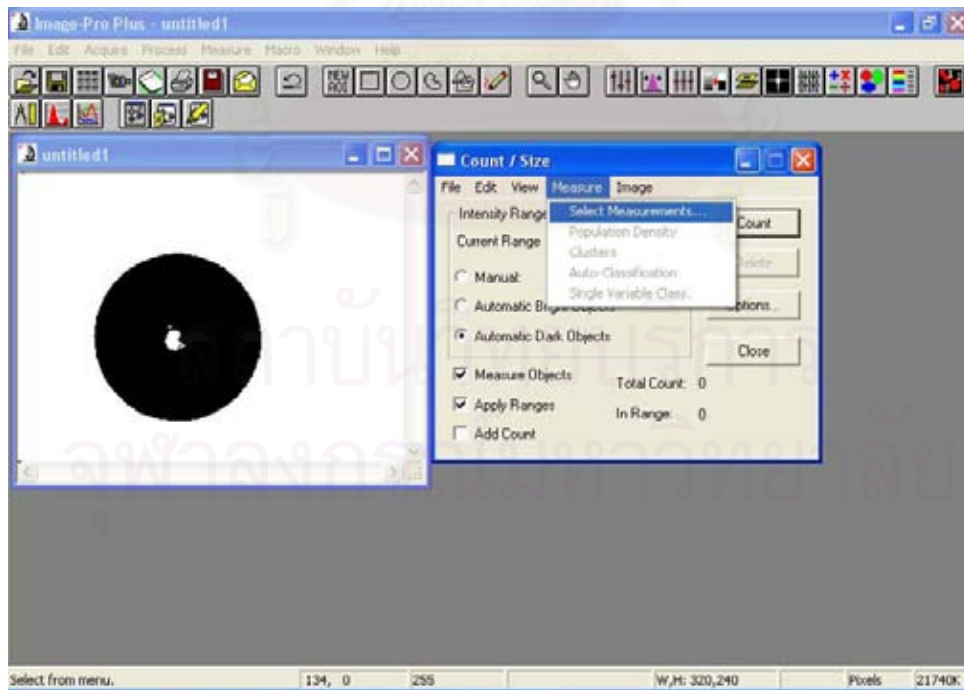
Figure D.8 Particle diameter measurement

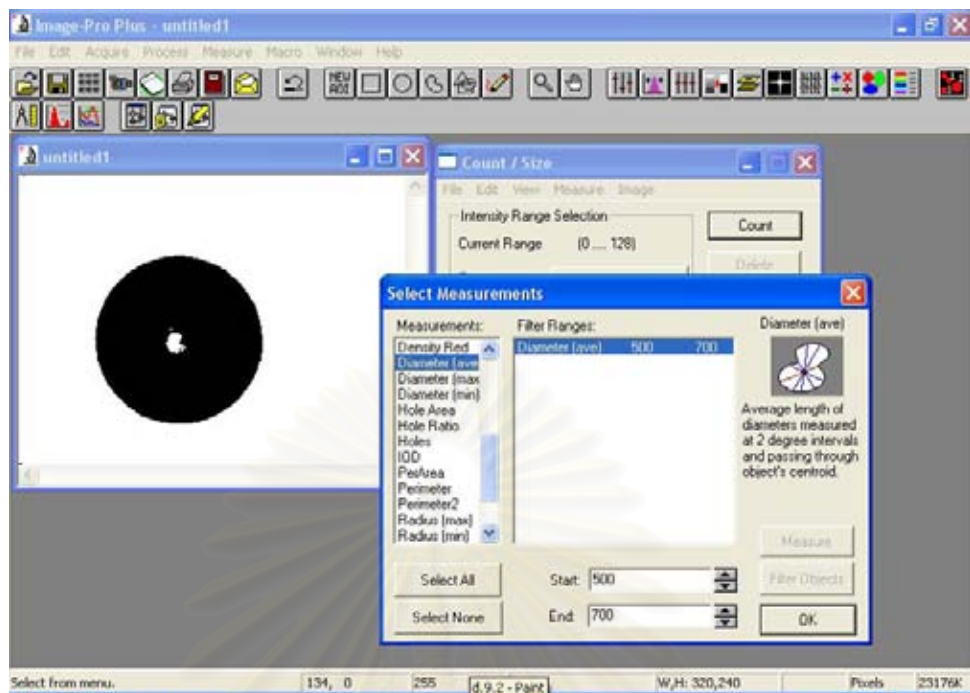**Figure D.9 Particle diameter measurement**

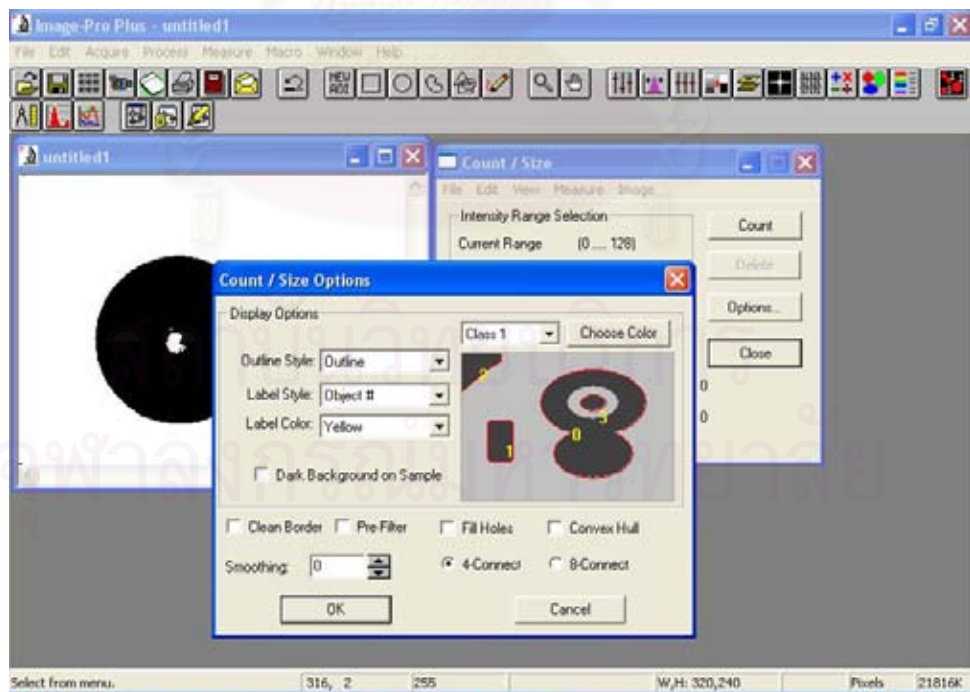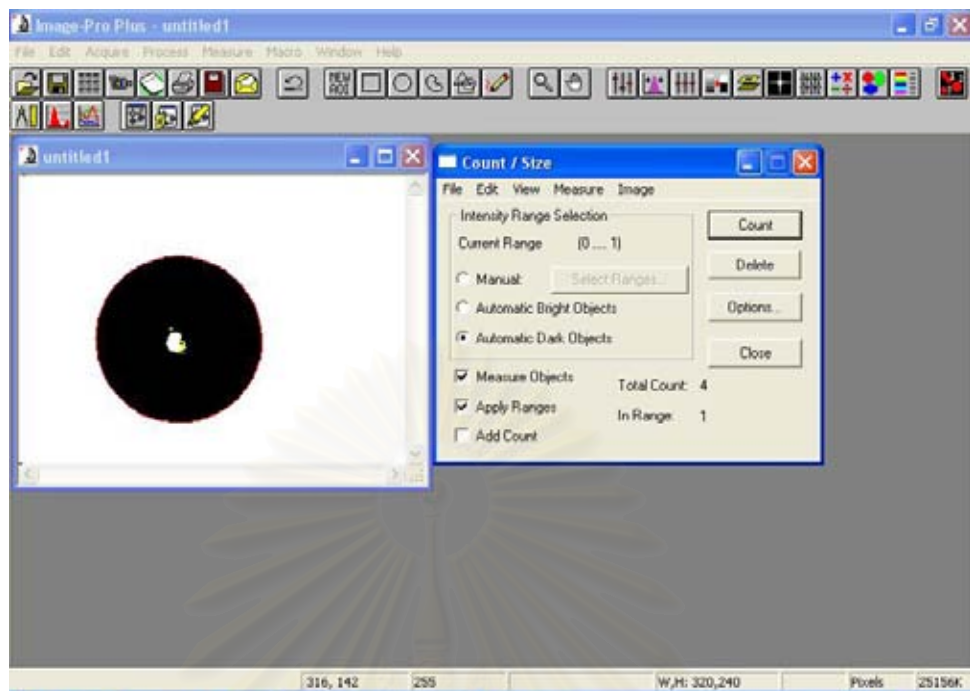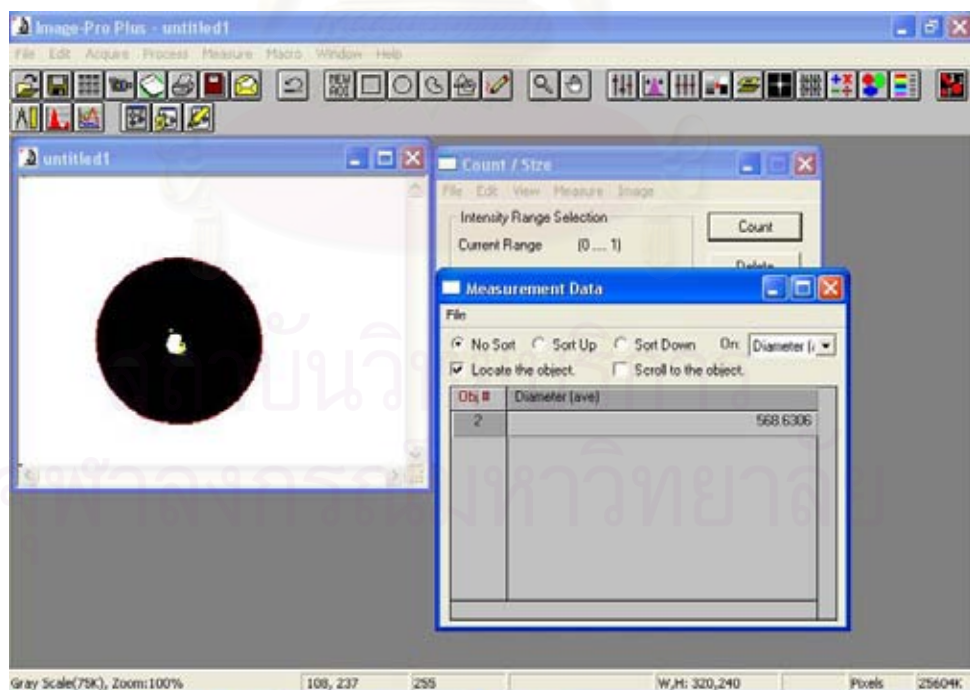**Figure D.10 Particle diameter measurement**

Figure D.11 Particle diameter measurement

Figure D.12 Particle diameter measurement

Figure D.13 Particle diameter measurement

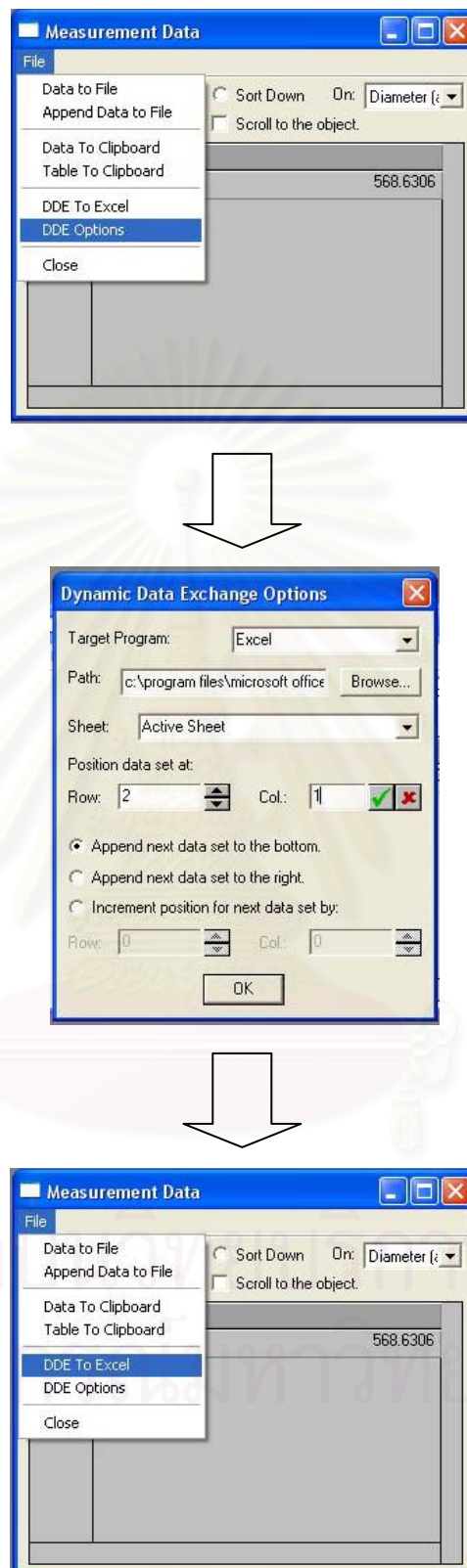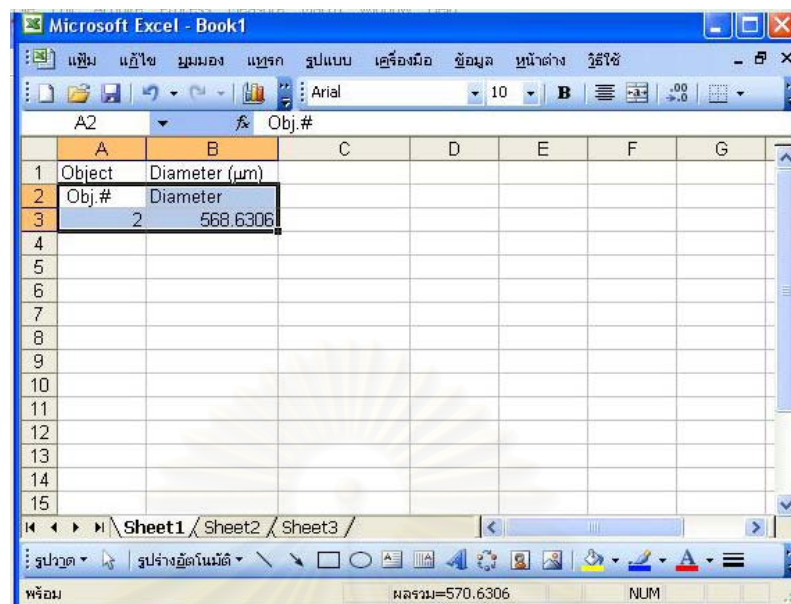**Figure D.14 Particle diameter measurement**

Figure D.15 Particle diameter measurement

VITA

Miss Yuwadee Phoonphetmongkon was born on August 27, 1980 in Udon Thani, Thailand. She studied in primary and secondary educations at Udon Thani Kindergarten School and Udonpittayanukoon School, respectively. In 2002, she received the Bachelor Degree of Science (Chemical Technology) from Chulalongkorn University. After that, she continued to study in Master Degree program at Chemical Engineering Department, Engineering Faculty, Chulalongkorn University with the master thesis entitled "Particle coating in fluidized bed coated enhanced with electrostaticity".